E-
Biomedical electrodes and neuroprothetic

Medical bioelectronic : Medical electrodes

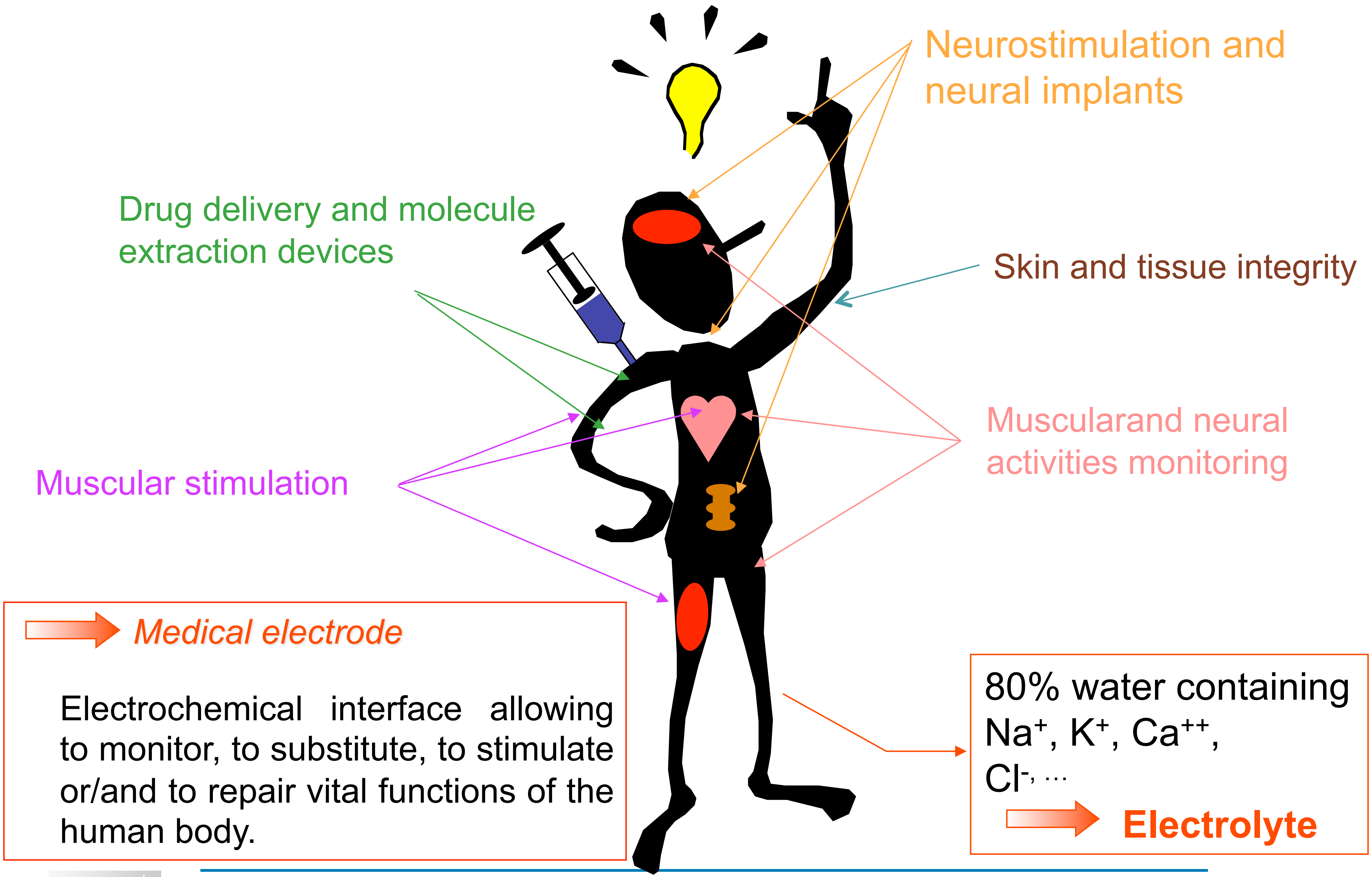

Neurostimulation and neural implants

Drug delivery and molecule extraction devices

Skin and tissue integrity

Muscularand neural activities monitoring

Muscular stimulation

Medical electrode

Electrochemical interface allowing to monitor, to substitute, to stimulate or/and to repair vital functions of the human body.

80% water containing Na^+, K^+, Ca^{++}, Cl^-, …

Electrolyte

Medical bioelectronic : Medical electrodes

Use	Electrode type	Signal	Materials	Application
Control	Monitoring	Potential	iron, Ag/AgCl, ceramic	ECG, EEG, EMG, EGG, ERG
Control	Impedance	modulated current	Ag/AgCl, iron	Skin-tissue impedance
Diagnostic	Reverse iontophoresis	Current périodic	Ag/AgCl + bioreceptor	Physiological concentrations (glucose…)
Stimulation	TENS	Current pulsed	Carbon	Muscular stimulation transdermic, analgesy
Stimulation	Neurostimulation	Current Pulsed HF	Pt, IrOx, TiN	Nerve stimulation, «deep brain stimulation »
Drug delivery	Iontophoresis	periodic current	Ag/AgCl	Systemic or local analgesy, local anesthesia, transfection, edeme, diabetes…
Drug delivery	Electroporation Electropermeabilisation	Current pulsed HF	Pt, iron	Local treatment of Surface cancers, peptides
Restoration	Electric wound healing	periodic current	Ag/AgCl, iron, Pt, Carbon	Restoration of chronic wounds

Bioelectronic implants and biocompatibility

Biocompatibility is a science that investigate the bilateral relation existing between implant (bio)materials and living host-tissues.

D.F. Williams

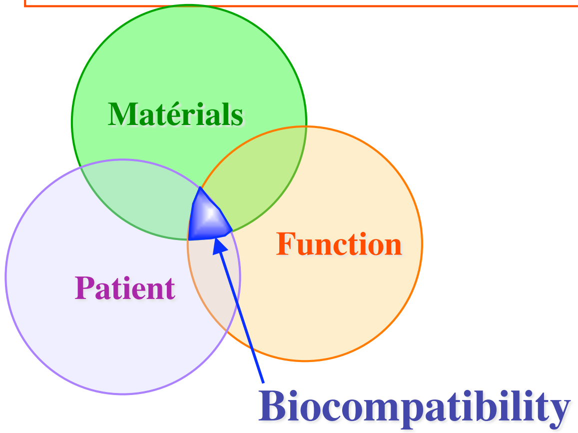

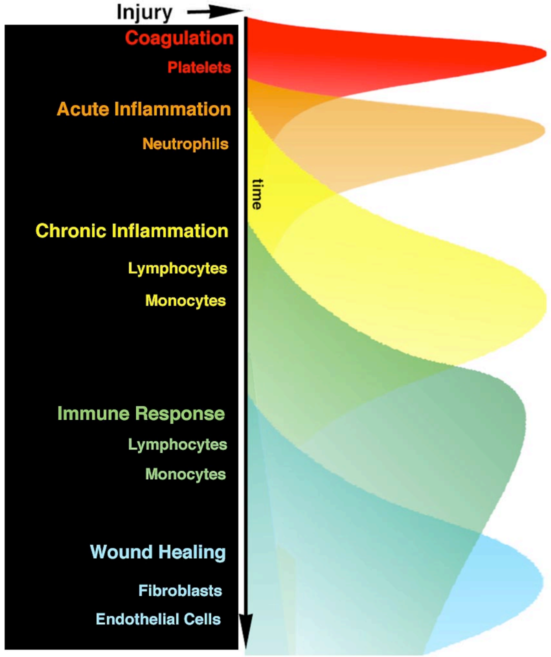

Important factors

- *cytotoxicity*
- *sensitivation*
- *irritation or réactivité intracutanée*
- *pyrogenicity*
- *toxicité systématique*
- *toxicités chronique et subchronique*
- *genotoxicité*
- *implantation*
- *haemocompatibilité*
- *Effets cancerigènes*
- *Impact sur la dégradation/ développement cellulaire*
- *Corrosion*

Evaluation

Electrochemistry
Surface caracterisation
Biological and clinical studies

F-
Biomedical electrodes and neuroprothetic

F.1- Materials used in biomedical electrodes

Nature of the electrochemical interface

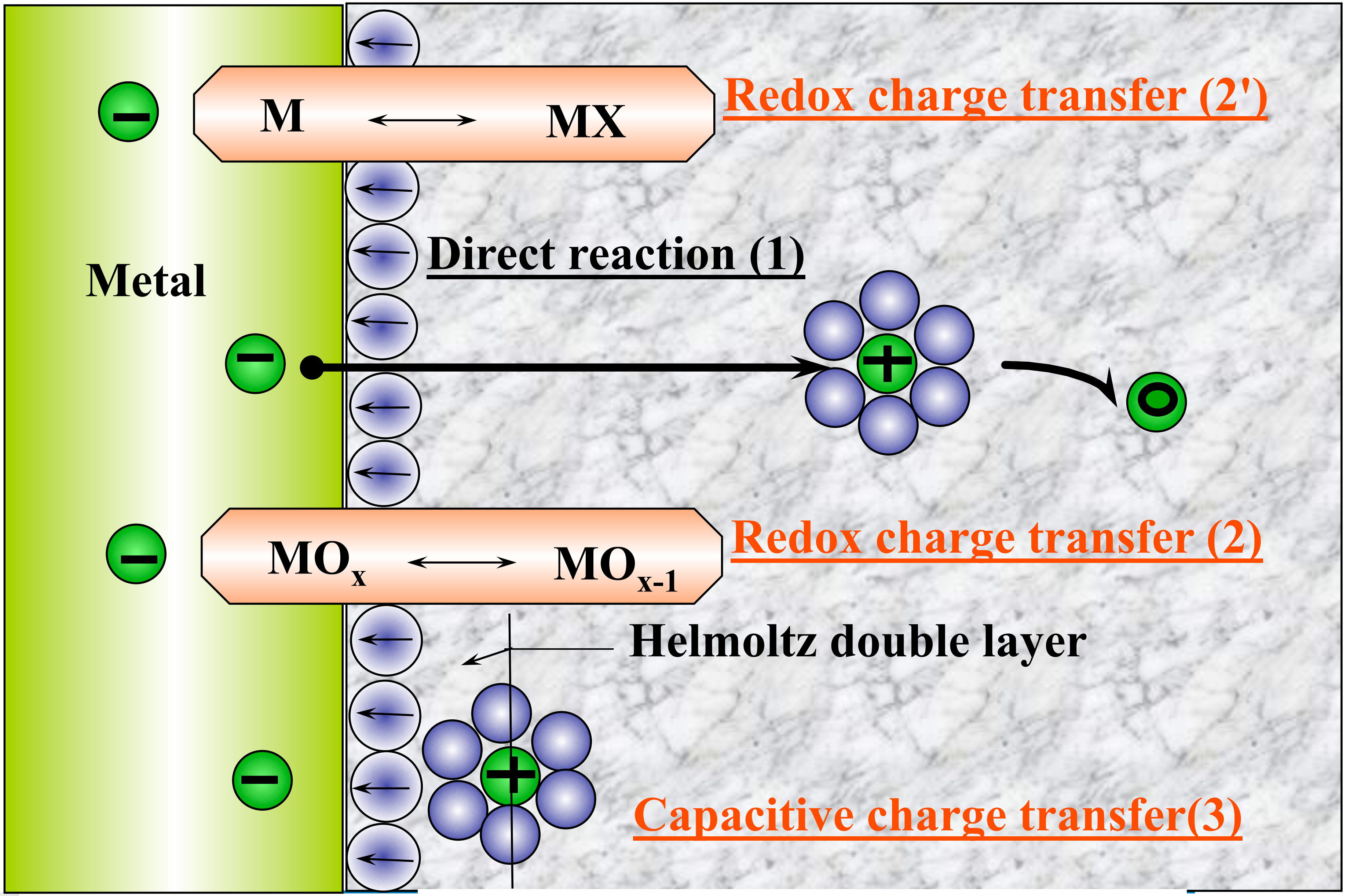

Redox charge transfer (2')

M ⟷ MX

Direct reaction (1)

Metal

$MO_x \longleftrightarrow MO_{x-1}$

Redox charge transfer (2)

Helmoltz double layer

Capacitive charge transfer(3)

Electrode

Electrolyte (Biological tissue)

Electrodes and polarization

- *Electrode materials are tipycally repartited in 2 families*
  - ○ **F**ully polarizable electrodes (***FP***)

    Irreversible behaviour

    Potentialstabilization around OCP

    Metal, Noble metal, carbon, TiN

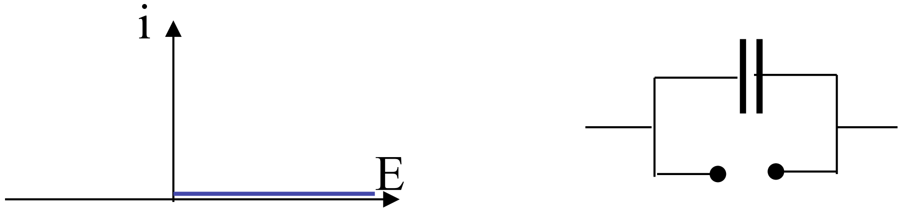

  - ○ **N**on-polarizable electrodes (***NP***)

    Reversible electrochemical behaviour

    Stable interface potential (redox couple)

    Ag/AgCl interface, IrOx…

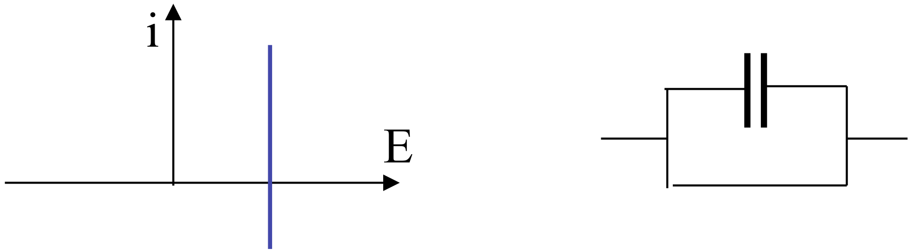

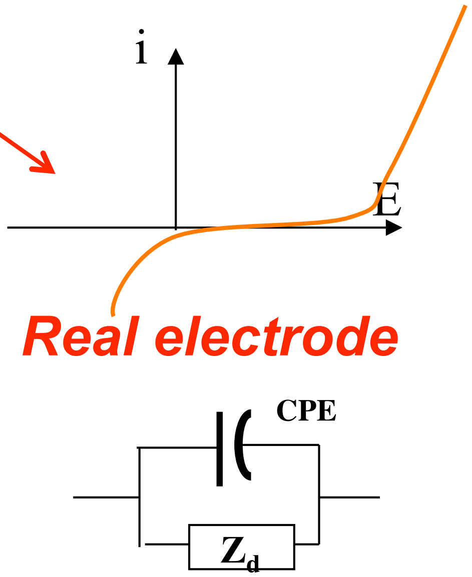

Real electrode

Electrodes impedance

Electrical circuit associated to the electrochemical interface

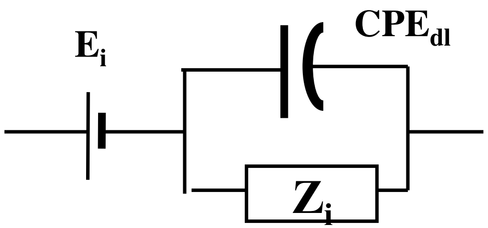

- **E_i** : interfacial potential or Open Circuit Potential

  Fixed by the more probable redox couple in solution
  Or by equilibrium between few different reactions

- **Z_i** : Charge Transfer Resistance or Spreading resistance

$$\boxed{Z_d = \frac{2\rho}{4r}}$$

ρ resistivity of the surounding solution
r electrode radius

- **CPE_{dl}** : Double layer pseudo-capacitance

$$\boxed{Z_C = \frac{1}{j\omega C}}$$

$$\boxed{Z_{CPE} = \frac{1}{Y(j\omega)^n}}$$

$0<n<1$

Electrode roughness
Uneven field distribution
Heterogeneous surface composition
Reaction rates distribution

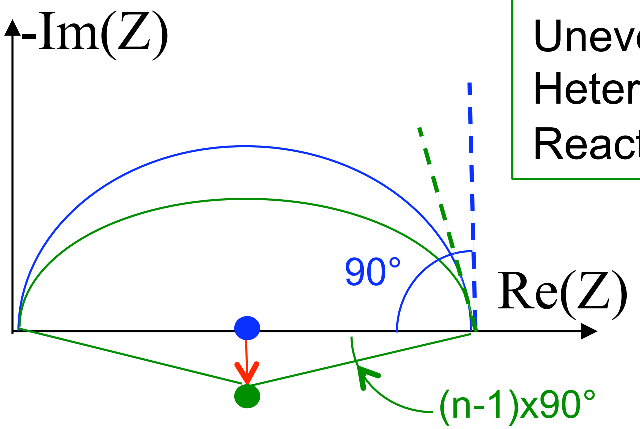

Typical electrode impedance response

- *Electrodes surounded by an electrolyte: the Randles model*

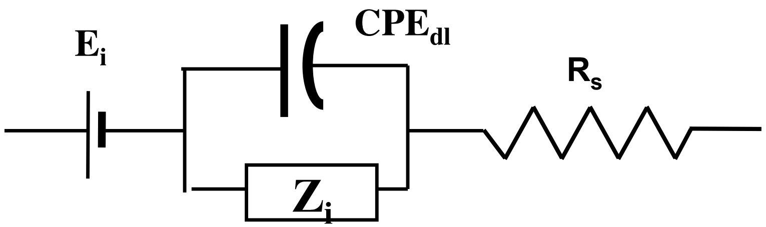

○ **R_s** : Electrolyte resistance

- For a pure capacitance

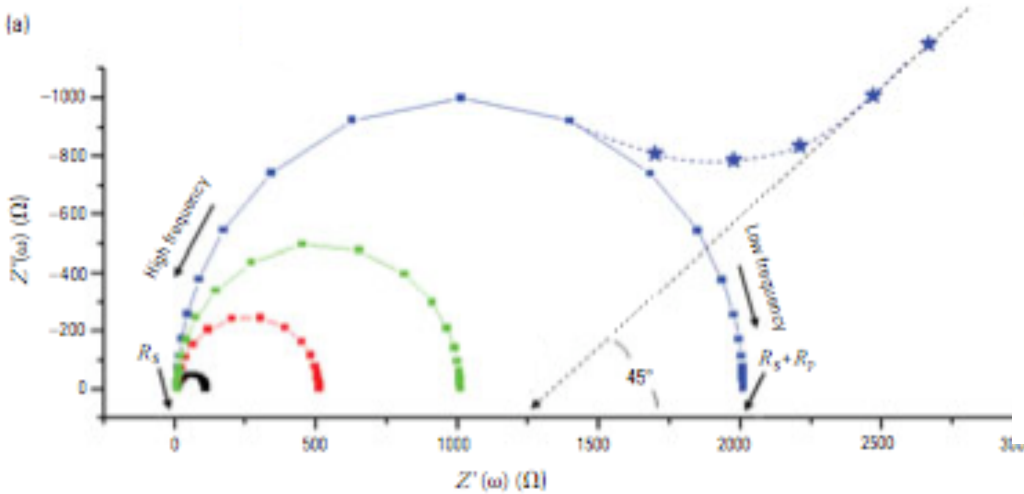

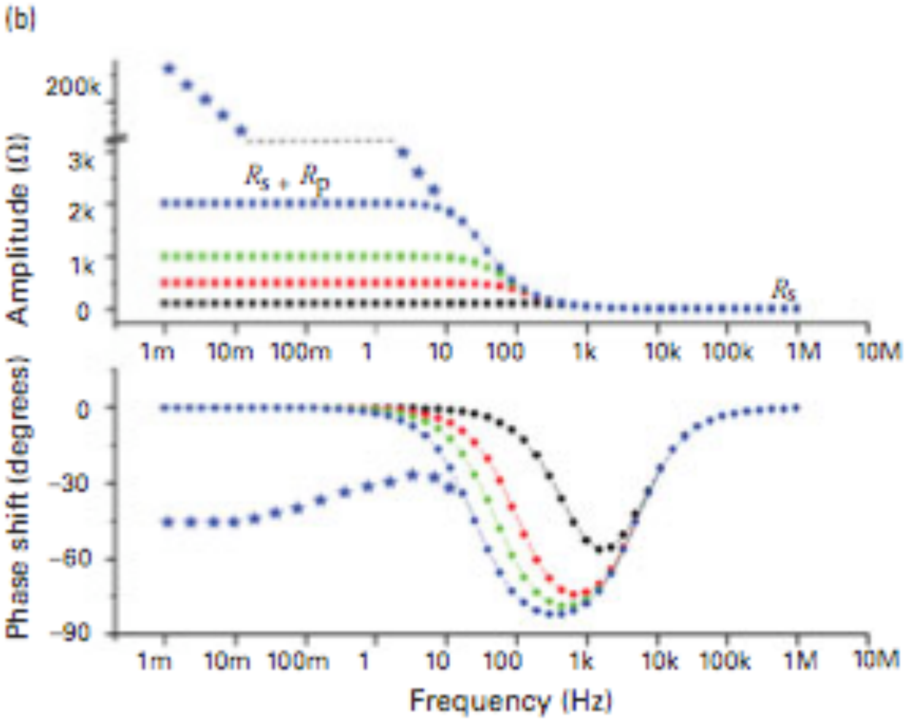

Carbon nanotube electrode (FP)

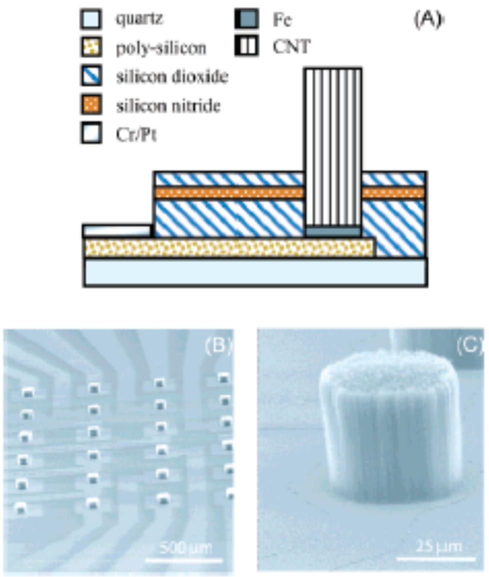

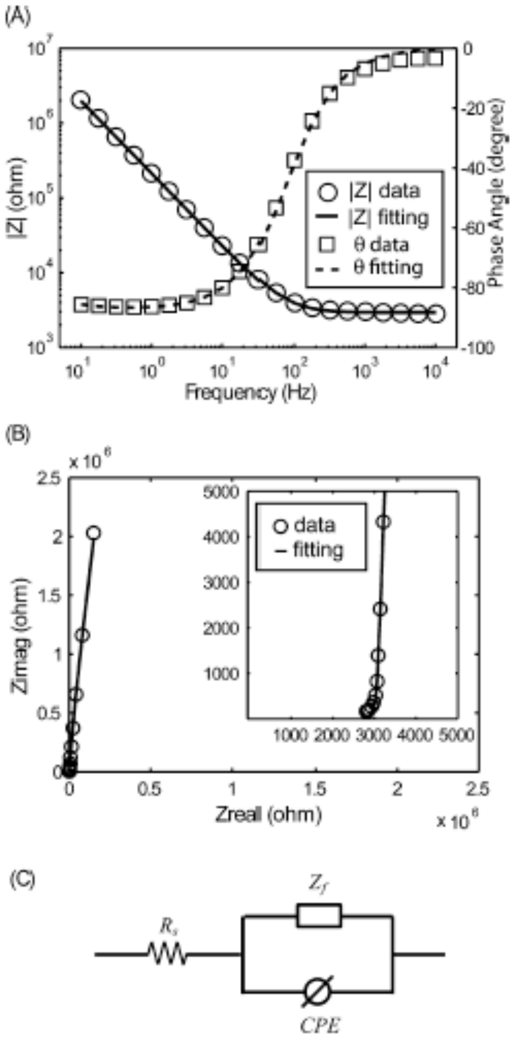

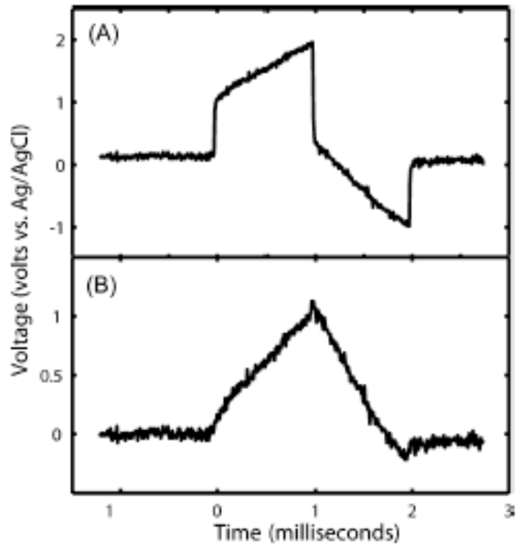

Figure 4. Measurement of the charge injection limit. (A) Voltage excursion of a functionalized CNT electrode (geometrical area = 5.7×10^{-5} cm²), under anodic-first symmetric biphasic current pulses (80 μA, 1 ms) and (B) with R_s subtracted.

- MWCNT hydrophobes
- Mouillage
  - ➡ Modification avec film de PEG-phospholipide

Table 1. Electrochemical Properties of Several Neural Electrode Materials

	CNT	bare Pt	IrOx
potential window (V)	2.5	1.5	1.5
charge injection limit (mC/cm²)	1−1.6	0.1−0.3	2−3
charge injection mechanism	capacitive	faradaic, pseudocapacitive	faradaic

Wang et al,
Nano lett. 6(2006) 2043

The TiN electrode (FP)

Rough TiN

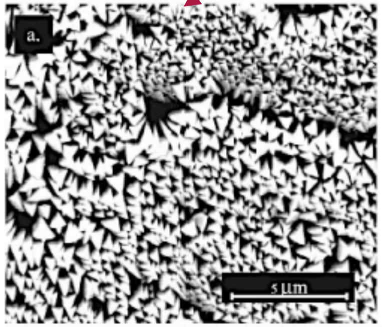

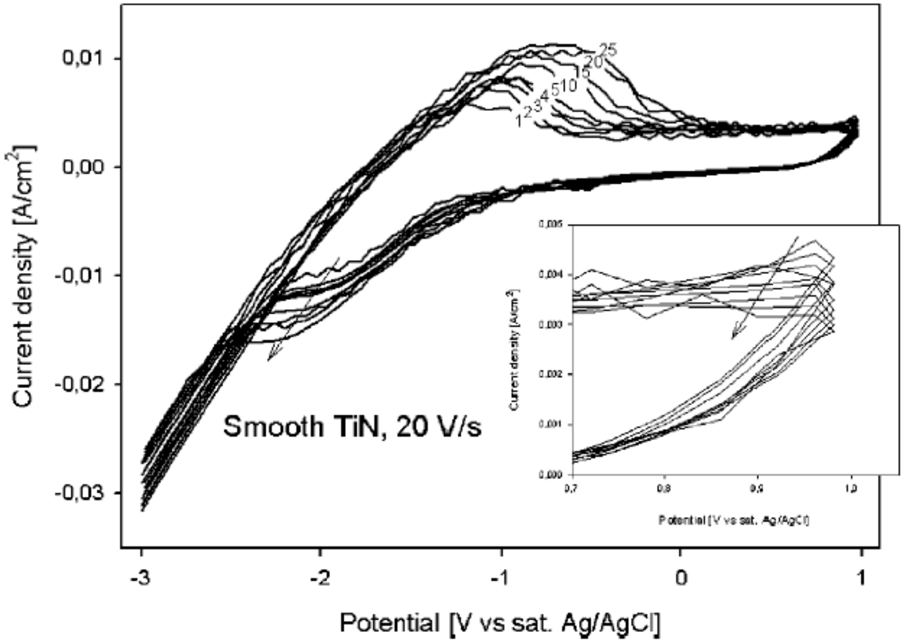

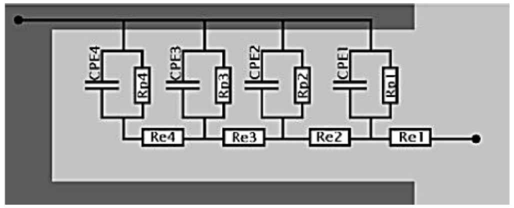

Figure 9. Transmission line model of pore.

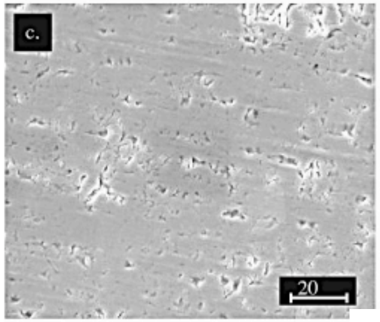

Smooth Ti

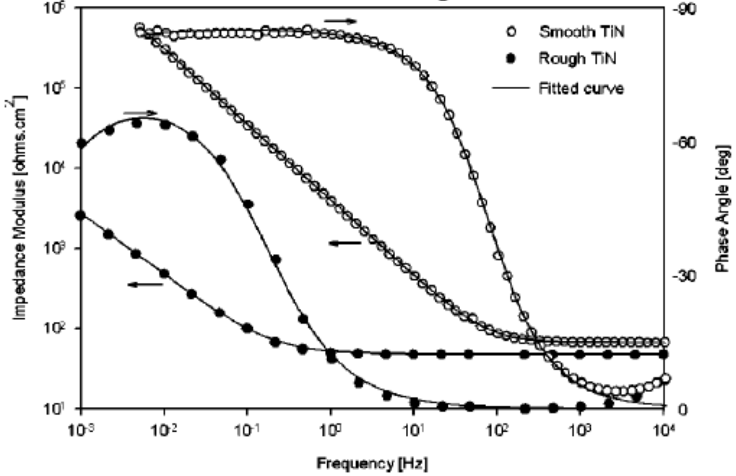
c. Smooth and rough TiN

Table I. Numeric values from spectra fitting. Range of the minimum of three measurements.

	R_p (Ω cm^{-2})	C (F/cm^2)	η
Smooth Pt	7.4-8.6 × 10^5	4.3-5.7 × 10^{-5}	0.91
Smooth Ti	2.3-3.4 × 10^7	1.6-1.7 × 10^{-5}	0.97
Smooth TiN on Ti	2.1-5.6 × 10^7	4.7-5.5 × 10^{-5}	0.91-0.94
Rough TiN	6.6-8.8 × 10^3	1.8-2.2 × 10^{-2}	0.82

***Norlin et al**, JECS 152 (2005) J7*

The gold electrode (FP)

Gold electrochemistry

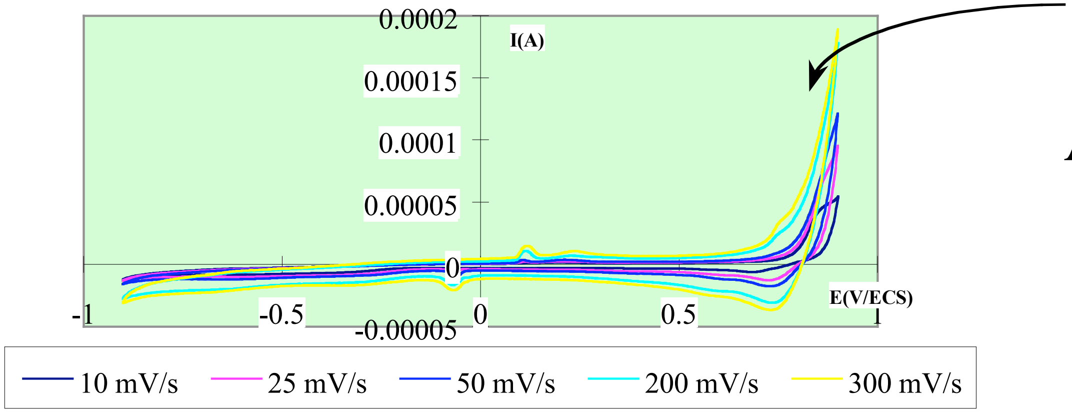

$Au(OH)_3(c)$

$$Au(OH)_3\,(c) + 4Cl^- + 3H^+ \leftrightarrow AuCl_4^- + 3H_2O$$

Oxigen reduction

$$O_2 + e- \leftrightarrow O_2^-$$

$$O_2^- + e- \longrightarrow O_2^{2-}$$

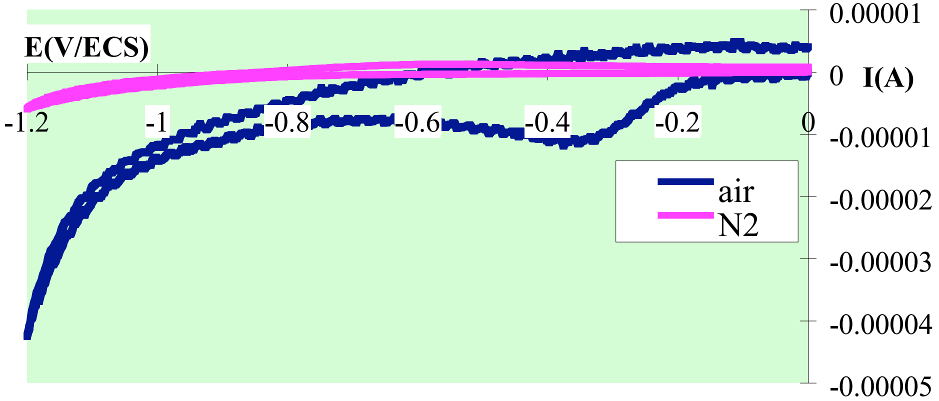

M. Hyland et al, *Analyst 121 (1996) 705*

The platinum electrode (FP)

- *Platinum electrochemistry*

Pt surface electrochemical behaviour

1. $Pt + H_2O \rightleftharpoons Pt_{(4)}OH + H^+ + e^-$
2. $Pt_{(4)}OH + H_2O \rightleftharpoons Pt_{(2)}OH + H^+ + e^-$
3. $Pt_{(2)}OH + H_2O \rightleftharpoons Pt_{(1)}O + H^+ + e^-$
4. $Pt_{(1)}O + H_2O \rightleftharpoons Pt_{(1)} O_2 + H^+ + e^-$

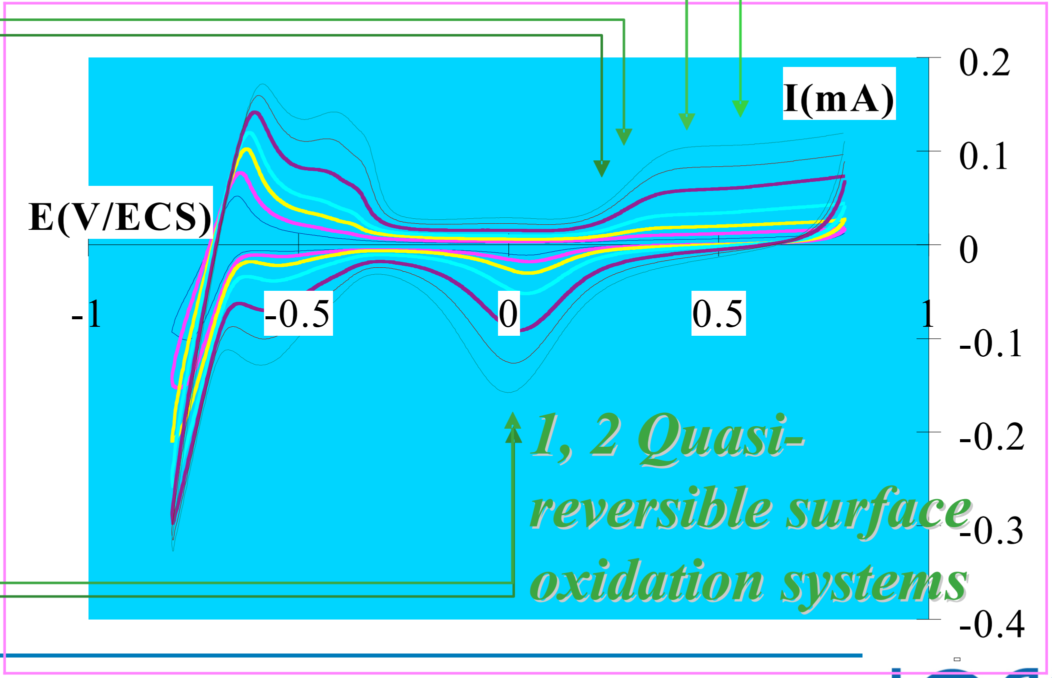

1, 2 Quasi-reversible surface oxidation systems

Different oxidation numbers of Pt

$$Pt \rightarrow \underbrace{Pt_4OH \rightarrow Pt2OH}_{Reversible} \rightarrow \underbrace{PtOH \rightarrow PtO}_{Ireversible}$$

Pt surface structuration and impedance

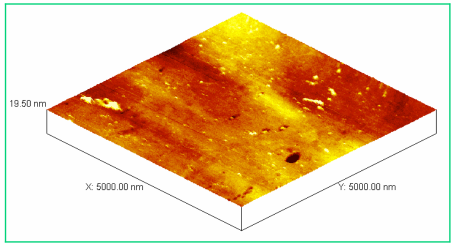

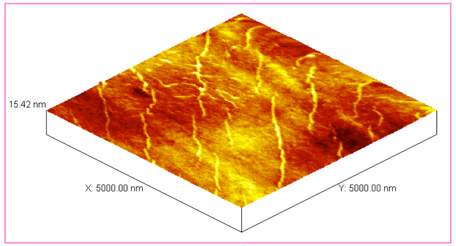

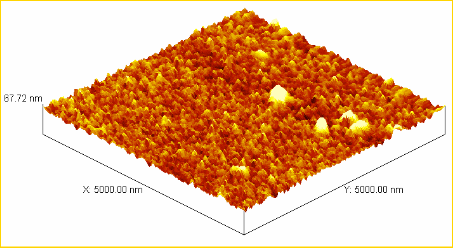

Electrode	Pt Foil	PI-Pt	PI-Cr-Au-Pt
Pt Processing	Bulk Pt	Sputtering	Electrodeposition
Roughness *nm*	0.89	1.06	6.88
Fractal Dimension	2.87	2.91	2.93
Electroactive area cm^2	0.06	0.09	0.8
% geometric area	30	46	408
$\mathbf{R_{CT}}$	33	40	44
$\mathbf{C_{eff}}$ $k\Omega$	1.1	2.09	96.7
n	0.883	0.833	0.820

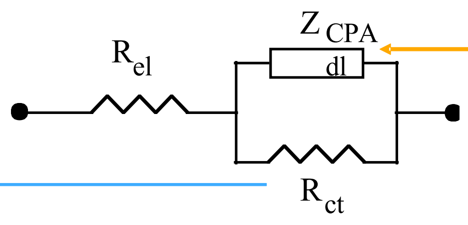

$$Z_{CPE} = \frac{1}{C(j\omega)^n}$$

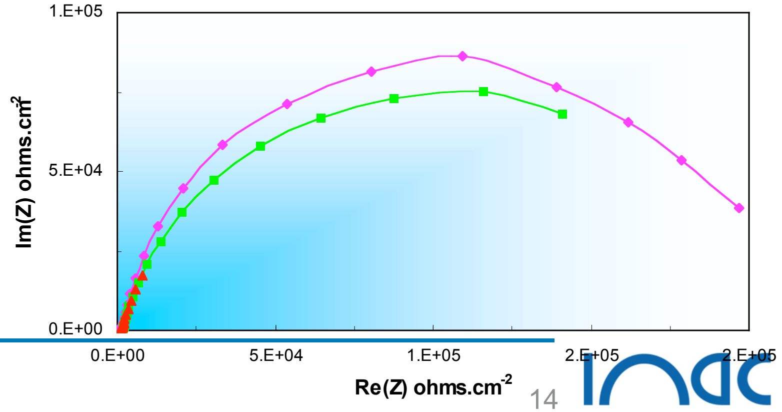

Mailley et al, *Bioelectrochem (2003)*

Platinum electrodes from electrodeposition

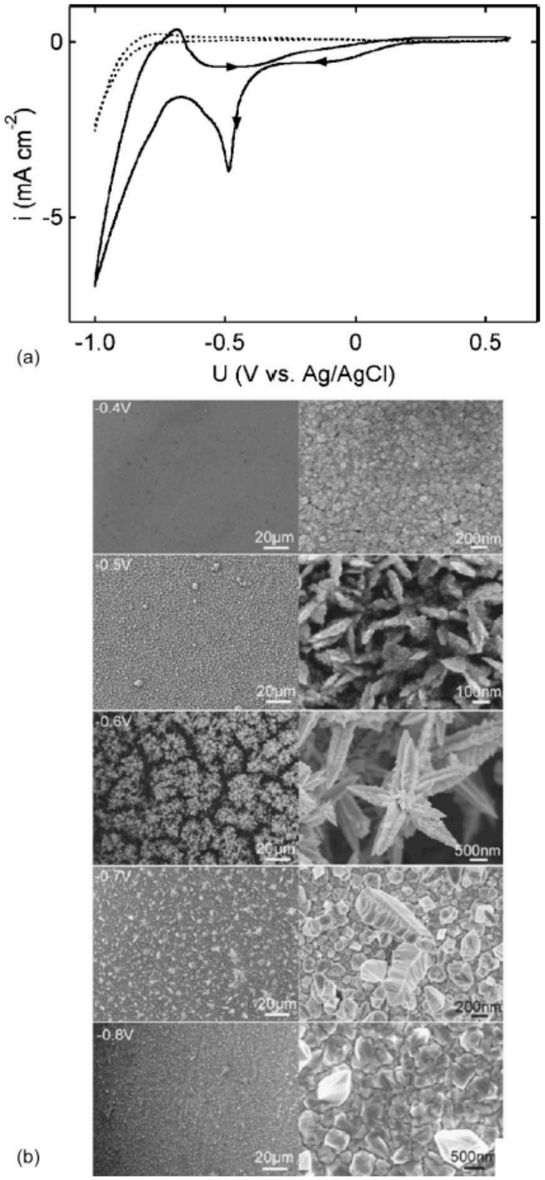

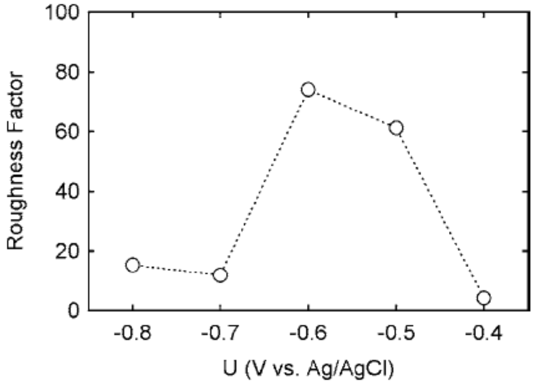

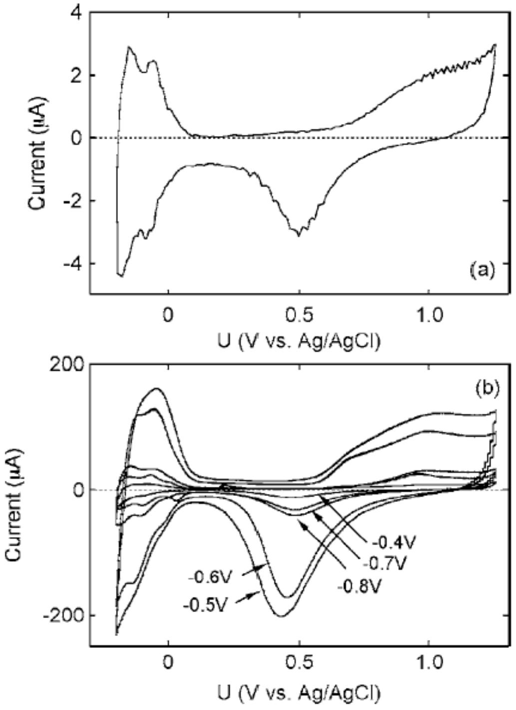

Figure 7. Current–voltage curves for (a) polycrystalline platinum microelectrode and (b) electrodeposited microelectrodes in 250 mM H_2SO_4, pH 1.8. The potential range was −0.2 to − 1.25 V, and the scan rate was 250 mV s^{-1}. The deposition potentials are indicated in the figure.

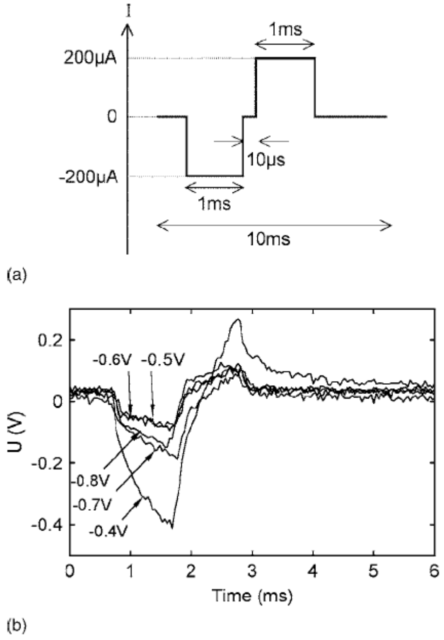

Figure 9. (a) Schematic illustration of the biphasic waveform. (b) Potential–time transients recorded for electrodeposited platinum microelectrodes.

Weiland et al, *JECS 153 (2006) C834*

The Ag/AgCl electrode (NP)

$$\left.\begin{array}{l} Ag \rightleftharpoons Ag^+ + e^- \\ Ag^+ + Cl^- \underset{K_{diss}}{\rightleftharpoons} AgCl \end{array}\right\} \quad Ag^+ + Cl^- \rightleftharpoons AgCl + e^-$$

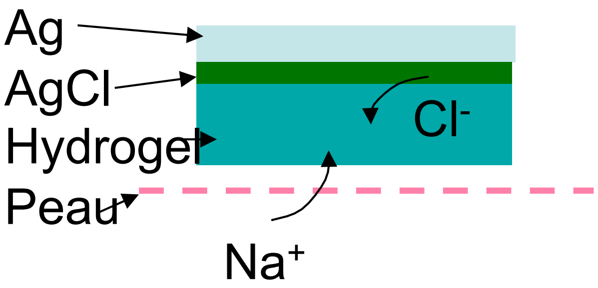

$$E_{Ind} = E^0_{AgCl/Ag} + \frac{RT}{F}\ln\left(\frac{1}{\left[Cl^-\right]}\right)$$

$$E_{ind} = E^0_{AgCl/Ag} + 0{,}0592\,pCl$$

$\rightarrow 0,222$ V/ESH

- Electrochemical equilibrium determined by endogenous species (Na^+, Cl^-)
- Very low polarization resistance
- Reusable or one shot

- Requires the use of a contact gel (contrary to FP electrodes)
- Poor robustness, photochemical degradation

Ag/AgCl electrochemical behaviour

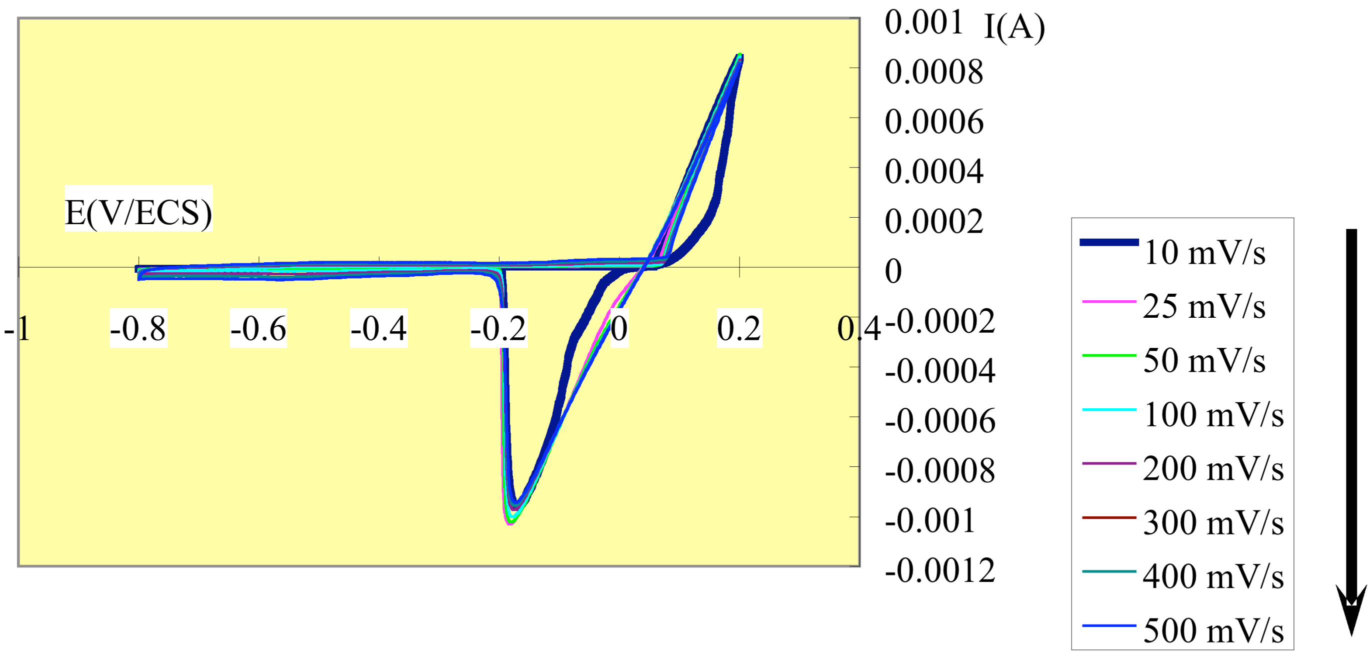

Scan
rate

Formation and consumption of crystalline compound AgCl

Rapide depolarisation andd polarisation of the interface

Hydrous iridium oxide electrodes (NP)

Structural Characterization

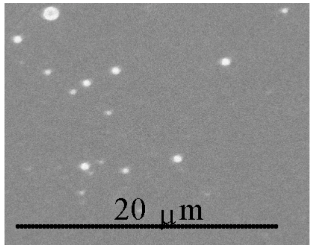

11 mC/cm^2

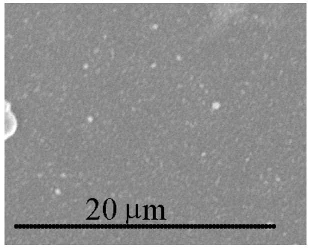

23 mC/cm^2

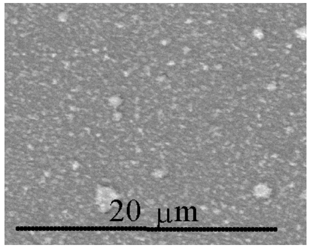

46 mC/cm^2

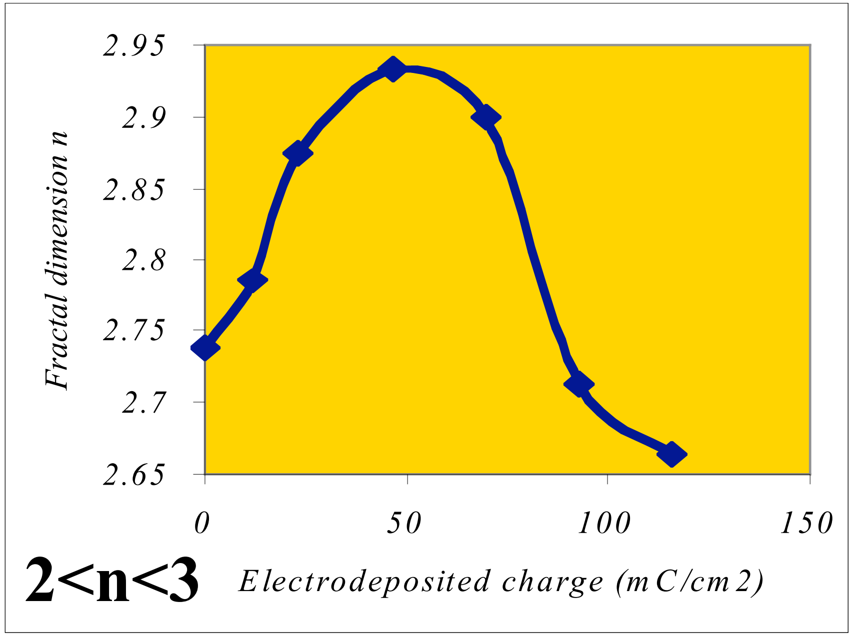

2<n<3

70 mC/cm^2

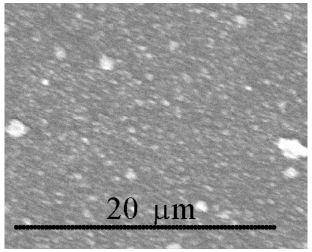

93 mC/cm^2

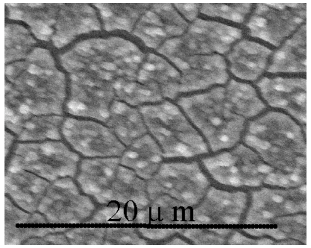

116 mC/cm^2

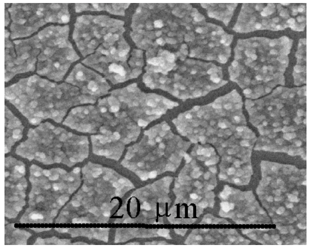

Mailley et al, *J mat Sci eng C (2002)*

IrOx electrochemical behaviour

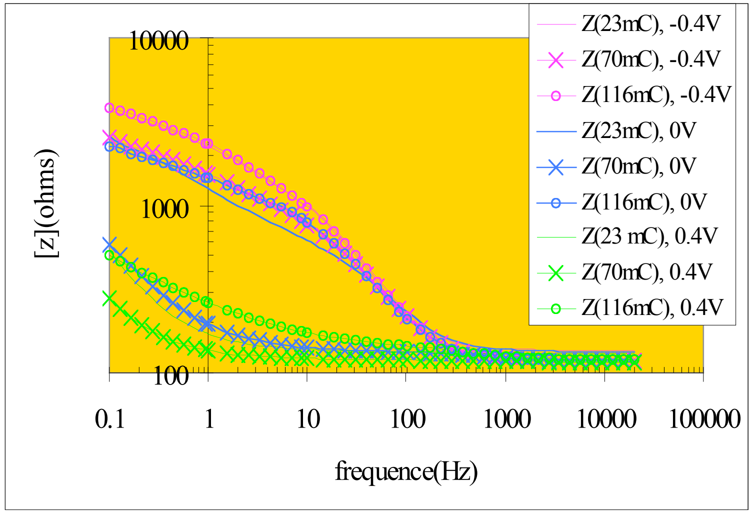

$$\mathrm{Ir(OH)\cdot 3H_2O \leftrightarrow Ir(OH)_2\cdot 2H_2O + H^+ + e^-}$$

$$\mathrm{Ir(OH)_2\cdot 2H_2O \leftrightarrow Ir(OH)_3\cdot H_2O + H^+ + e^-}$$

$$\mathrm{Ir(OH)_3\cdot H_2O \leftrightarrow Ir(OH)_4 + H^+ + e^-}$$

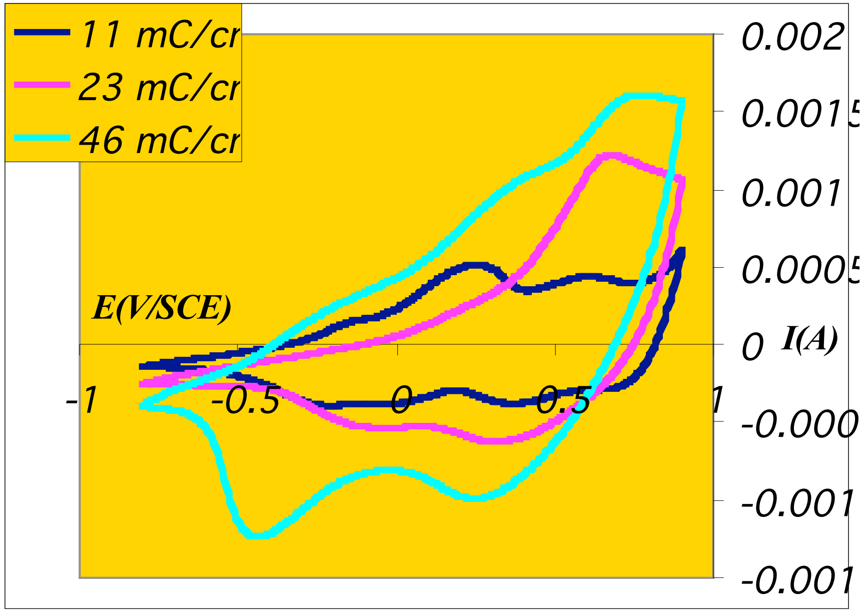

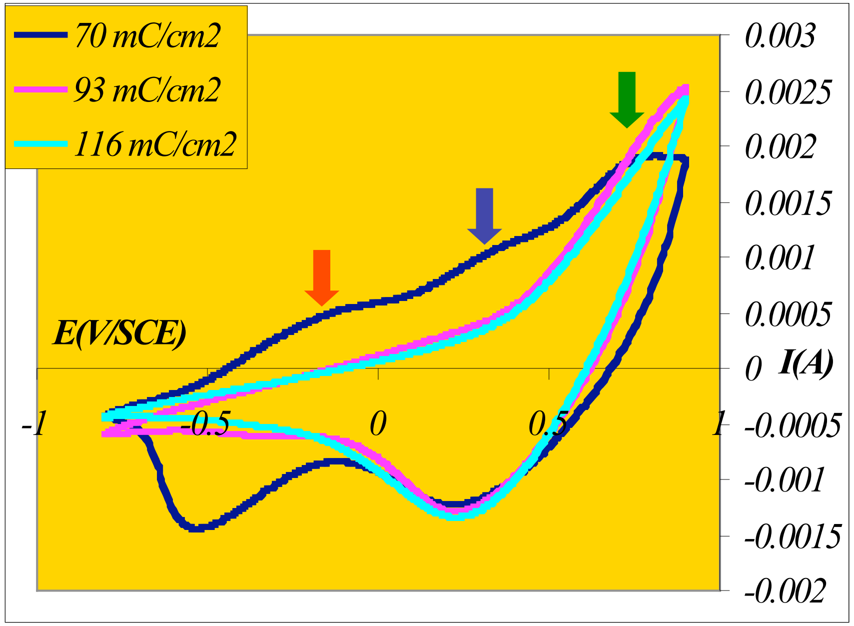

IrOx from sputtering and electroactivation

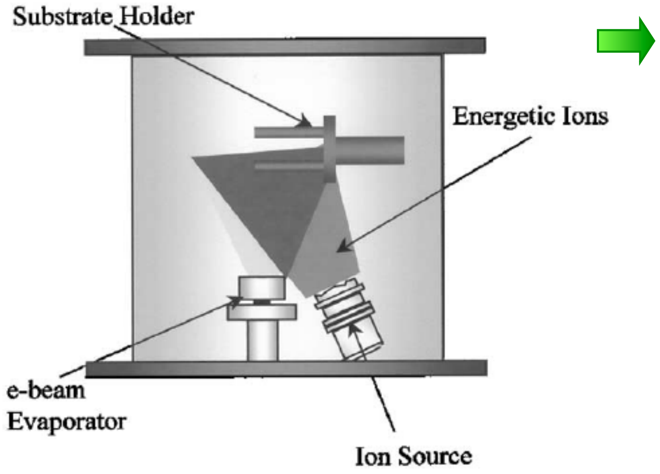

➡ Ir deposition by pulverisation (under Ar plasma)

⬇

Activation through electrochemical cycling in H_2SO_4 0.1 M

⬇

Formation of $IrOH_4$ ➡

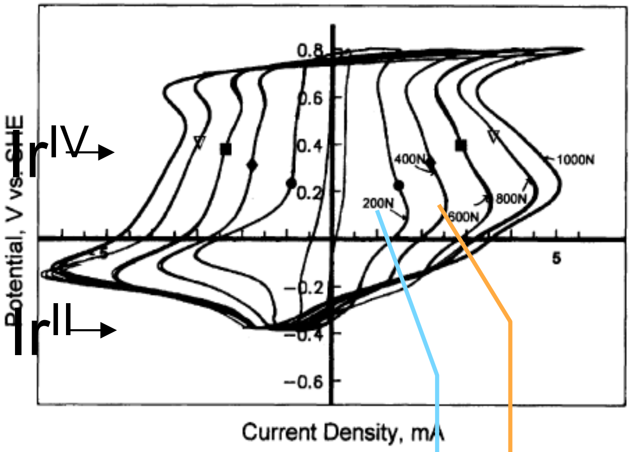

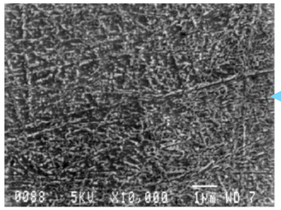

(a) 300-cycle

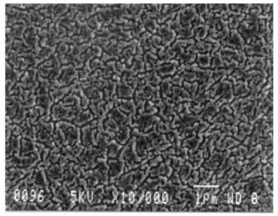

(b) 500-cycle

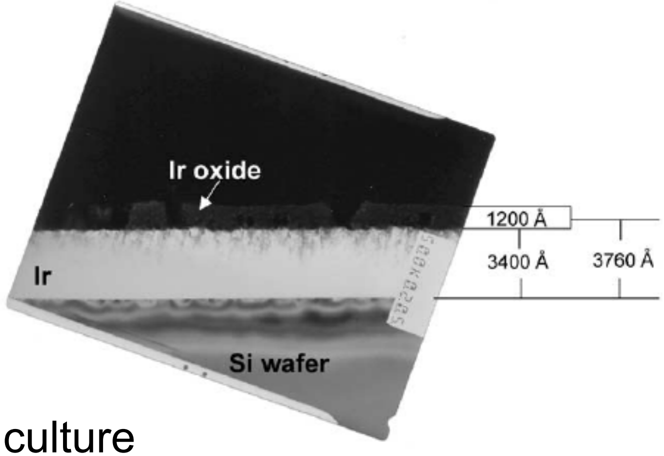

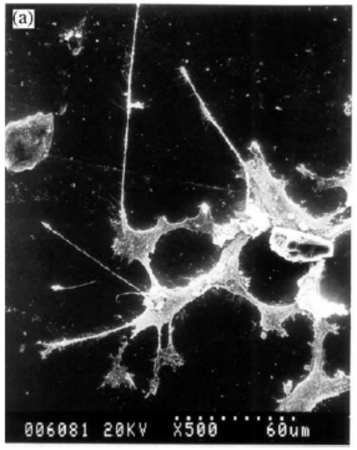

⬇

Biocompatibility : PC 12 cells culture

Lee et al, *Biomaterials 24 (2003) 2225*

Sputtered IrOx under Oxygen plasma

Direct IrOx deposition magnetron pulverisation under Ar/O_2 plasma

In situ oxidation

Porosity depends on O_2 flux

Final electrochemical activation

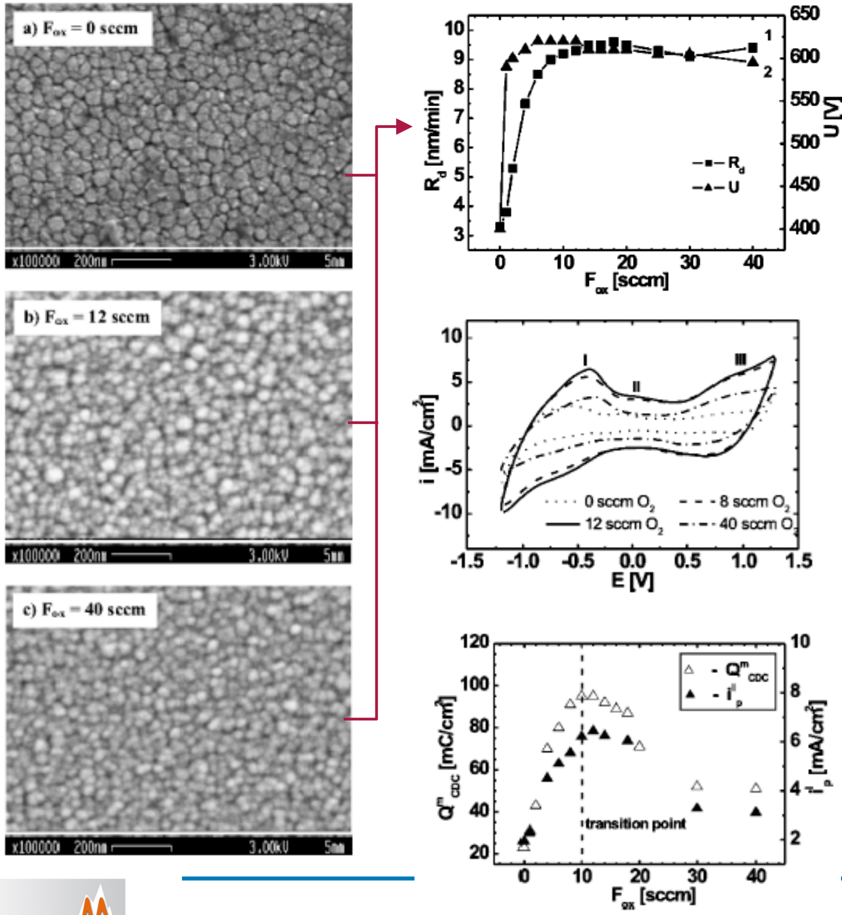

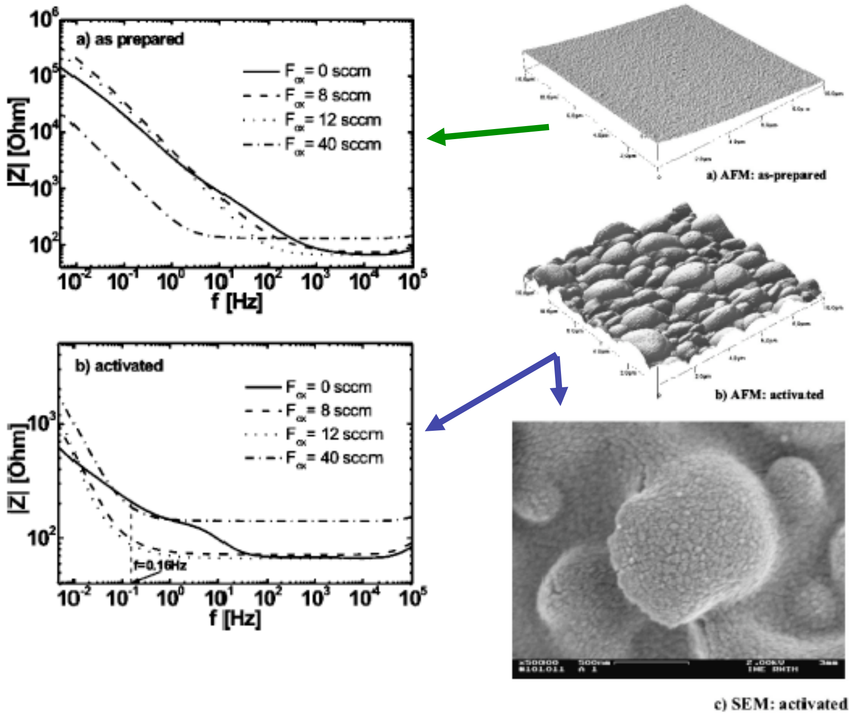

Slavcheva et al, *JECS 151 (2004) E226*

Comparison betwen FP and NP electrodes

Weiland et al, *IEEE Trans. Biomed. Eng. 49 (2002) 1574*

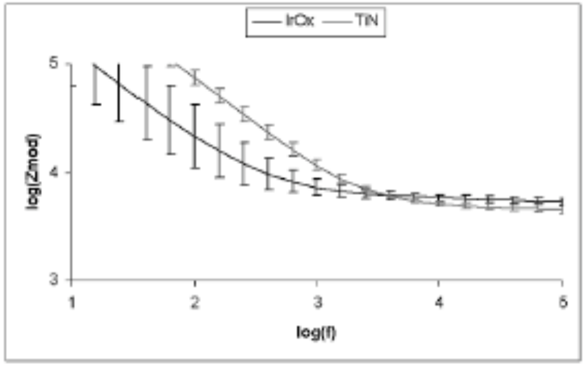

(a)

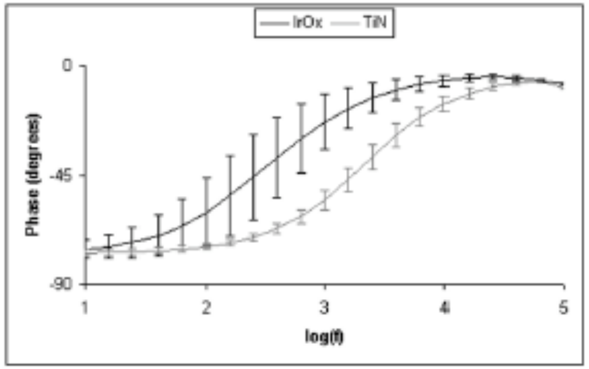

dc +300 mV 5 mV rms

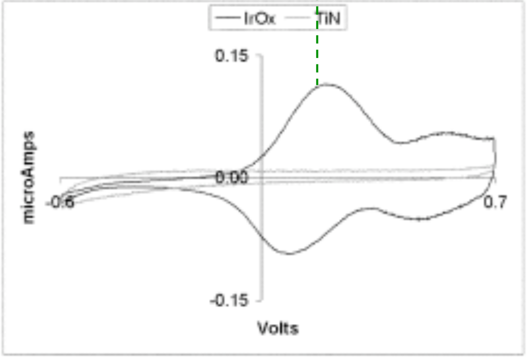

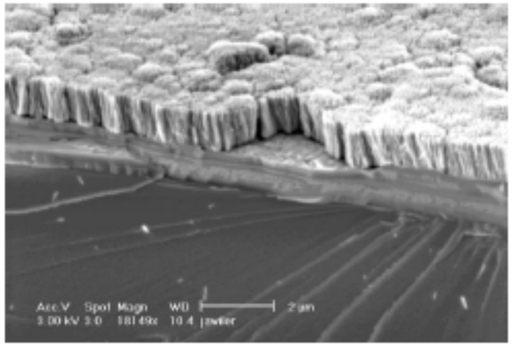

TiN rugueux

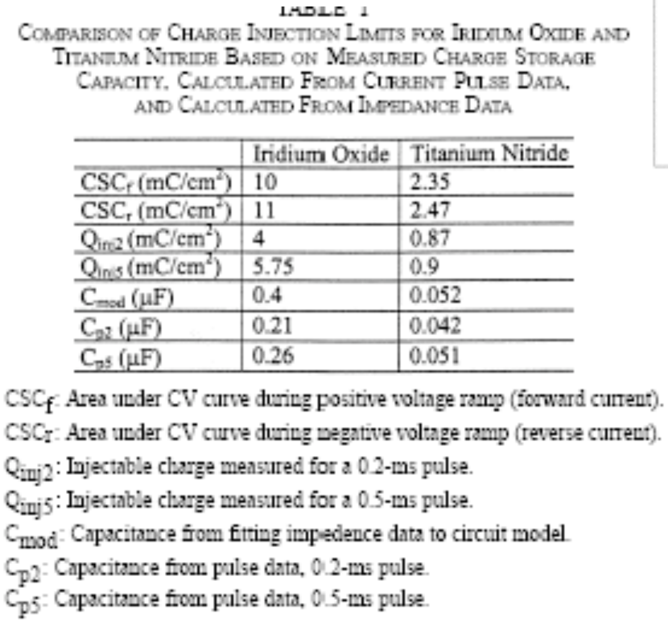

TABLE I

COMPARISON OF CHARGE INJECTION LIMITS FOR IRIDIUM OXIDE AND TITANIUM NITRIDE BASED ON MEASURED CHARGE STORAGE CAPACITY, CALCULATED FROM CURRENT PULSE DATA, AND CALCULATED FROM IMPEDANCE DATA

	Iridium Oxide	Titanium Nitride
CSC_f (mC/cm^2)	10	2.35
CSC_r (mC/cm^2)	11	2.47
Q_{inj2} (mC/cm^2)	4	0.87
Q_{inj5} (mC/cm^2)	5.75	0.9
C_{mod} (µF)	0.4	0.052
C_{p2} (µF)	0.21	0.042
C_{p5} (µF)	0.26	0.051

CSC_f: Area under CV curve during positive voltage ramp (forward current).
CSC_r: Area under CV curve during negative voltage ramp (reverse current).
Q_{inj2}: Injectable charge measured for a 0.2-ms pulse.
Q_{inj5}: Injectable charge measured for a 0.5-ms pulse.
C_{mod}: Capacitance from fitting impedence data to circuit model.
C_{p2}: Capacitance from pulse data, 0.2-ms pulse.
C_{p5}: Capacitance from pulse data, 0.5-ms pulse.

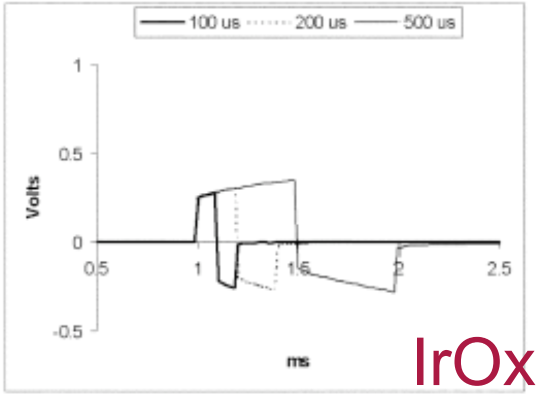

IrOx

(b)

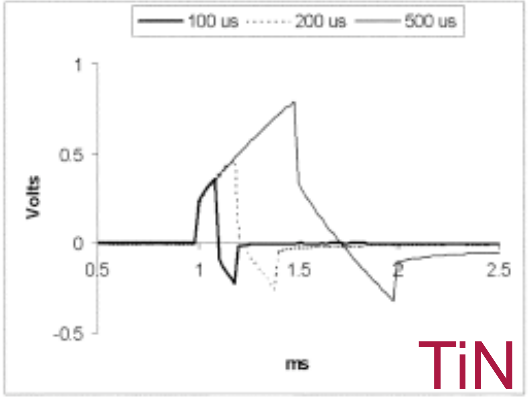

TiN

Pulse 50 µA
Surface 4000 µm²

F-
Biomedical electrodes and neuroprothetic

F.2- Biomedical electrodes for skin/ tissue survey and transdermal applications

Skin anatomy

Skin → Living system in perpetual renewing
→ Skin surface renewing cycle : 7 to 14 days

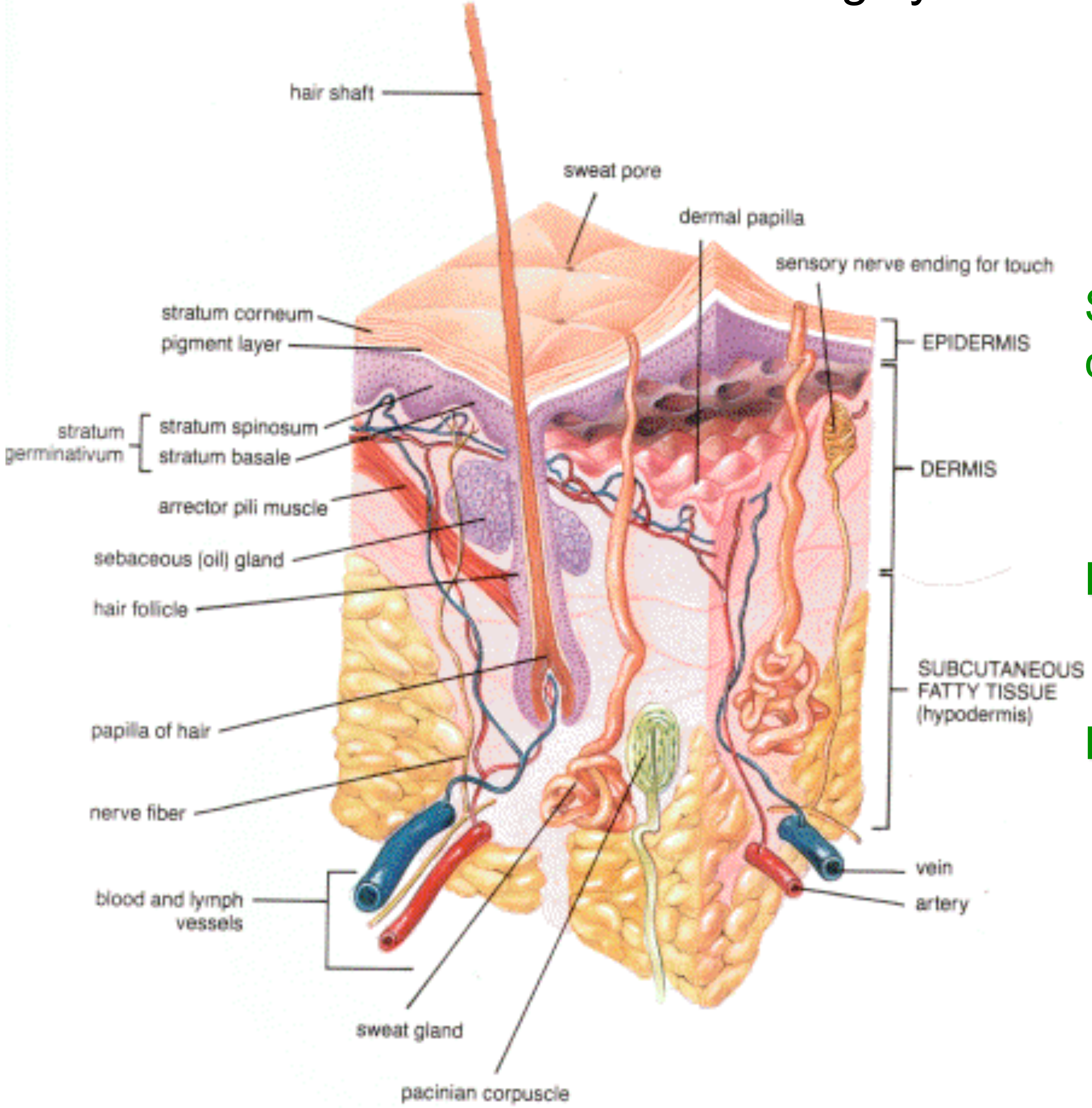

Low hydration
High impedance

Stratum corneum
- Dead cells
- Hydrophobic keratinocytes
- + skin appendages
- Thickness 10-20 µm

Epidermis
- More hydrated
- Thickness 2mm

Dermis
- Electrolytic media
- High vascularization

Skin impedance

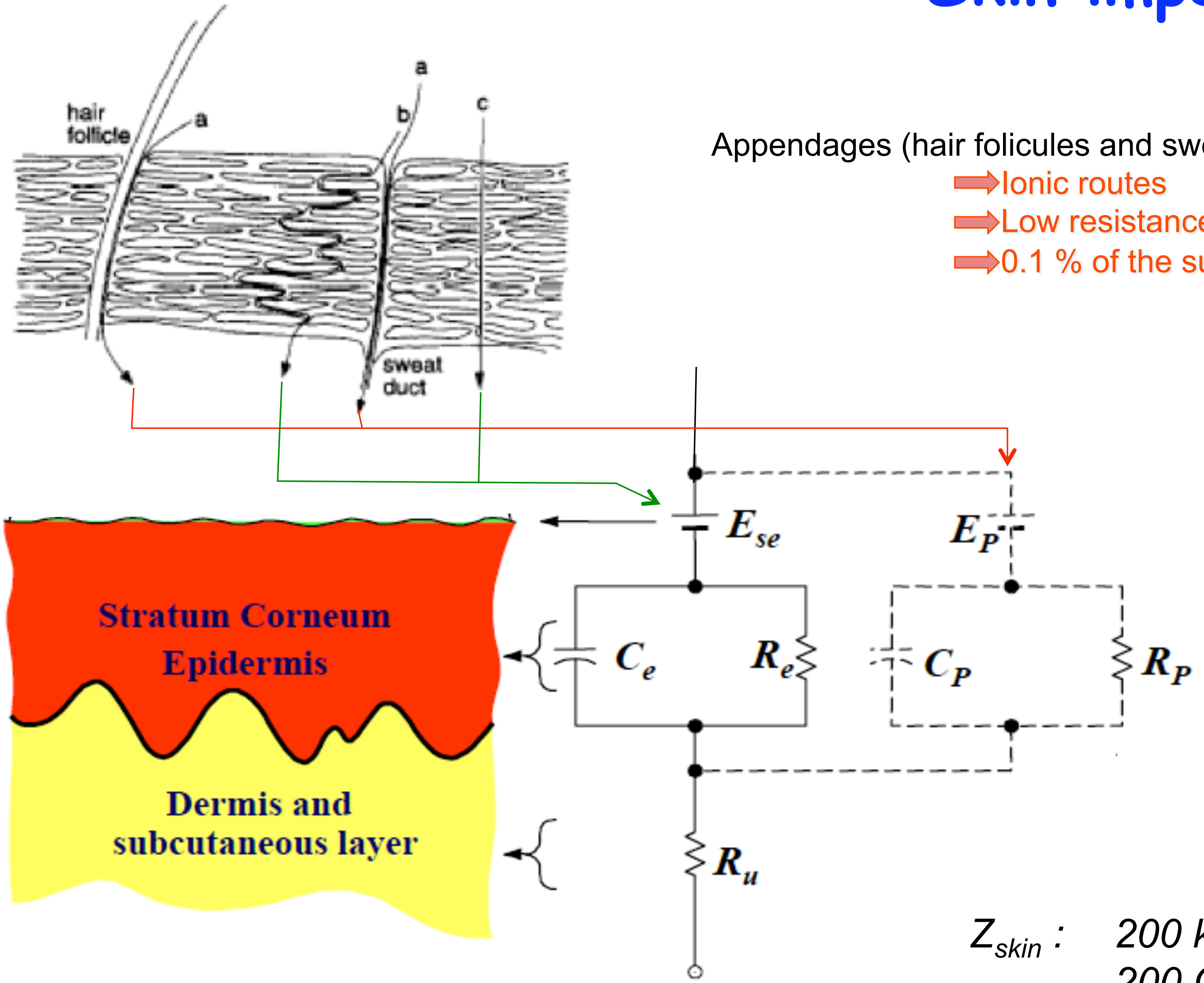

Appendages (hair folicules and sweet ducts)

- ⇒Ionic routes
- ⇒Low resistance
- ⇒0.1 % of the surface

Z_{skin} : 200 kΩ at 1Hz
200 Ω at 1MHz

Skin electrodes functionnal requirements

Contact with human body

- **B**iocompatibility associated to class I biomedical devices
  Skin iritation, sensitization
- **B**iocompatibility of Class IIA (injury, short term penetration, iontophoresis)
  Use of biocompatible materials
  No leakage of dangerous species or material degradation

Quality of the mechanical contact

- **C**onstant pressure
- **E**venly distributed pressure on the same pad or between different electrodes
- **N**o disconnection or displacement of the electrodes during measurement

→ *Motion artefacts*
Low f noise

Quality of the electrochemical contact

- **N**o drift in electrode impedance
- **L**ow interface impedance (large surface)
- **N**o corrosion of the electrode materials
- **E**venly distributed current lines (in case of high current densities)

Skin electrode impedance behaviour

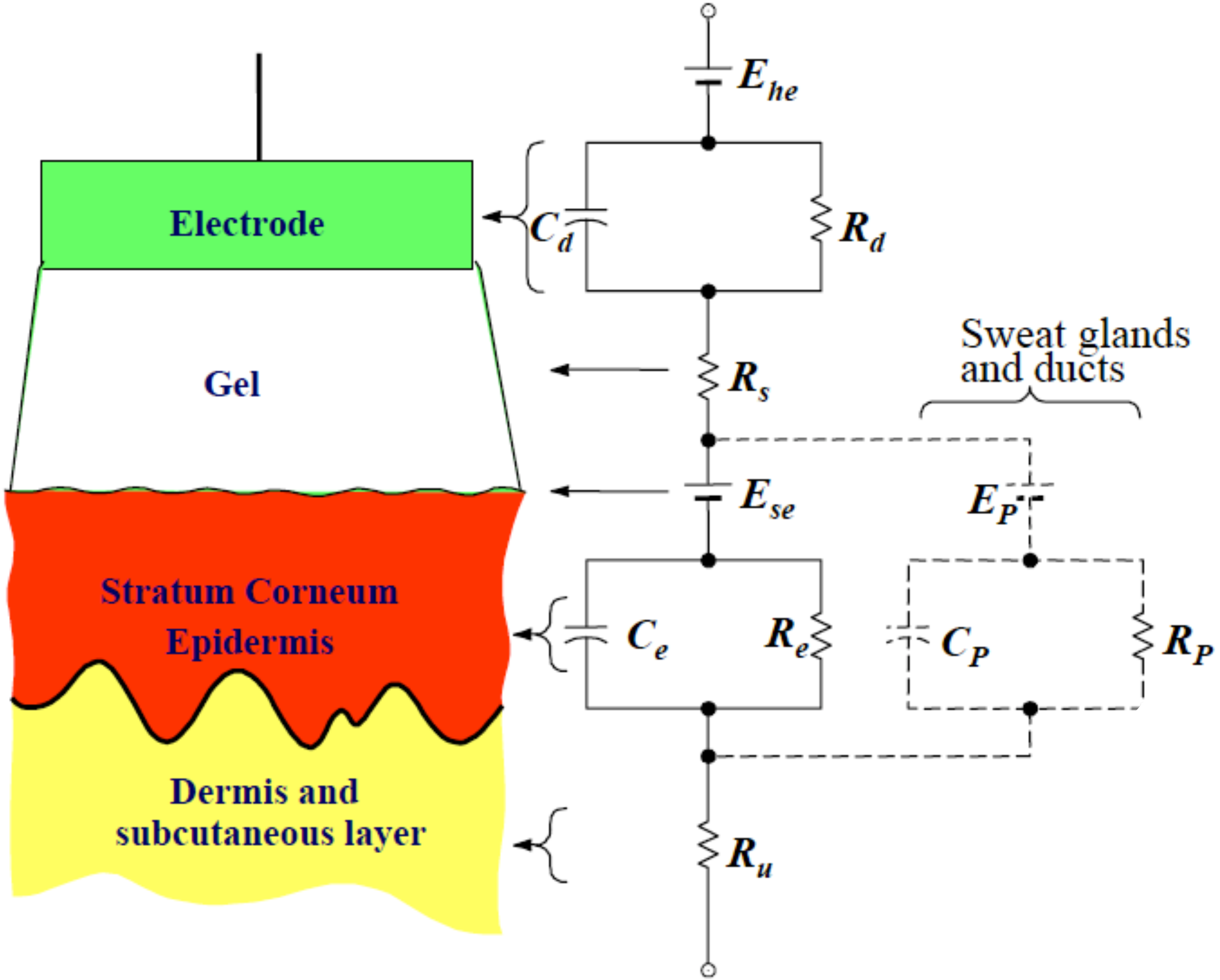

Electrode-Skin interface and hydration

Capacitance increase with hydration ratio
Skin resistance decrease with hydration
Marked influence of the ionic concentration

Essentially for NP electrodes

For NP electrodes, contact gel is required

Quality of the electrical contact
Optimized electrochemical charge transfer
Decrease of the stratum corneum resistance
Decrease of motion artefacts
Decrease influence of sweating

2 types of gels ⇨ **Viscous gels** *(contact gel)*

R_{SC} 5 à 500 Ω
High salt containt ($\nearrow C_{SC}$)
Karaya gum, Klucel….

⇨ **Hydrogel**

Highly conformable
Adhesion
R_{SC} 800 à 8000 Ω
High salt containt($\nearrow C_{SC}$)
PEG, PVP, ...

Classical FP electrodes

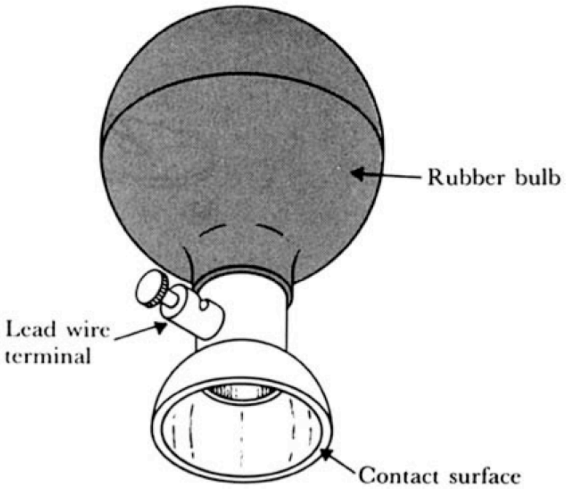

Suction electrode

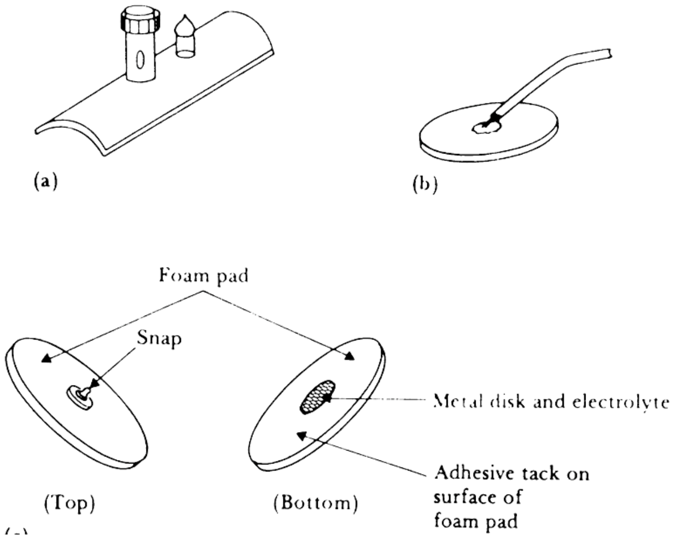

Metal pad electrodes

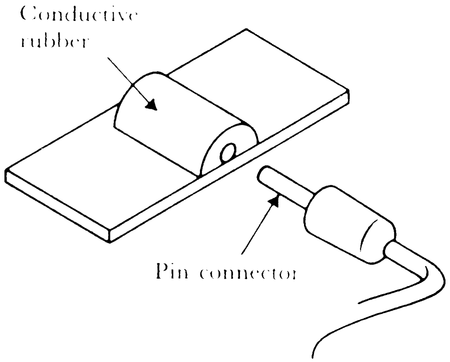

Flexible carbon-rubber electrode

Classical NP electrodes

Electrodes using contact gels (reusable)

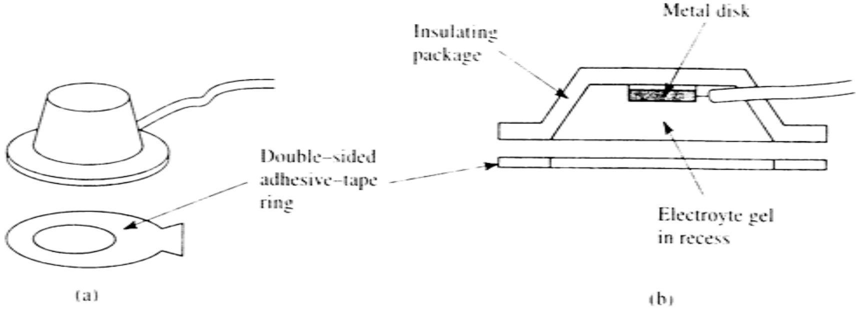

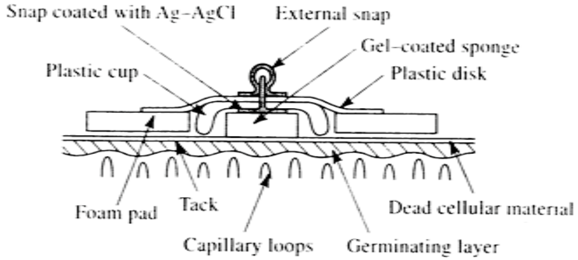

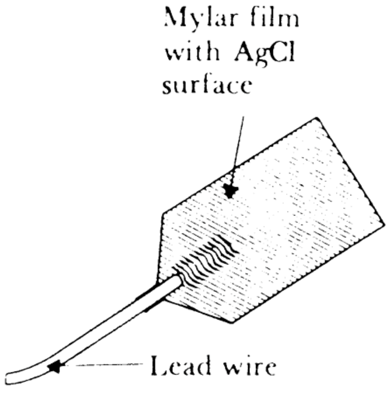

One-shot screen printed electrodes using hydrogel

Minimum configuration in bioimpedance assay

- ***Two electrodes assay***
  - **I**mpact of the cell geometry

    Current densities, field penetration depth
  - **S**ensed area

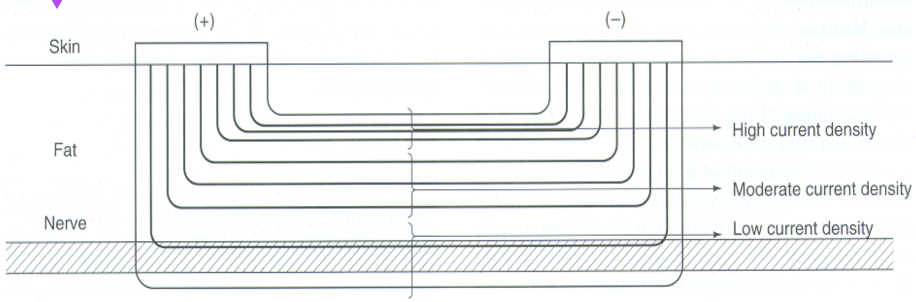

Increased electrode spacing gives rise to larger current densities in deep tissues

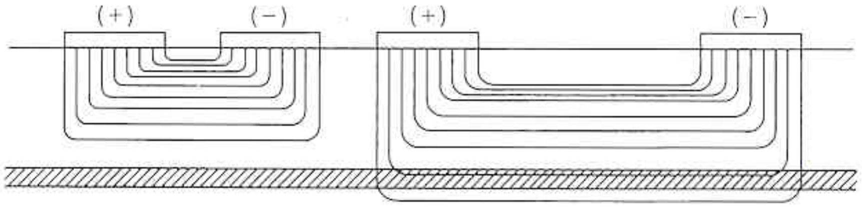

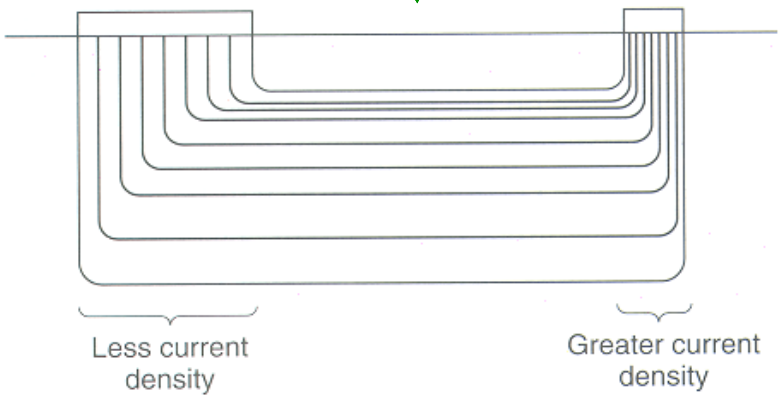

Dispersive electrode (counter electrode)

Sense electrode (working electrode)

Bioimpedance spectroscopy of blood pooling

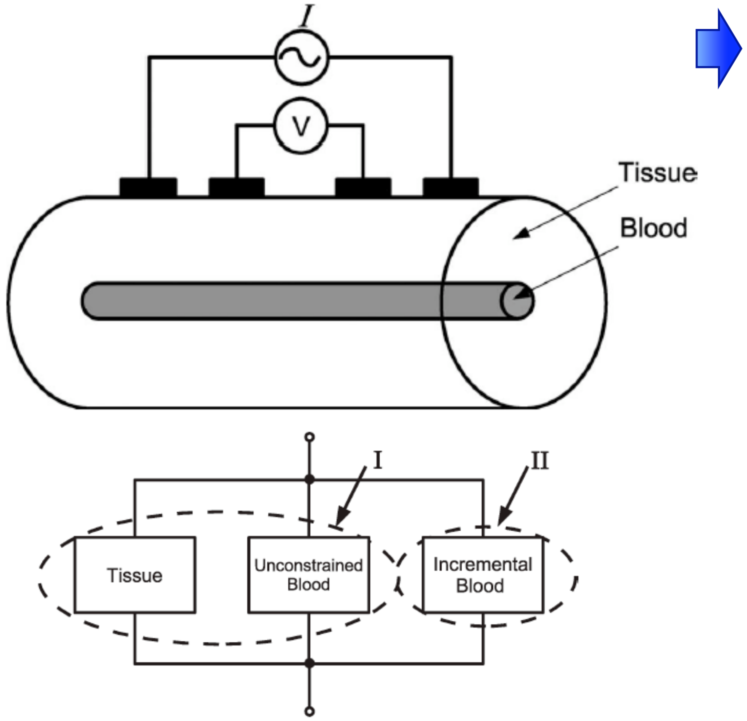

Fig. 2. In terms of the electrical structure, the measured forearm is modeled as three components in parallel. Tissue and static blood are grouped as part I (with impedance Z_{I}), whereas incremental blood is labeled part II (with impedance Z_{II}). During unconstrained status, the model is represented by part I; during blood pooling, the model is part I paralleled with part II due to the infused blood volume.

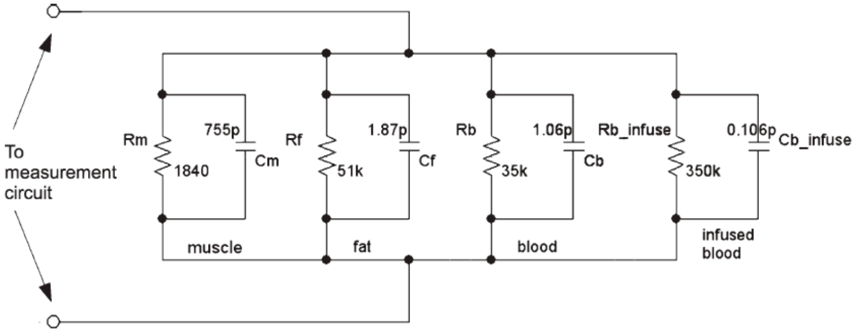

Four probes assay

- **L**imited influence of SC
- **S**ensing of blood pooling

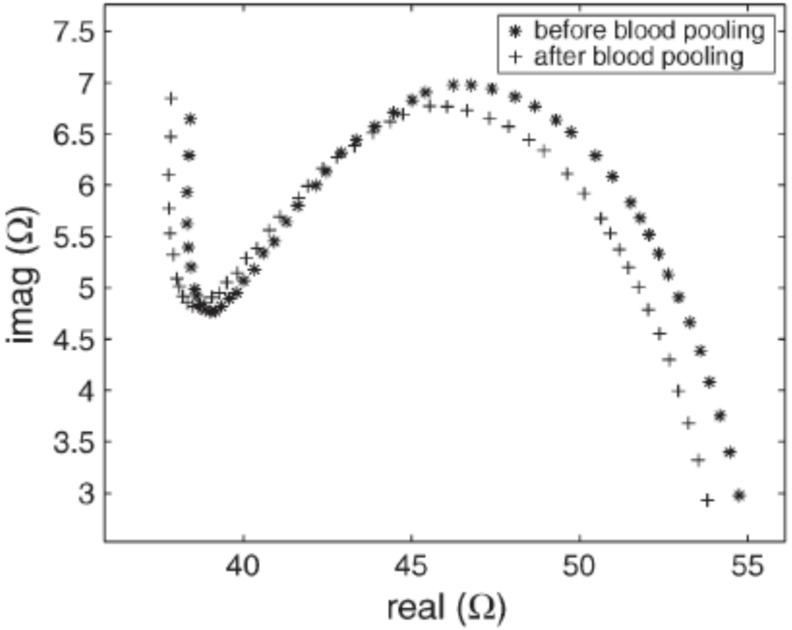

Dai et al, *IEEE Trans. Intrument. Measur. 58 (2009) 3831*

Handheld miography probe

Multiple probe system based on two concentric sqare electrodes array

- **M**easurement of neuromuscular desease
- **O**rientation of the current injection acording to muscular fibers orientatio
- **F**P gold plated electrodes fabricated on a circuit board

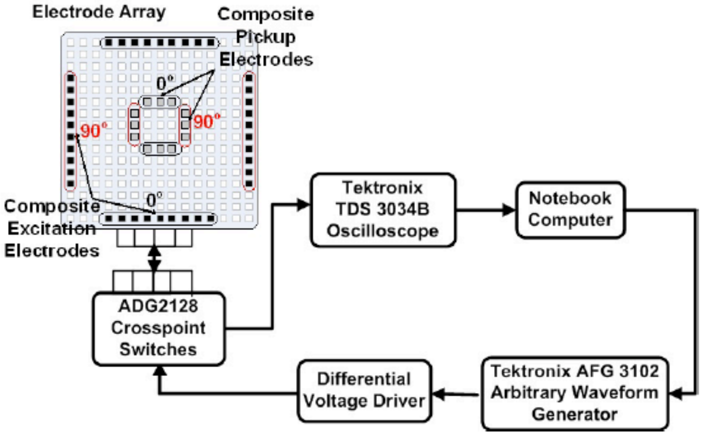

Fig. 1. Concept diagram of EIM measurement system. Electrode array shown as a rectangular array.

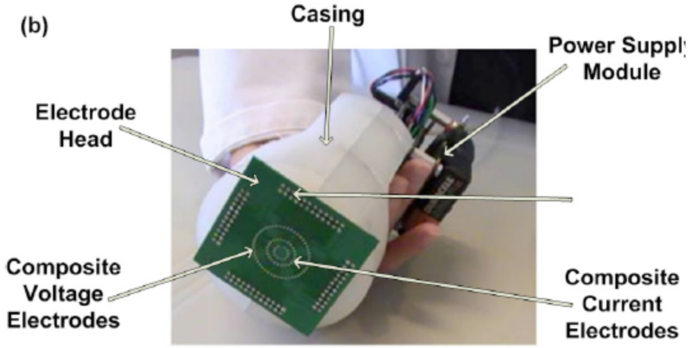

Fig. 2. (a) System diagram of reconfigurable electrode head. (b) Assembled reconfigurable electrode head with the rectangular electrode grid concept depicted in Figure 1 replaced by an array consisting of concentric rings of individual electrode elements.

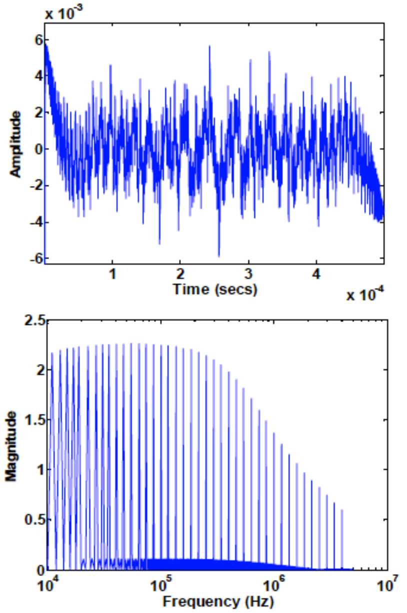

Fig. 4. Time and frequency domain plots of the input signal containing a number of tones at logarithmically spaced frequencies.

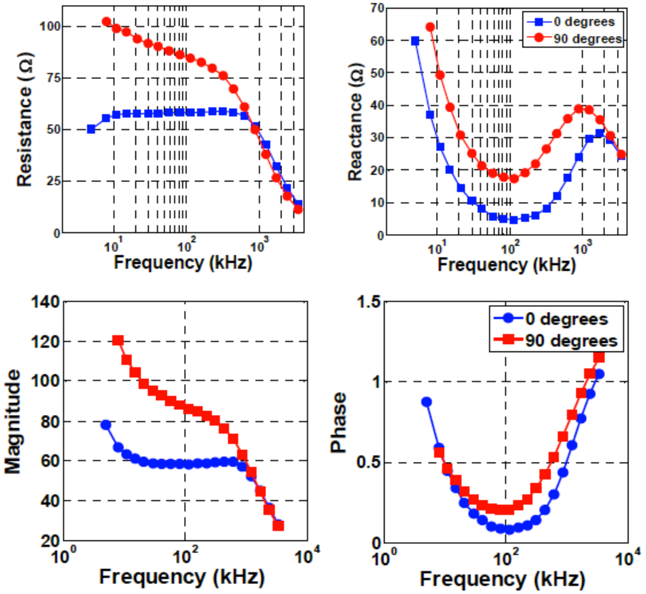

Fig. 5. Impedance plots showing the anisotropic current conduction properties of muscle tissue. The test was carried out using a piece of beef which shows clear muscle fiber bundles.

***Ogunnika et al, proceeding of** IEEE EMBS conference. (2008) 3566*

Fake fingers in biometric fingerprints

Detection of fake fingers owing to field penetration depth

- Increased injection electrodes distance
- Detection of added fake tissue due to change in impedance behaviour
- FP gold plated electrodes (no gel that may cause « short-circuit »)

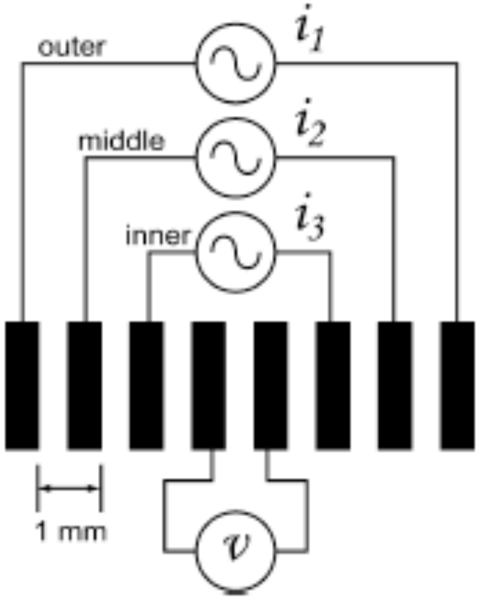

Fig. 1. Electrode array with three alternative current injecting electrode sets and one set of voltage pick-up electrodes. Electrode width and separation is 500 μm.

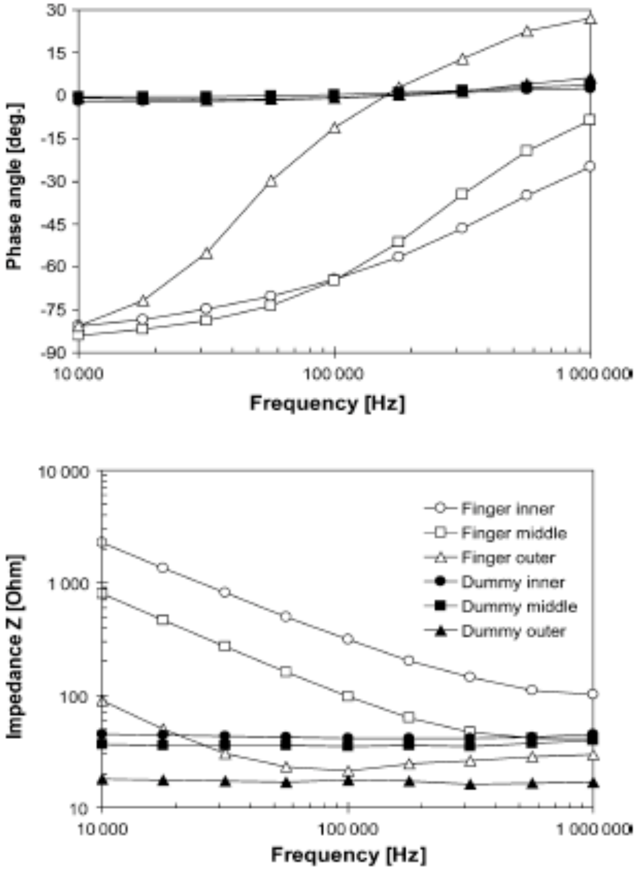

Fig. 2. Measured impedance modulus response for one live finger and "gummy" fake finger according to recipe by Matsumoto et al. [1]. Frequency range 10 kHz–1 MHz. Captions "inner, middle and outer" refer to the electrode set used for current injection (see Fig. 1).

Martinsen et al, *IEEE Trans. Biomed. Eng. 54 (2007) 891*

Handheld FP device for carcinoma detection

- ***Detection of basal cell carcinoma conversely to benign lesions and normal skin***
  - FP gold plated electrodes without gel (hand pressure)

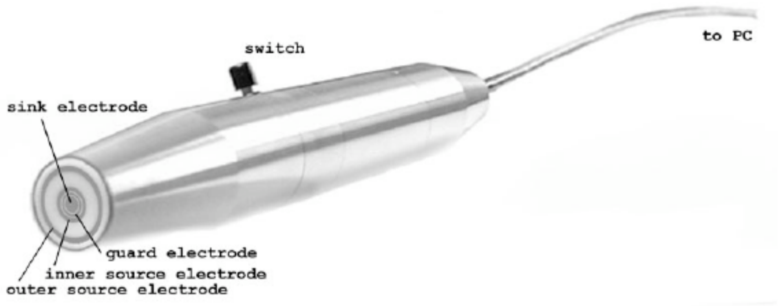

Fig. 1. Hand-held probe used to measure impedance.

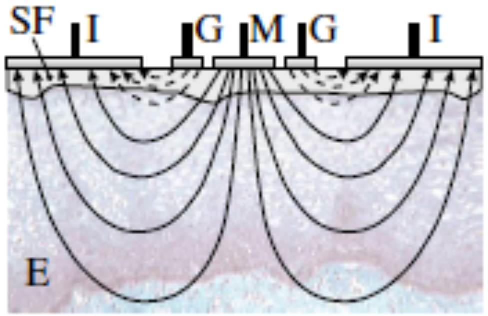

Role of the guard electrode

Depth penetration

trometer and were based on a comparison of four indexes: mag-ni (PIX), real-part index (RIX), and imaginary-part index (IMIX), defined as [11]

$$\mathrm{MIX} = \frac{abs\left(Z_{20\ \mathrm{kHz}}\right)}{abs\left(Z_{500\ \mathrm{kHz}}\right)}$$

$$\mathrm{PIX} = \arg\left(Z_{20\ \mathrm{kHz}}\right) - \arg\left(Z_{500\ \mathrm{kHz}}\right)$$

$$\mathrm{RIX} = \frac{\mathrm{Re}\left(Z_{20\ \mathrm{kHz}}\right)}{\left(Z_{500\ \mathrm{kHz}}\right)}$$

$$\mathrm{IMIX} = \frac{\mathrm{Im}\left(Z_{20\ \mathrm{kHz}}\right)}{abs\left(Z_{500\ \mathrm{kHz}}\right)}$$

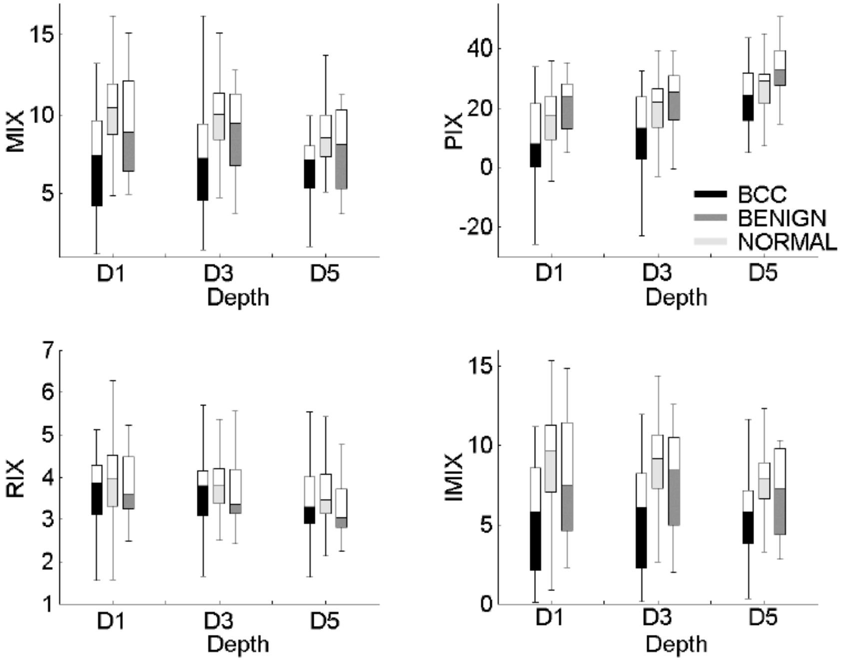

Beetner et al, *IEEE Trans. Biomed. Eng. 50 (2003) 1020*

From topical bioimpedance to treatment

- Electroporation of the bilipidic layer
- Medicine inclusion

$\Delta\mu$

Electroosmosis

Hydrophilic drug
Intra-cellular target

Topic injection of anticancer drugs (Cisplatine, Bléomycine)

Tumor treatment of superficial tissues

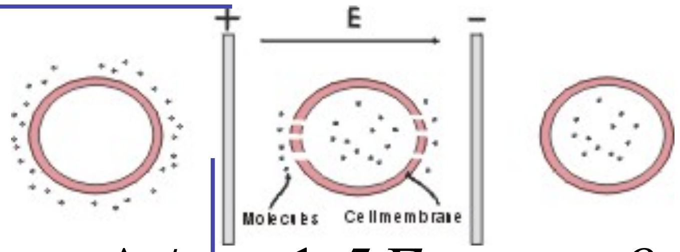

$$\Delta\phi_m = 1.5 E_{ext} r \cos\theta$$

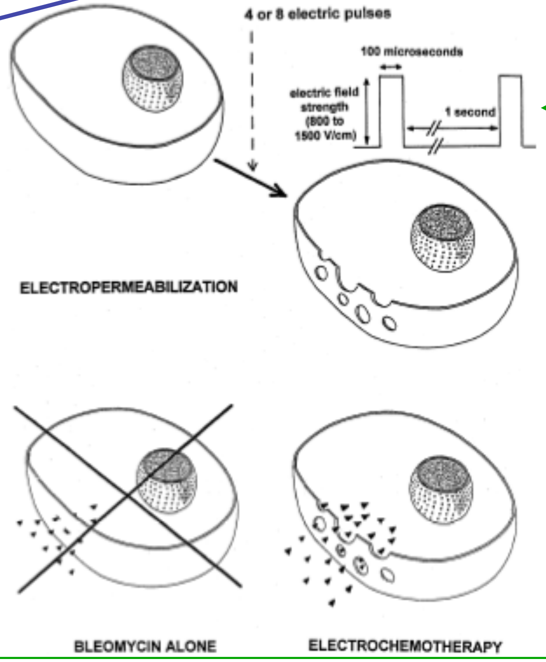

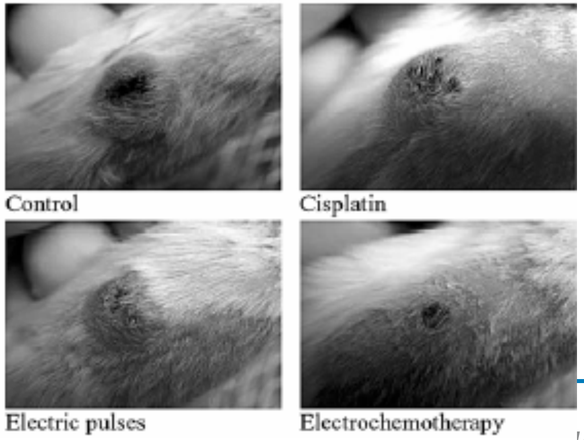
Control
Cisplatin
Electric pulses
Electrochemotherapy

Tumor treatment using Bleomycine
- 4-8 pulses of 100 µs, f = 1Hz
- 1000-1500 V m^{-1}(skin), 800 V m^{-1}(mucous)

L. Mir et al, *Bioelectrochem. Bioenerg 38(1995) 203*

L. Mir et al, *Advanced Drug Delivery Reviews 35 (1999) 107*

Topic electrochem treatment of cancer cells

Cliniporator *L. mir et al.*

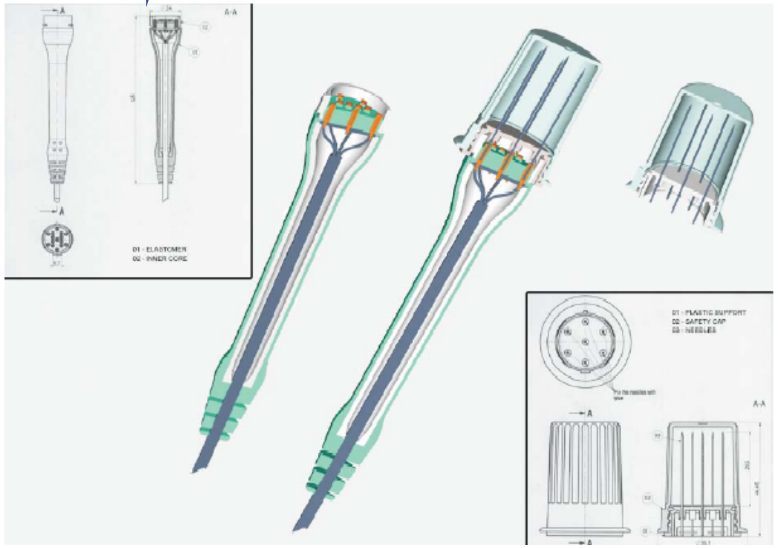

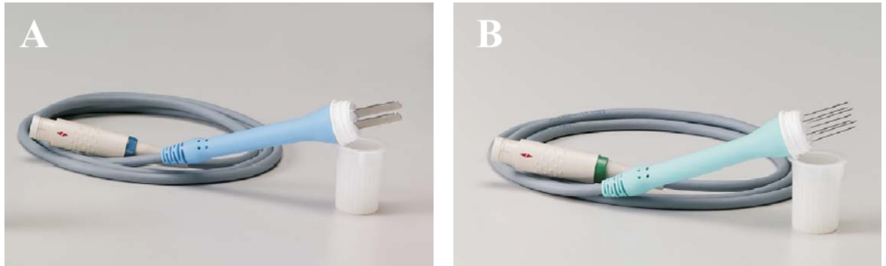

FP stainless steel electrodes

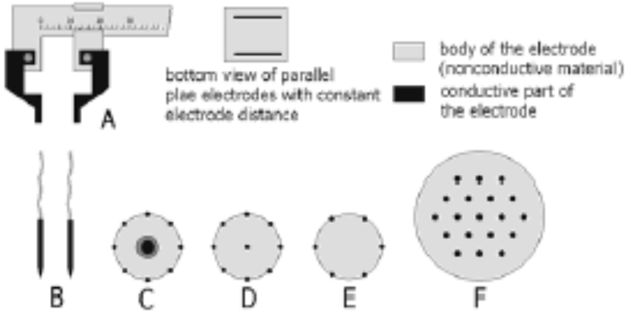

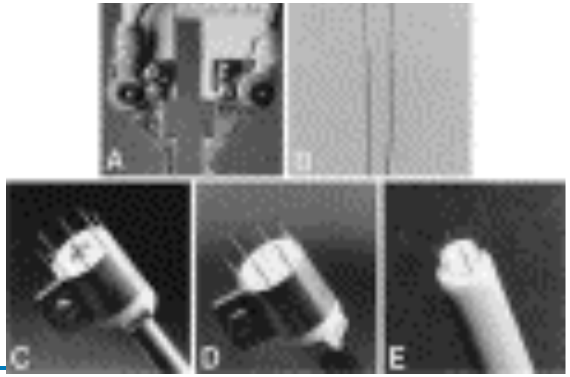

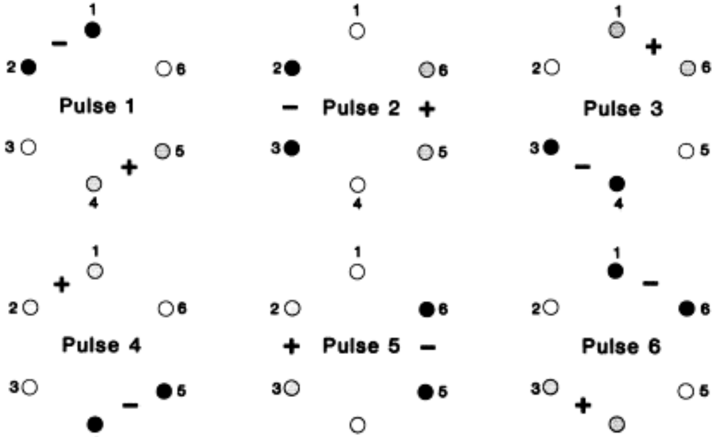

Bipolar electrodes
Sequentially activated by pairs

R. Heller al, BBA *1334 (1997) 9*

Dry minimaly invasive NP electrodes

Detection bioelectric signal with NP dry electrodes

- **N**P IrOx penetrating electrodes
- **M**inimize motion artefact and stratum corneum impedance
- **P**ossible generation of multielectrodes array
- **N**o risk of gel short circuit

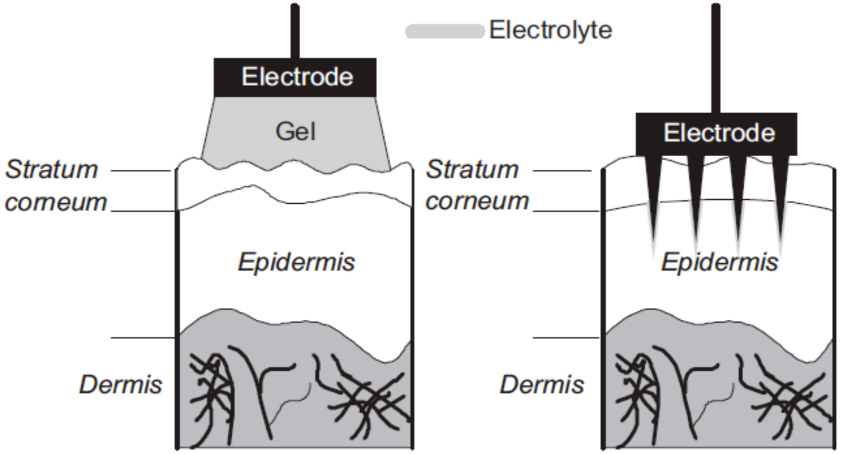

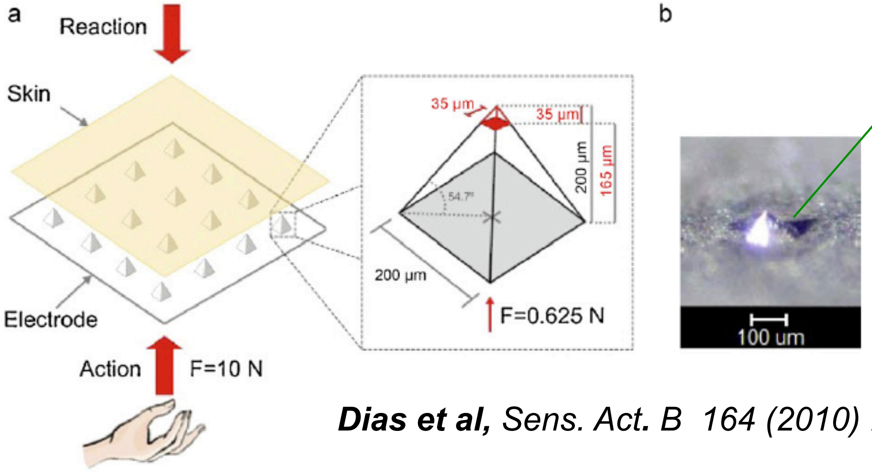

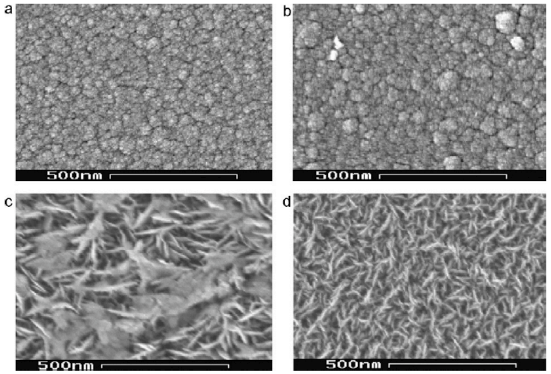

SEM images of IrO thin-film surfaces deposited at different oxygen flows: (a) 2 sccm; (b) 3.5 sccm; (c) 6.5 sccm; (d) 10 sccm.

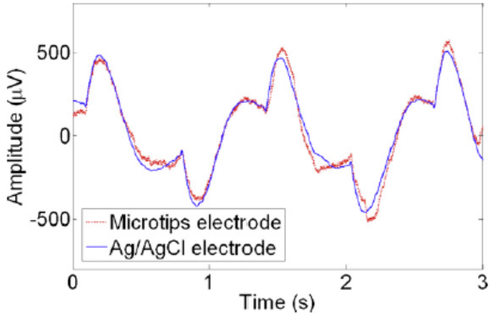

Fig. 11. Time-domain recorded signals from both the control Ag/AgCl electrodes (blue solid line) and the microtips electrode with IrO coating (red dashed line) during an EOG experiment. (For interpretation of the references to color in this figure legend, the reader is referred to the web version of the article.)

Dias et al, *Sens. Act. B 164 (2010) 28*

Impedance tomography

Xray section image from thorax
Calculated current lines repartition (blue)
between 2 electrodes within the thoracic cage
submitted to bending associated to conductivity
change

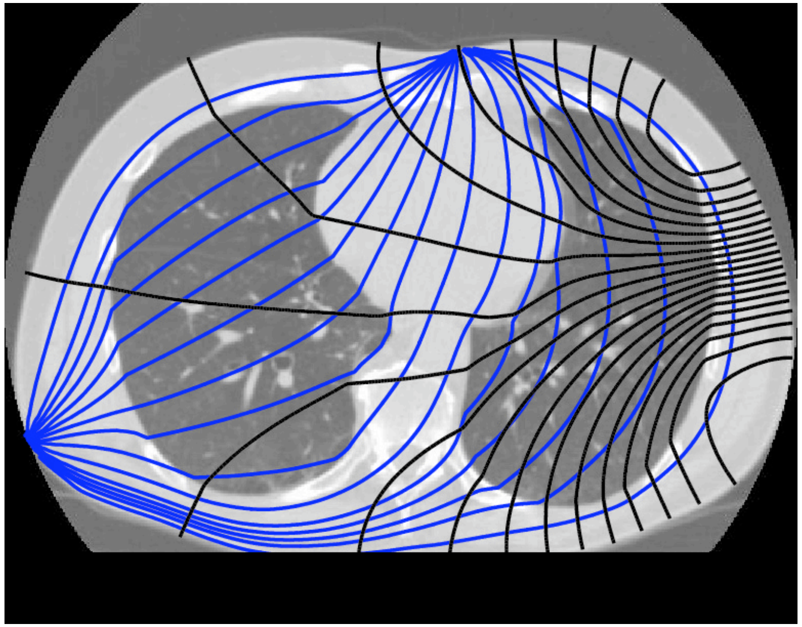

Tomographic impedance image reconstructed
from sequential mesurements between varying
pairs of electrodes

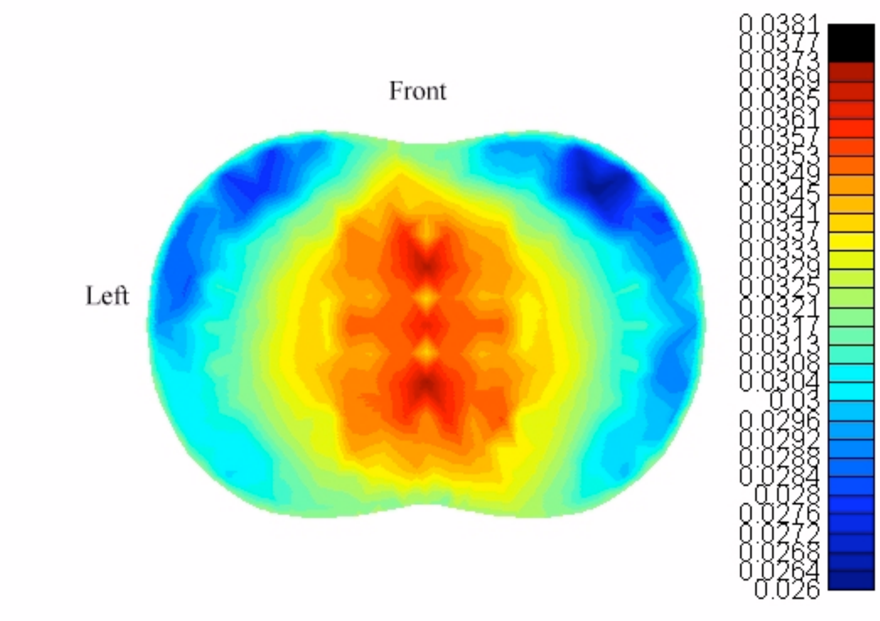

➡ ***Detection/imaging of tumors , fat, respiratory process, haemoragic strokes…***

Breast cancer detection

Non invasive and predictive detection of breast cancer using FP electrodes array

- **C**omplementary to X-Ray mamography (80 % false positive)
- **M**odification of electrical behaviour in the tumor
- **H**igher permitivity (Cm decrease) and higher resistance
- **C**urrent line bending due to local modification of conductivity
- **1** pair of injection electrodes, n pairs of probes (sequentially moved)

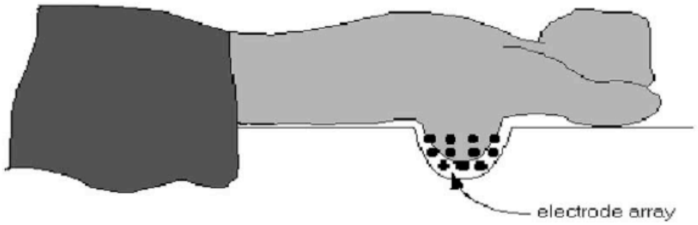

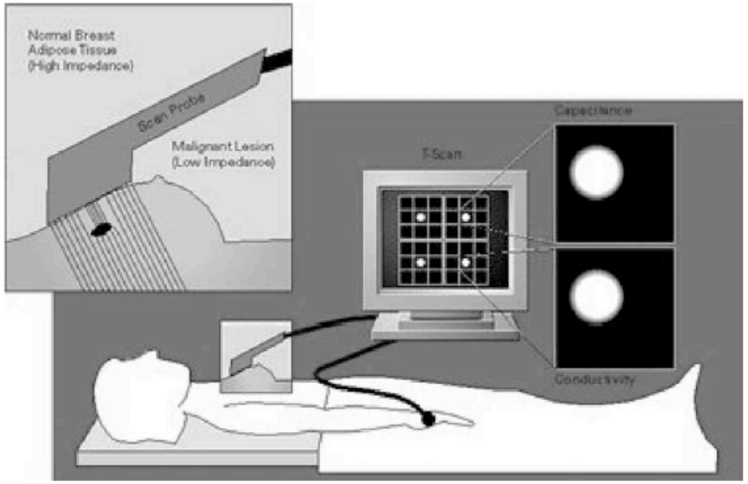

Breast maping using the commercialy available T Scan 2000 device

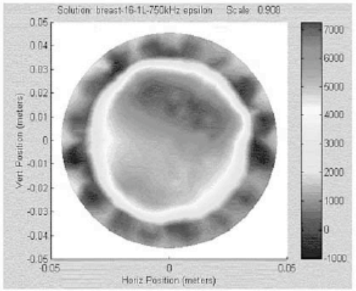

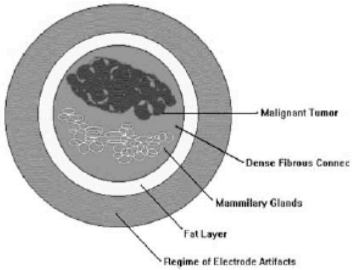

Low sppatial resolution
Penetration depth (3.5 cm)
Uncontrolled echanical pressure
Contact artefact of some FP electrodes

Zou et al, *Med. Eng. Phys. 25 (2003) 79*

Human abdominal fat imaging

Non invasive tomography of fat tissues (viceral fat)

- **M**echanical design to ensure reproducible skin connection
- **F**P electrodes in stainless steel (32 probes)
- **A**pplied stimulus 1mA rms 500 kHz

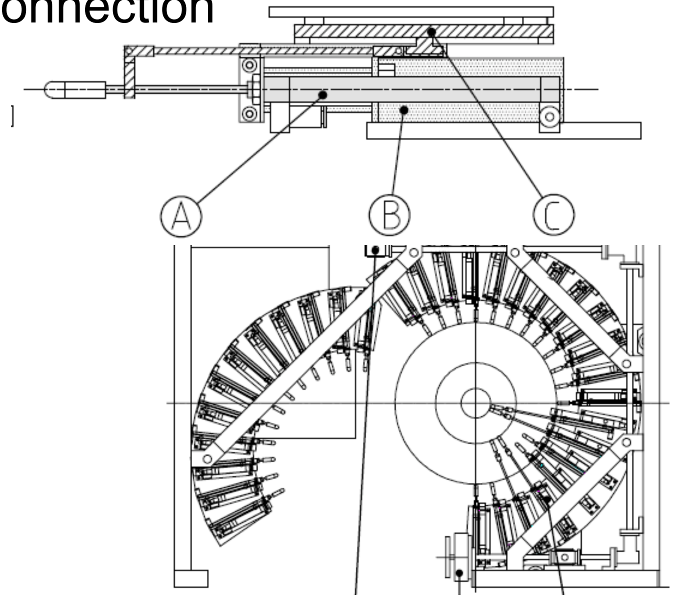

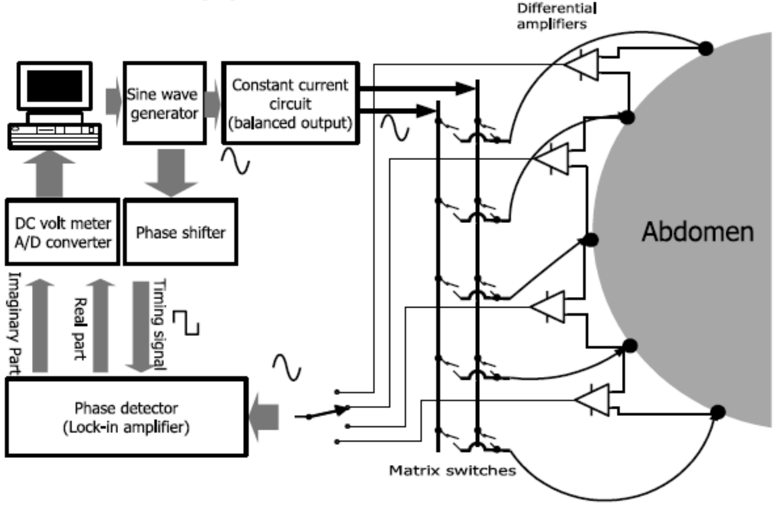

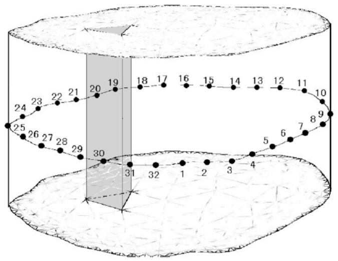

Figure 4. Schematic drawing of the model abdomen. Each of the triangular prisms was assumed to have the same conductivity.

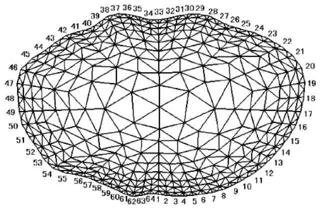

Figure 5. Discretization in the cross-section of the abdomen for the finite element method.

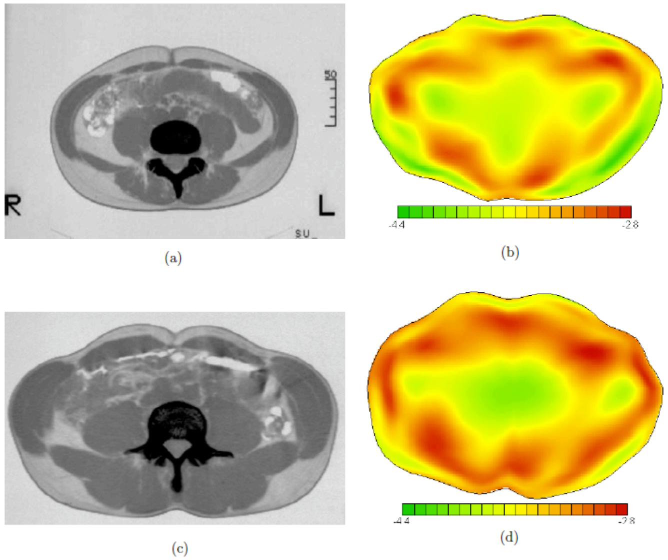

Yamaguchi et al, *Physiol. Meas.315 (2010) 963*

PEDOT NP electrodes for tomography

Dry NP electrodes

- Redox behaviour ensured by PEDOT doping
- Good skin contact and low noise

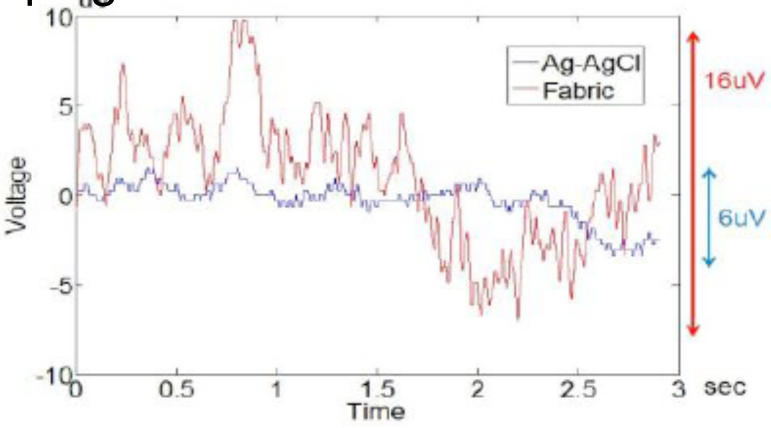

(a) Fabric coated PEDOT (b) PEDOT fiber (×50,000 magnification)

Figure 1. Fabric material for a button-type dry electrode.

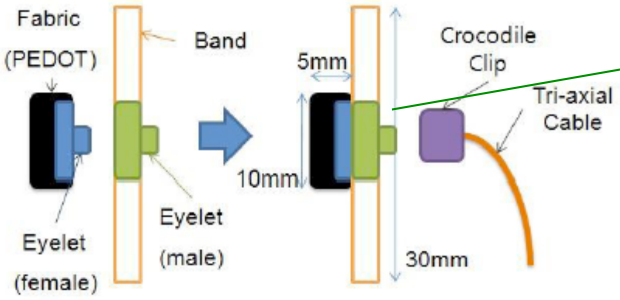

Figure 4. Button electrode design.

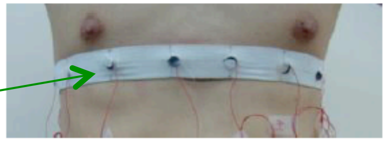

Figure 9. Electrode belt around the human chest.

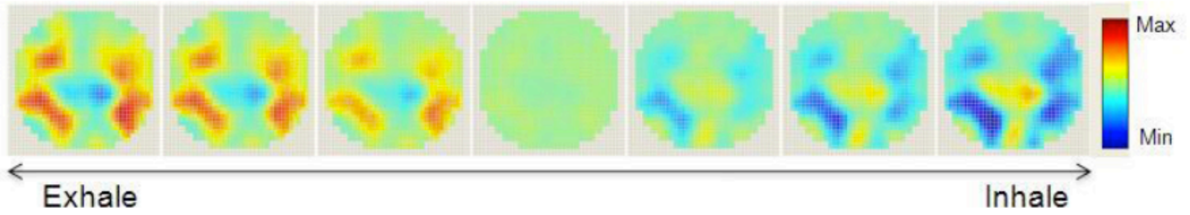

Figure 10. Time-difference images of the human chest using the electrode belt.

Bi **Wi et al,** *J. Phys. : Conf. Series 224 (2010) 012006* ic

Transdermal drug delivery : iontophoresis

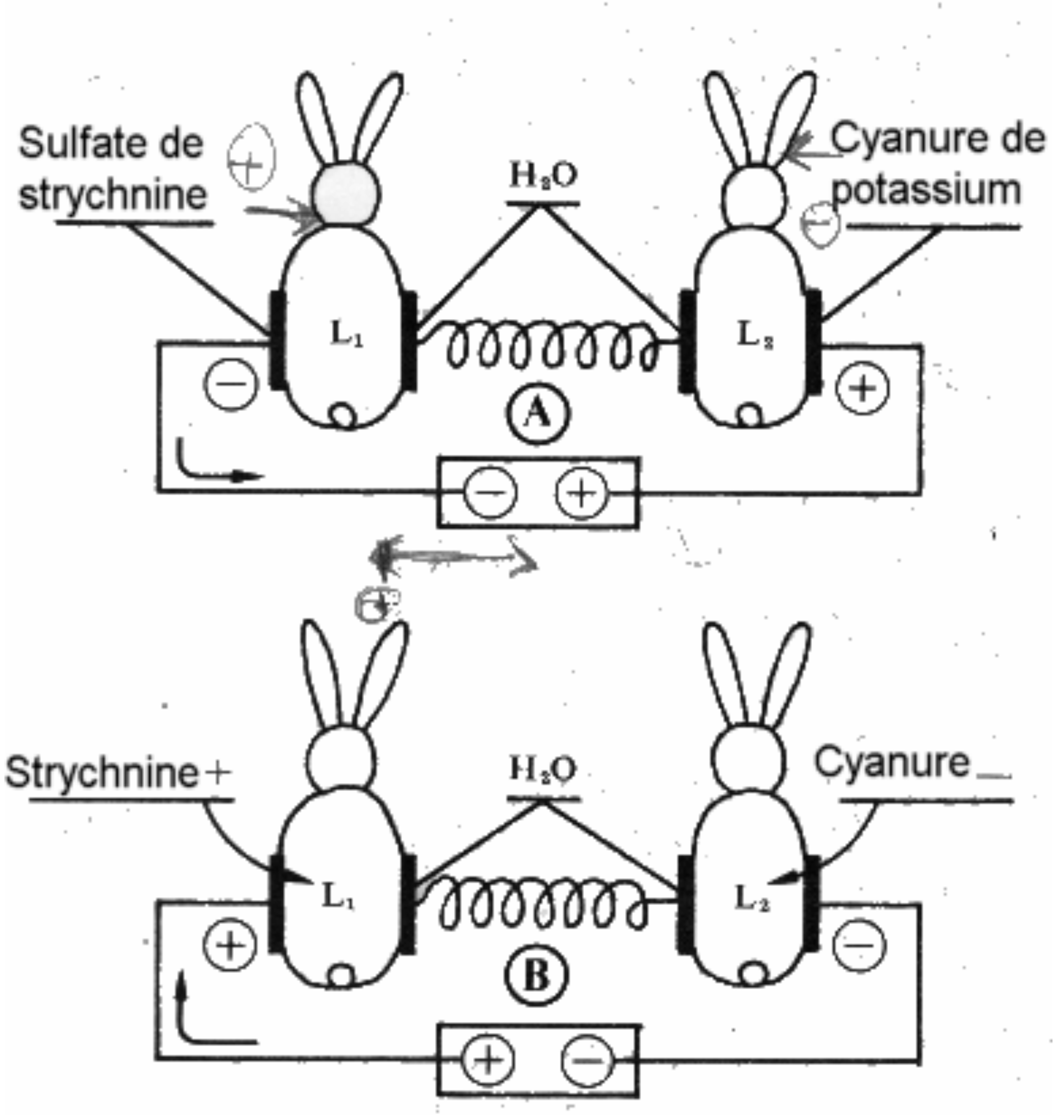

- Pivati 1747
- Leduc 1900

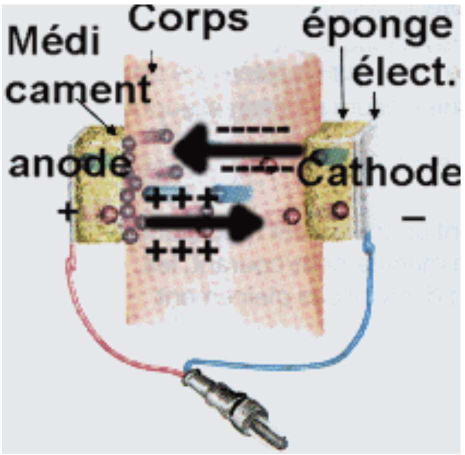

Iontophoresis mechanism

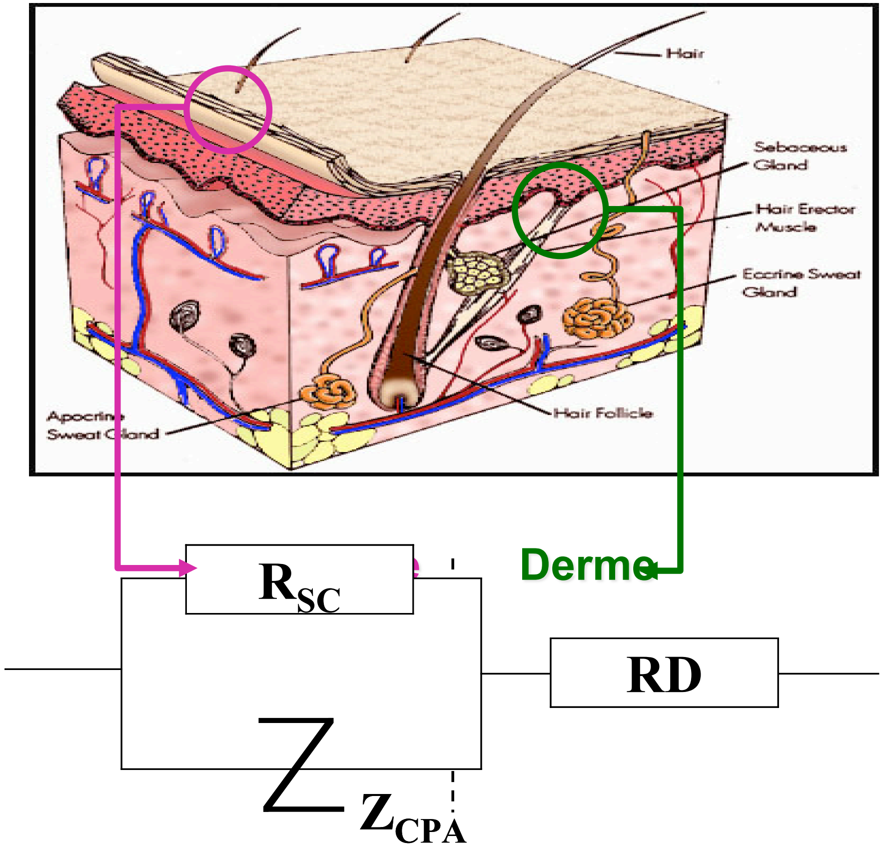

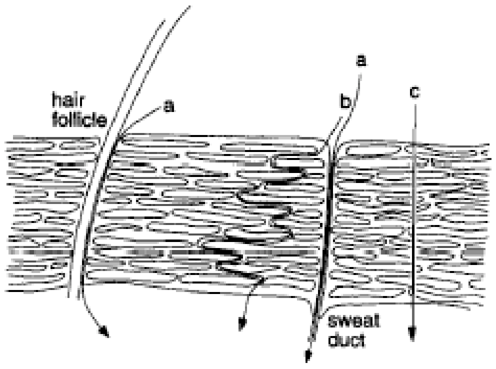

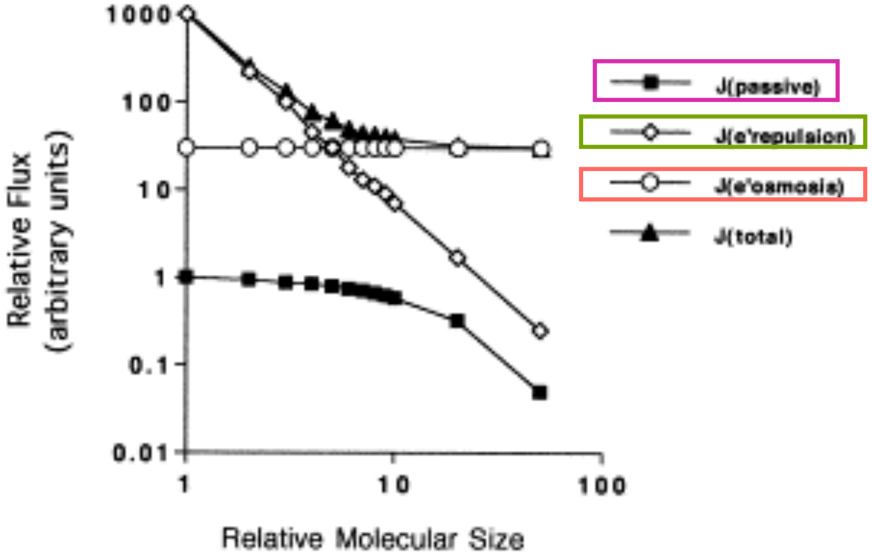

Nernst Einstein

$$\vec{J}_i = -D_i.\vec{\nabla}C_i - z_i u_i C_i F.\vec{\nabla}E + C_i\vec{v}_f$$

Diff. *Mig.* *Conv.* → Electroosmosis

$$J = \varepsilon\left\{-HD\left[\frac{dC}{dx}+\frac{CzF}{RT}\frac{d\psi}{dx}\right]\pm WvC\right\}$$

ε : tortuosité-porosité de l'épiderme
H : interaction peau / mouvements brownien et migratoire
W : interaction peau / flux convectif

Electrode design and lifetime

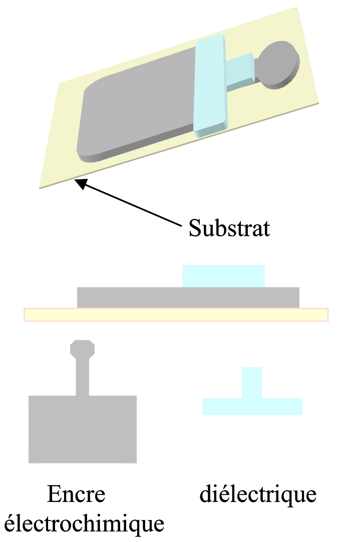

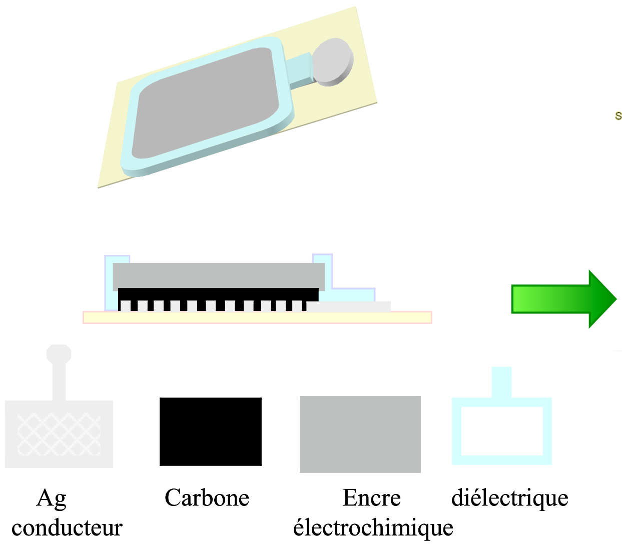

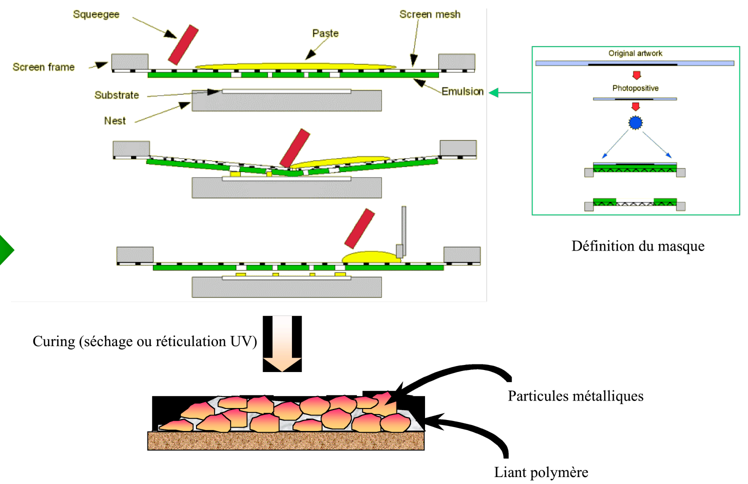

Principe de la sérigraphie

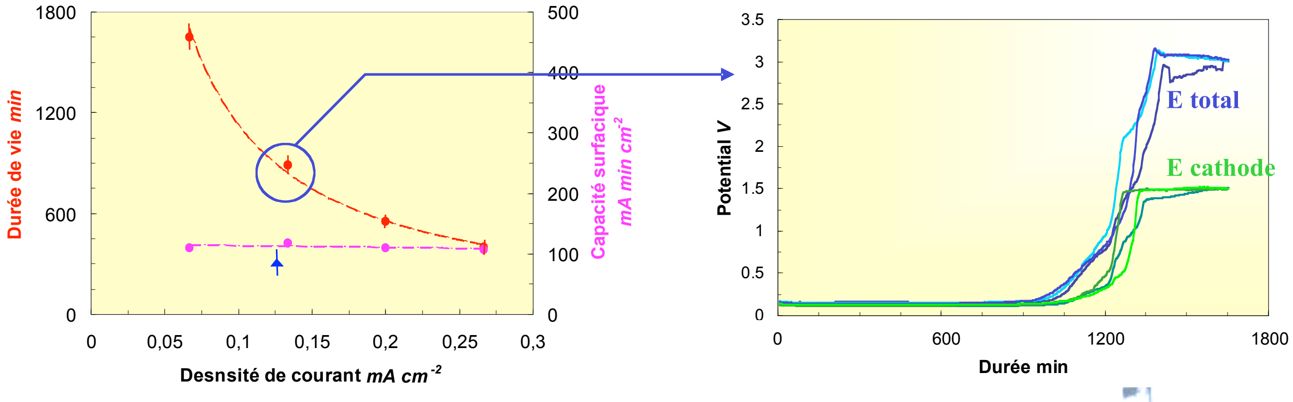

Durée de vie

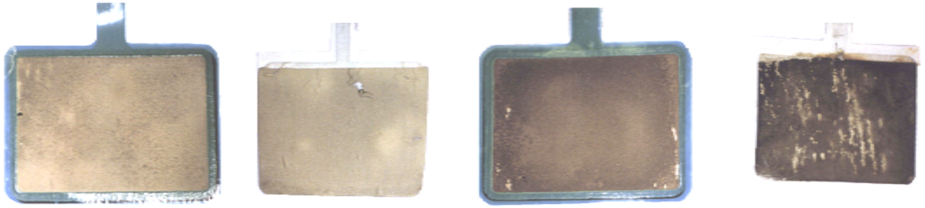

Electrode materials

Electrical capacity

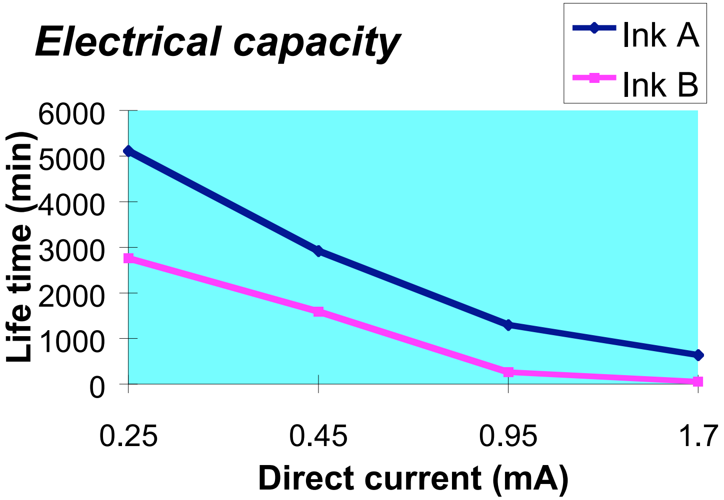

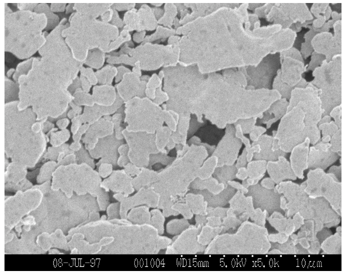

Acheson PM406

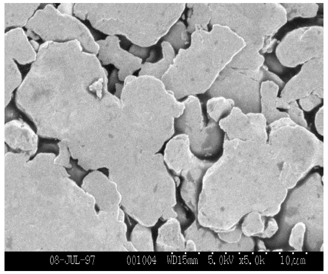

Acheson PM403

Potentiodynamic curve

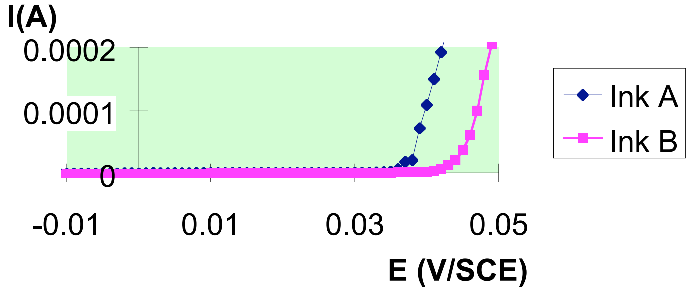

Impedance characterisation

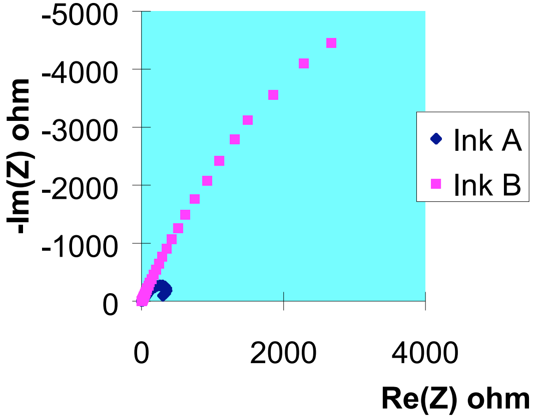

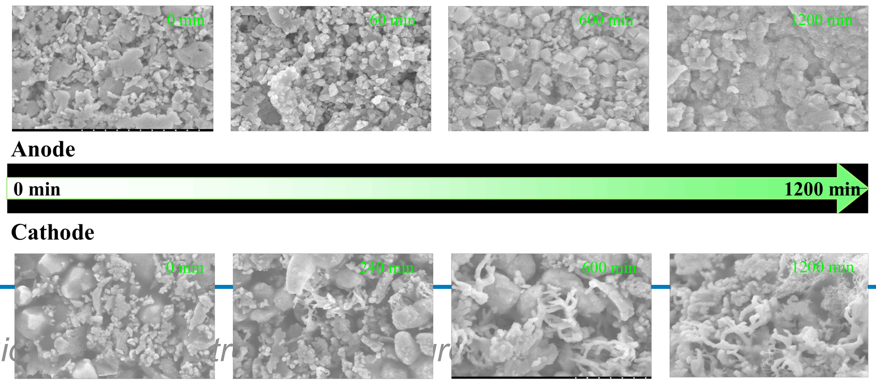

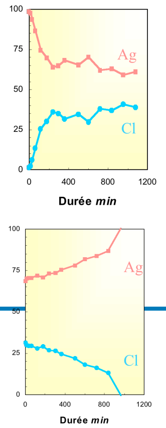

Iontophoresis device design

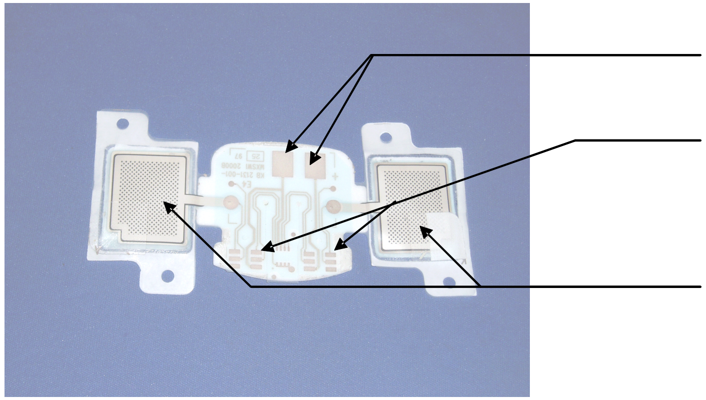

Connecteurs pile

Connecteur générateur de courants

Electrodes

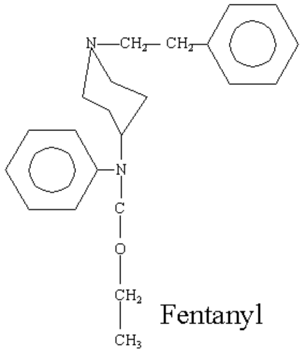

Fentanyl

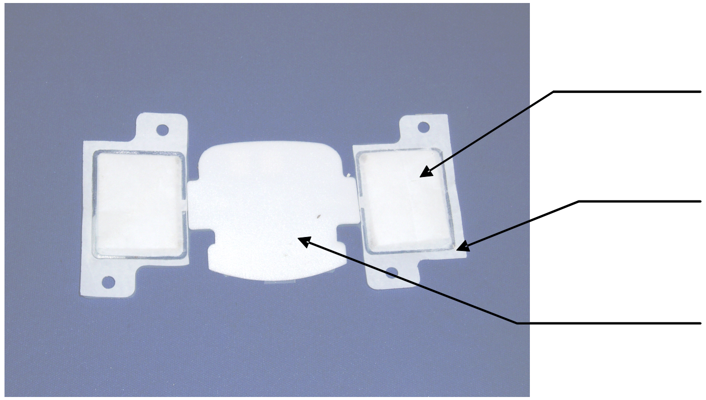

Réservoir recouvert d'une membrane de maintient

Scellage de la membrane

Mousse adhésive double face

- Therapy duration
- Current repartition
- Device size
- Complex electronic
- Process

Design evolution

In vivo degradation of the anode ?

- Polarity inversion
- Pulsed signals in place of DC
- Ring regeneration electrode...

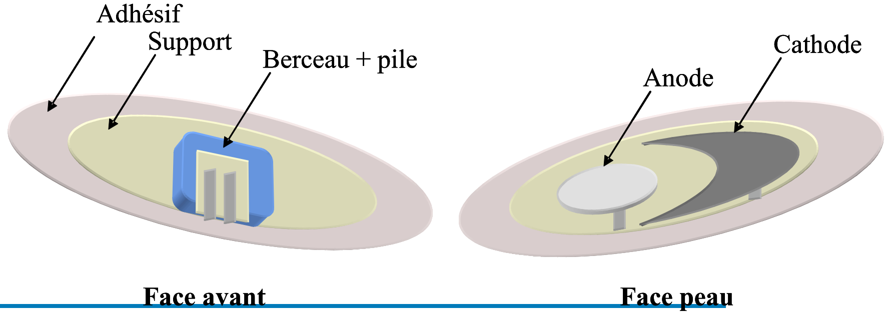

QUELQUES SYSTEMES EXISTANTS

- Traitements topiques (analgesie locale, anaesthesie locale)
  - Phoresor de IOMED (electrodes TransQ)

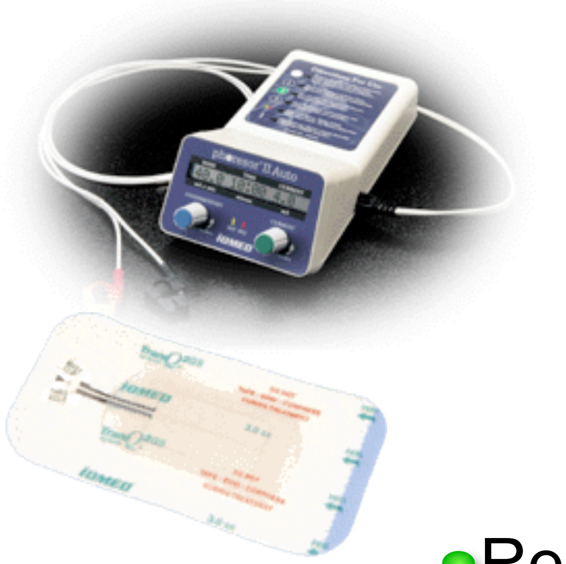

  - ADIS de Advance

  - Relion de TM Systems (applications veterinaires)

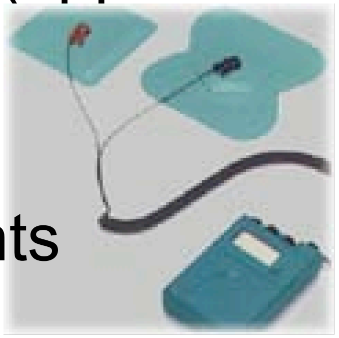

- Pas de systemes pour des traitements systemiques longs
  - Diabete, douleur chronique ou post-operatoire, hormonotherapie.

1.3.2- IONOPHORESE INVERSE

- Extraction du glucose par voie electroosmotiq
  - Dosage non invasif du taux de glycemie
  - Mesure continue en temps reel

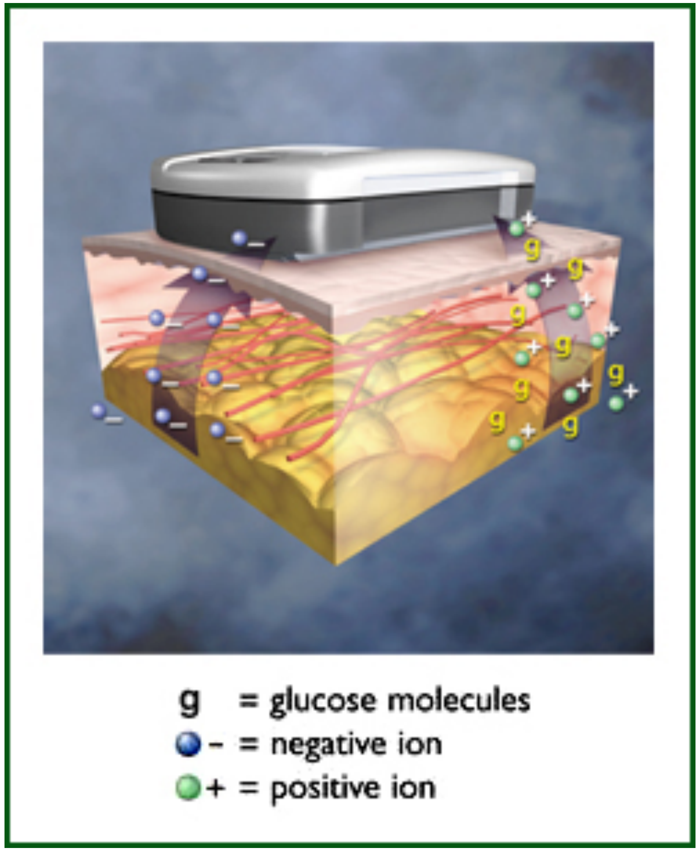

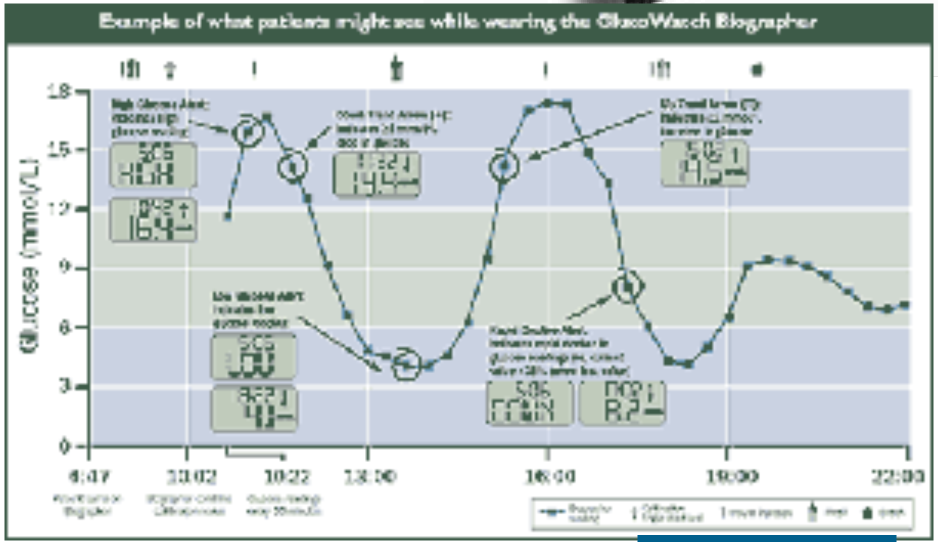
Example of what patients might see while wearing the GlucoWatch Biographer

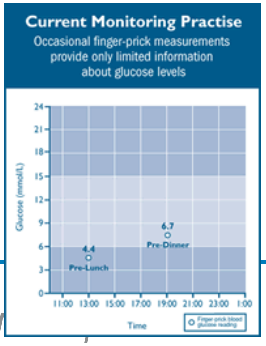
Current Monitoring Practise

Occasional finger-prick measurements provide only limited information about glucose levels


The G2 Biographer

Frequent glucose readings provide trend information to help identify opportunities for improved control

Cygnus Intl., Becton-Dickinson

F-
Biomedical electrodes and neuroprothetic

F.2- Implant electrodes for nerve stimulation

Functionnal neurostimulation: Cuff electrodes

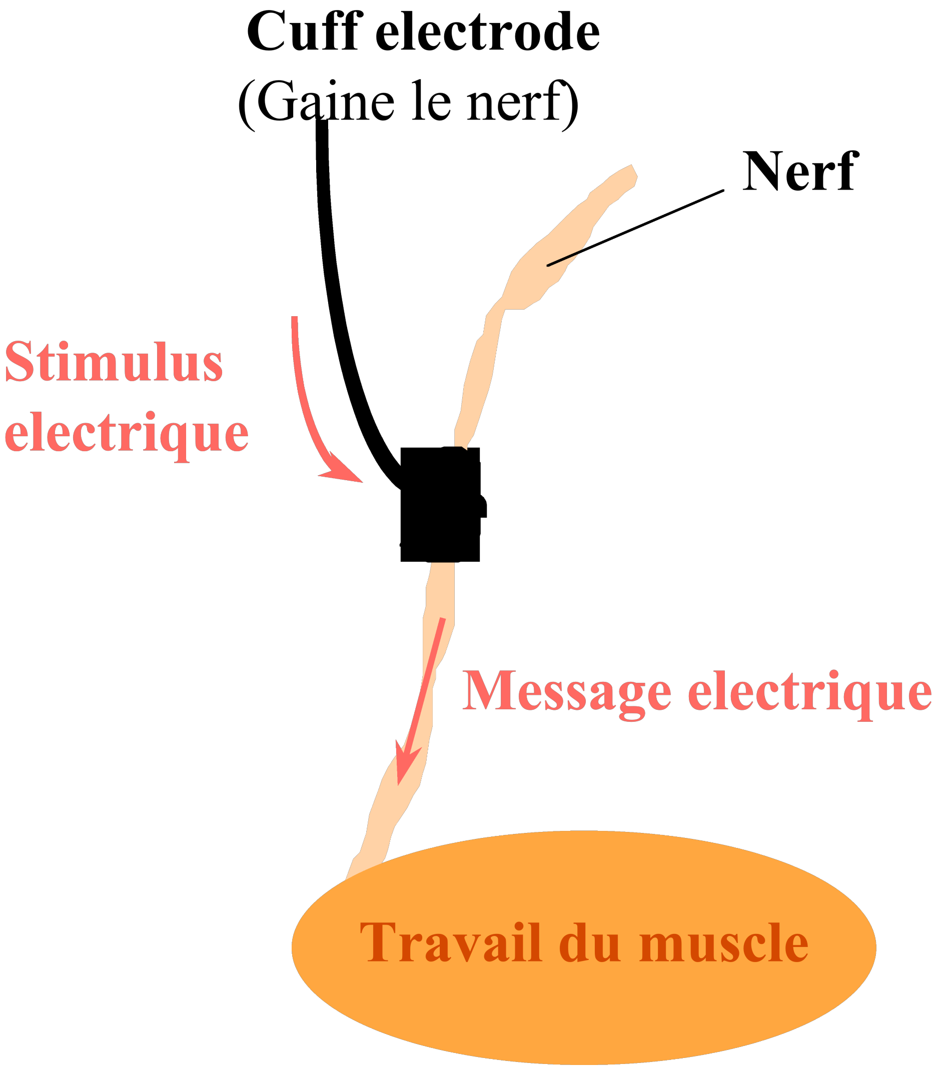

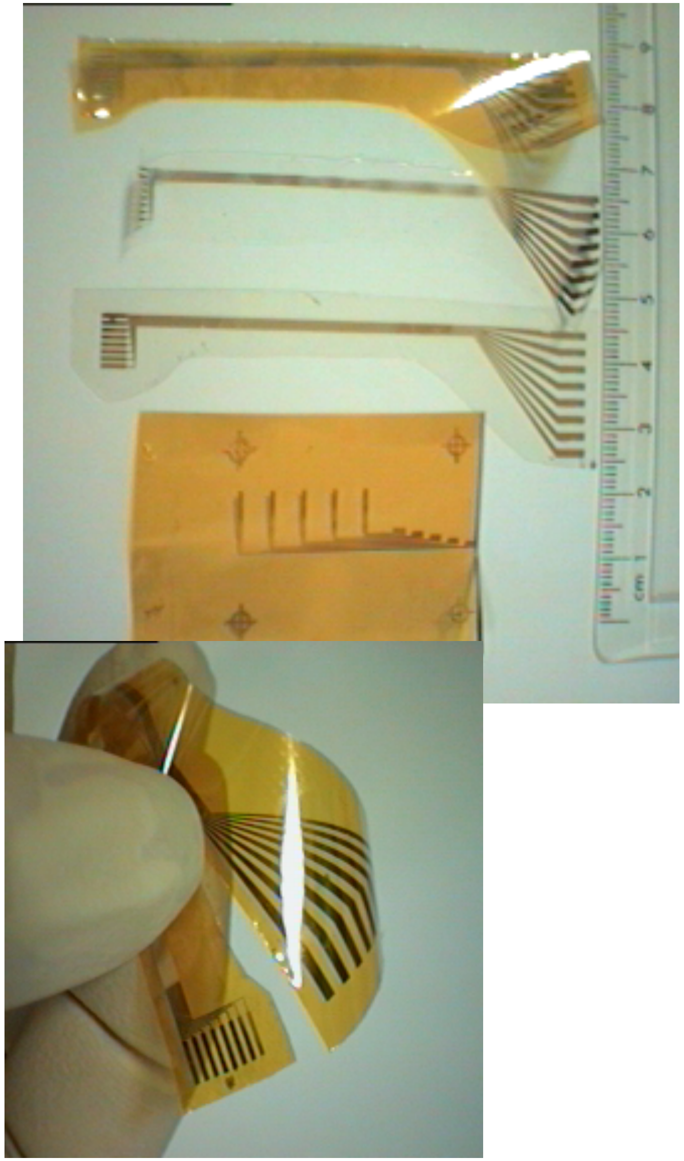

Mailley et al,, Mat Sci. Eng C, 21 (2002) 167

Functionnal neurostimulation: Cuff electrodes

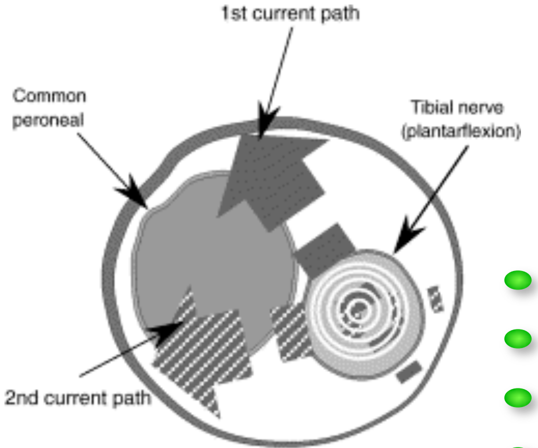

Cross section of sciatic nerve

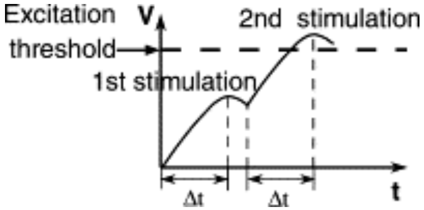

- Bipolar electrodes(paires)
- 2 application directions
- Current sequences
- Selective excitation

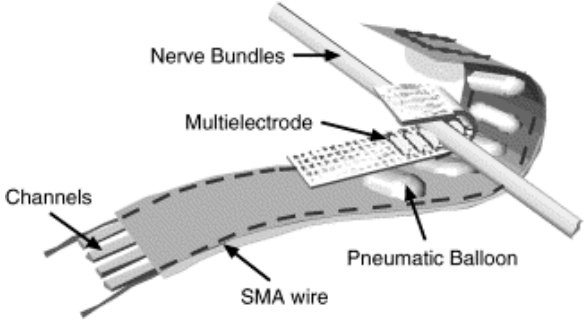

Process of fabrication

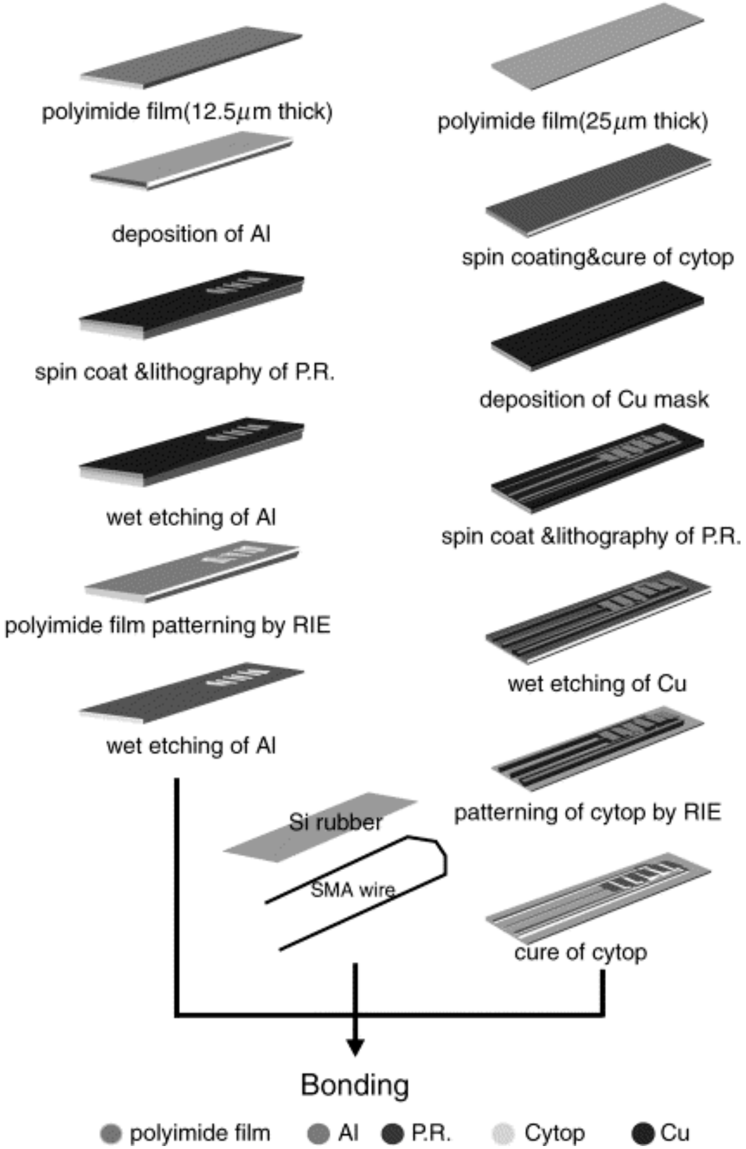

Mechanical contact on the nerve

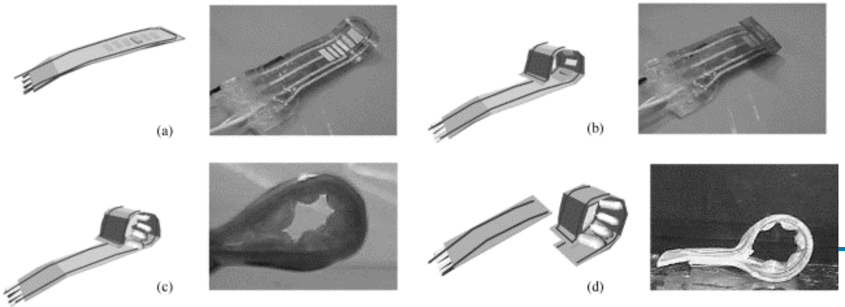

Konishi et al, Sensors & Actuators B, 83 (2002) 60

Functionnal neurostimulation: intraneuronal electrodes

Array of 128 needles
Silicon/Ir/SiO2
LIGA technology

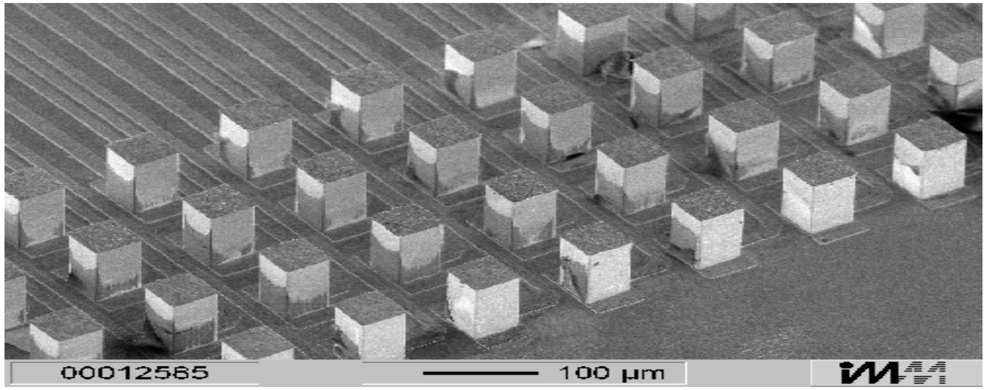

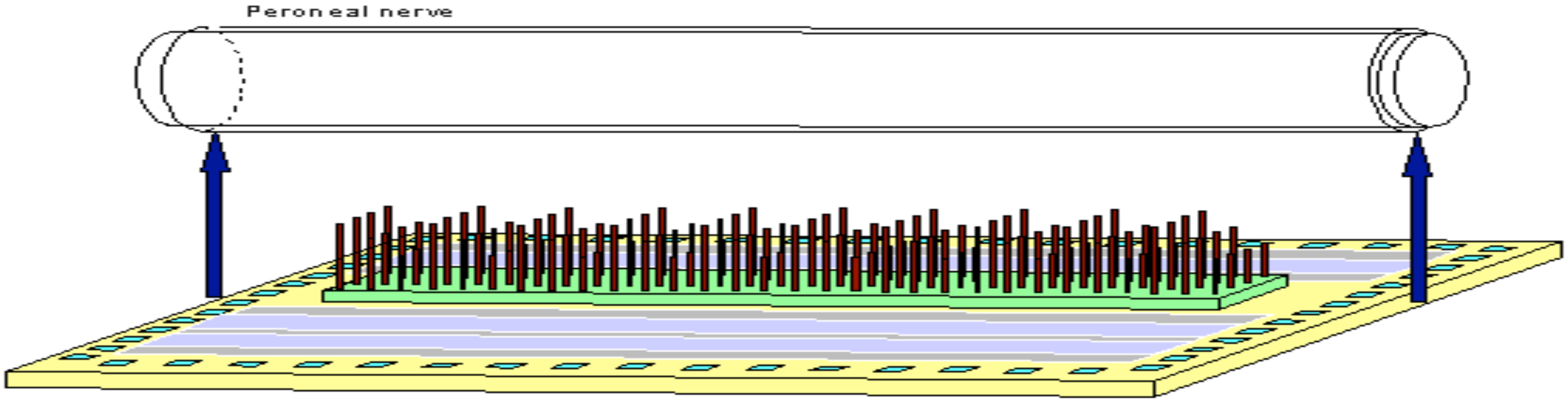

Functionnal neurostimulation: intraneuronal electrodes

Planar microelectrode array (*Universities of Michigan, Stanford, Utah and Surrey*)

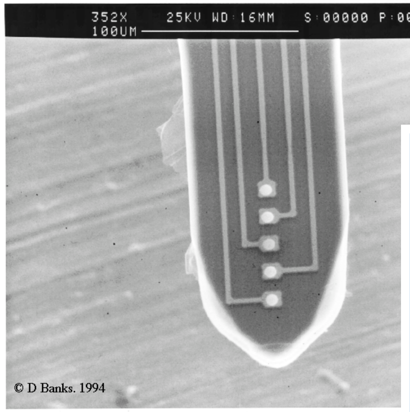

© D Banks. 1994

4 microelectrodes

Silicon, SiO_2, polyimide

IrOx, Au, W, Ni, Pt ou TiN

SiO_2, Si nitride, Polyimide, PMMA

Photolithography

Penetration in the brain tissues

- S/B
- Insensitive to movement
- Injury and friction

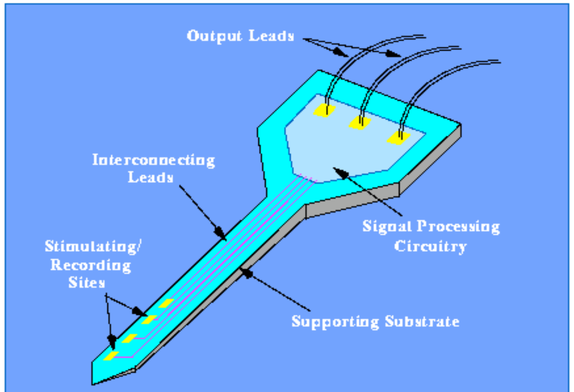

Figure 1: Basic structure of a micromachined multielectrode probe for recording and/or stimulation of the central nervous system.

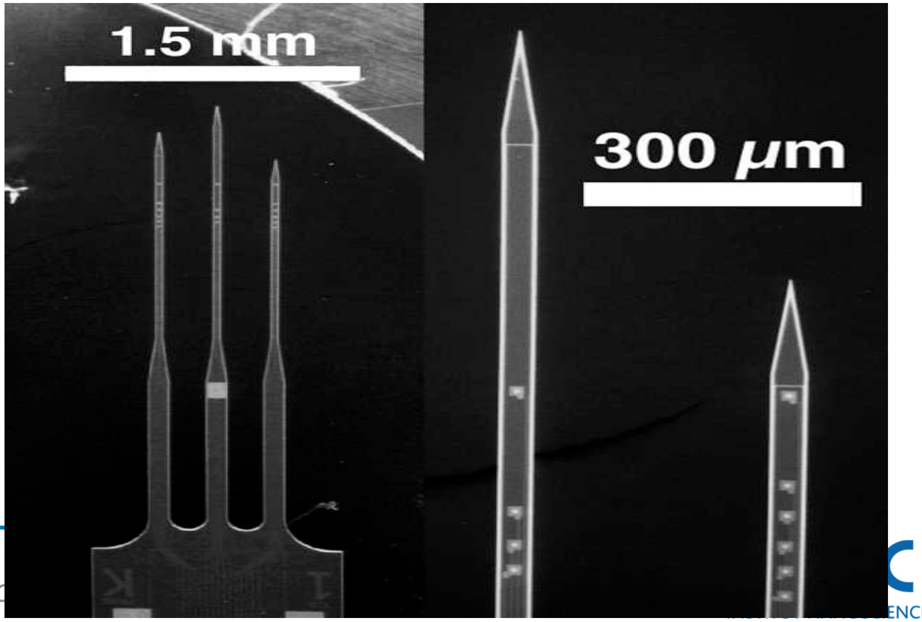

Functionnal neurostimulation: intraneuronal electrodes

After implantation:

Biofilm formation
Adsorption of proteins
Adsorption of lipides
Tissue growing

Increase of interfacial impedance

Loose of efficacy
Risk in tissue burning
Difficulty in explantation

Before Implantation

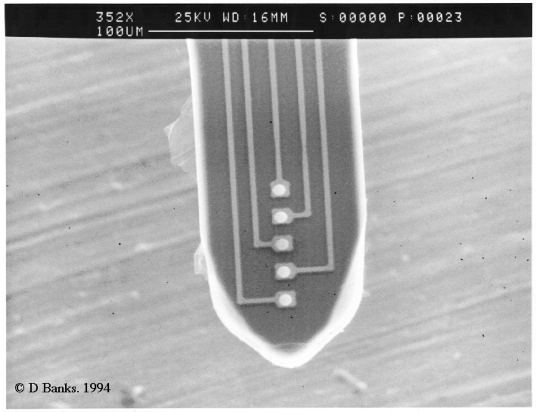

© D Banks. 1994

After implantation

Functionnal neurostimulation: flexible nerve plate electrodes

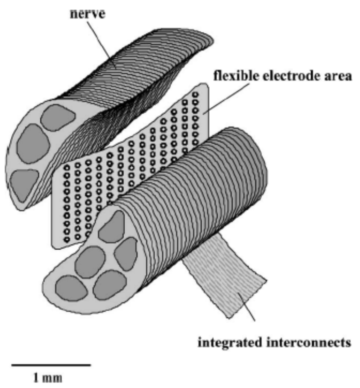

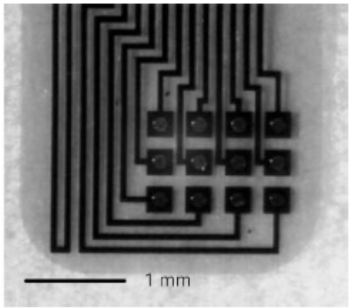

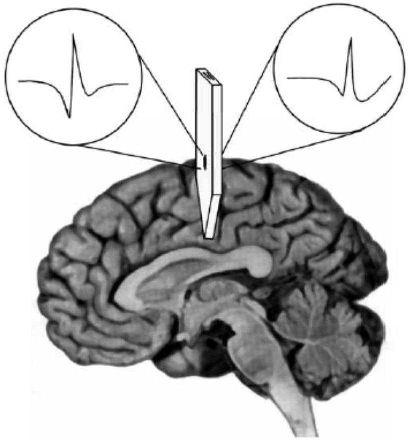

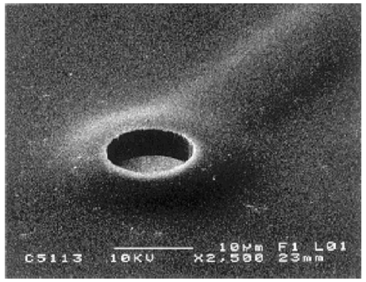

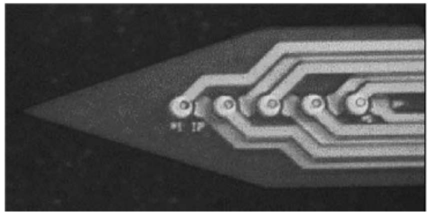

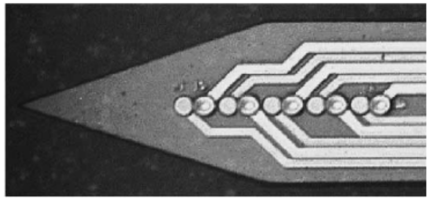

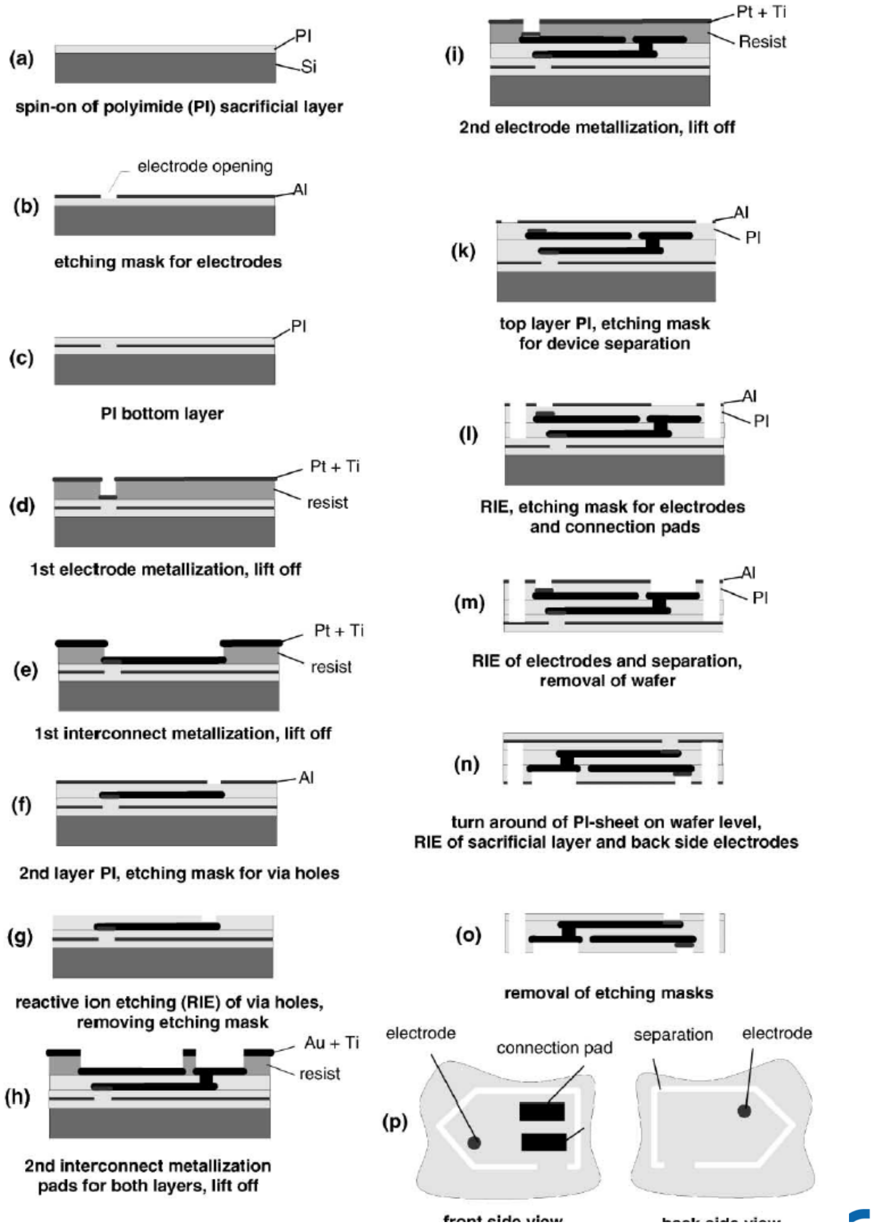

Steiglitz et al, Sensors & Actuators B, 83 (2002) 8

Functionnal neurostimulation: sieve electrodes

Microring electrode array for cuted nerve

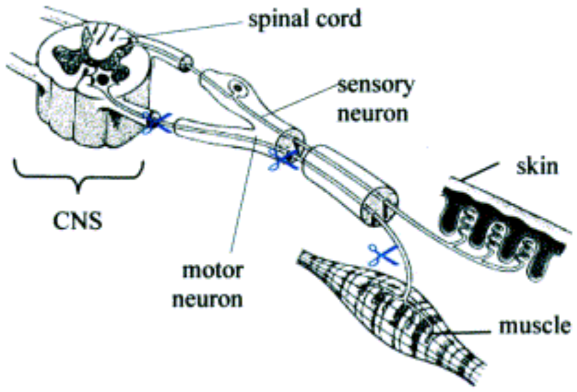

✂ : possible sites of peripheral nerve lesions

Fig. 1

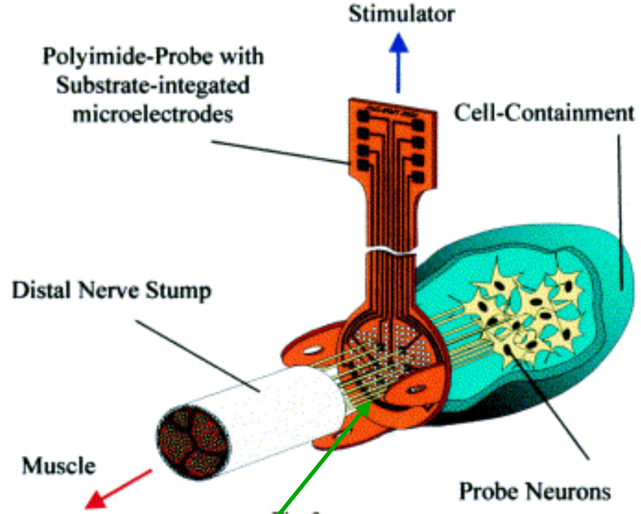

Fig. 3

Nerve growth trough te electrode appertures

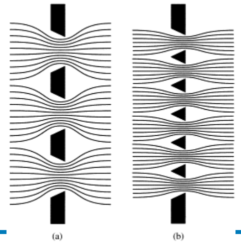

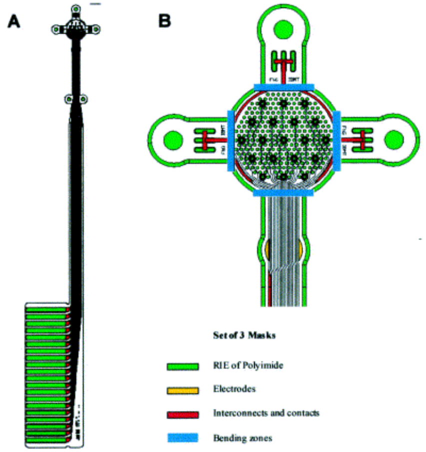

Fig. 4

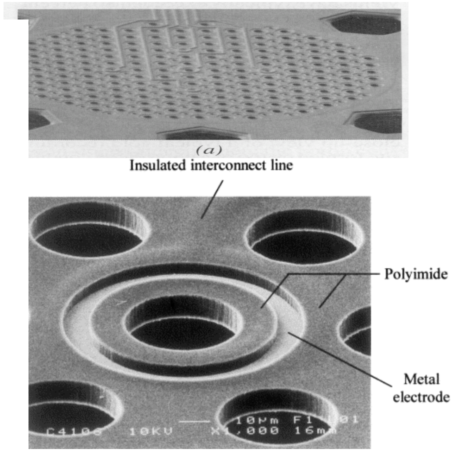

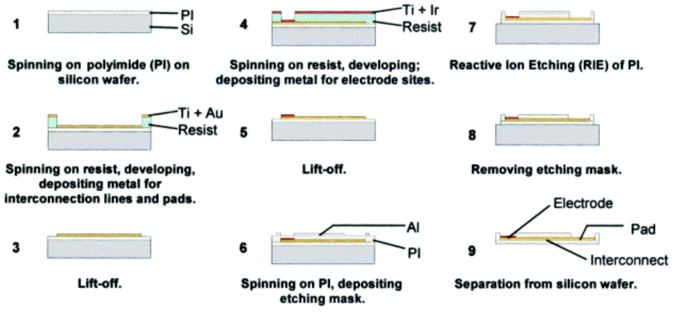

1 Spinning on polyimide (PI) on silicon wafer.

2 Spinning on resist, developing, depositing metal for interconnection lines and pads.

3 Lift-off.

4 Spinning on resist, developing; depositing metal for electrode sites.

5 Lift-off.

6 Spinning on PI, depositing etching mask.

7 Reactive Ion Etching (RIE) of PI.

8 Removing etching mask.

9 Separation from silicon wafer.

Fig. 5

Electrical field distribution

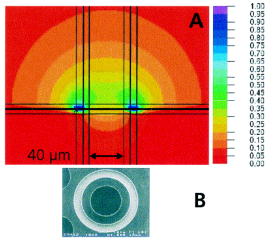

Fig. 6

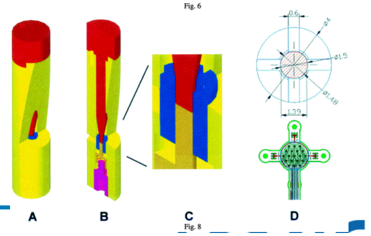

Fig. 8

Steiglitz et al, *Biosensors & Bioelectronics, 17 (2002) 685*

Cochlear implants

Hearing system ➡ Deafness → Ossicles (Mechanical) → Cochlea (biochemical)

➚accoustic level amplifier

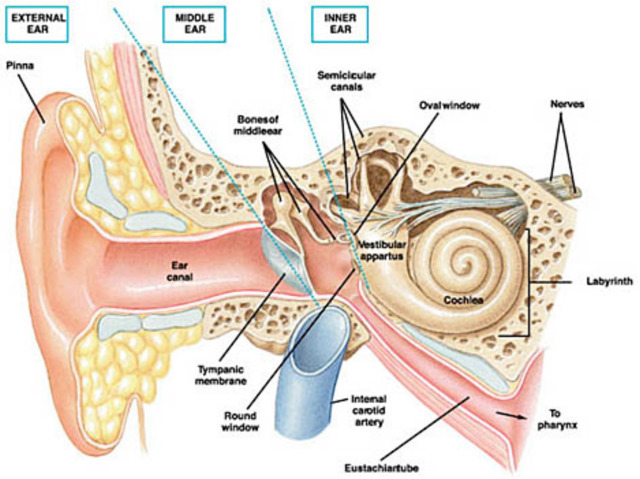

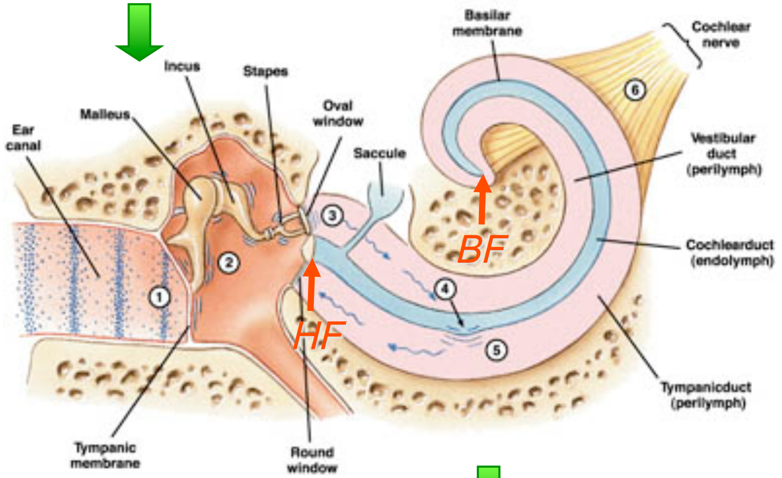

Resonator (tectorial-basilar membranes)
Transduction chemo-mechanic

Hair cells

sensorineuronal

Electrostimulation

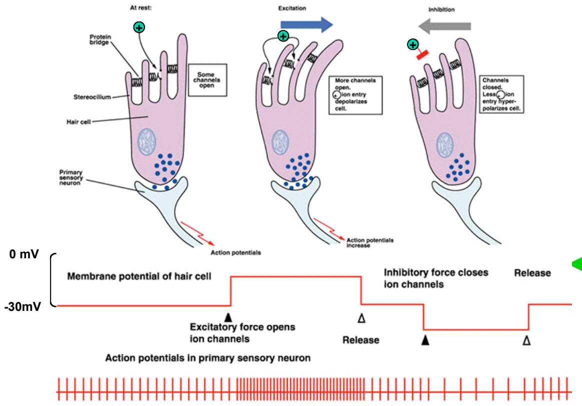

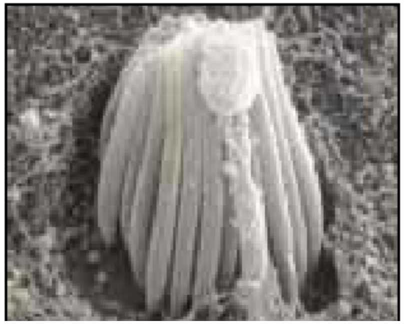

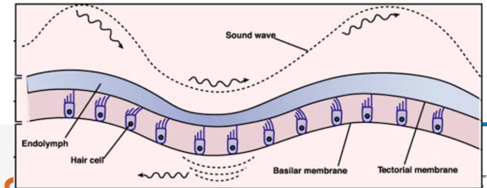

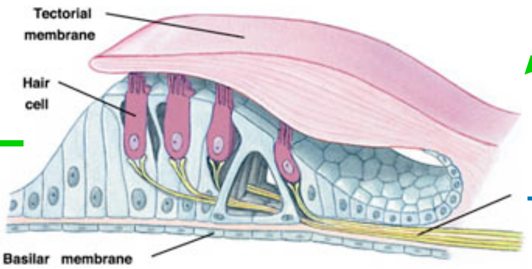

Cochlear implants

Electrostimulation

Shunt of the bi-membrane resonator
Detection and binary transduction of sounds
Transfer to the implant through coils

Number of data to implement?

Nombre d'électrodes ?

30 000 nerve terminaisons!!!

Phone research
Voici mimicking
8 lines

Array of 22 electrodes
Placed in series

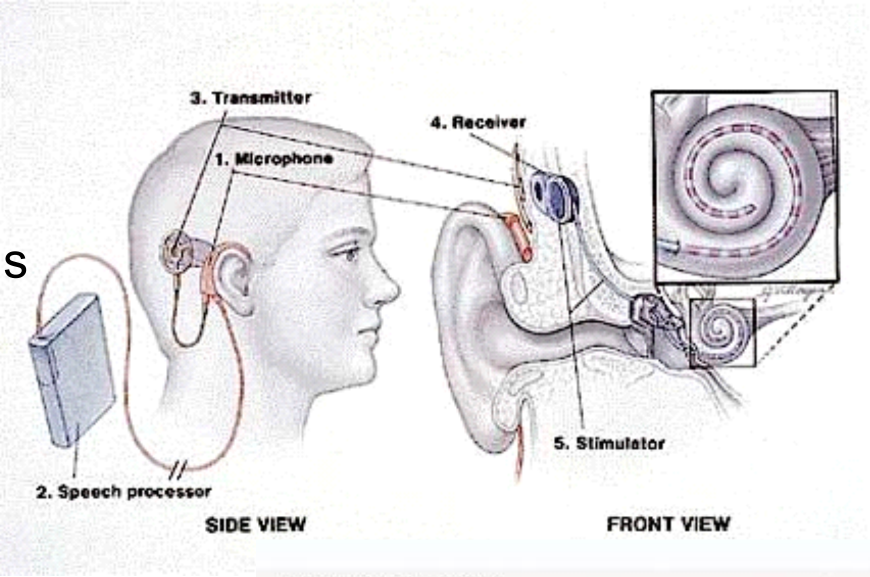

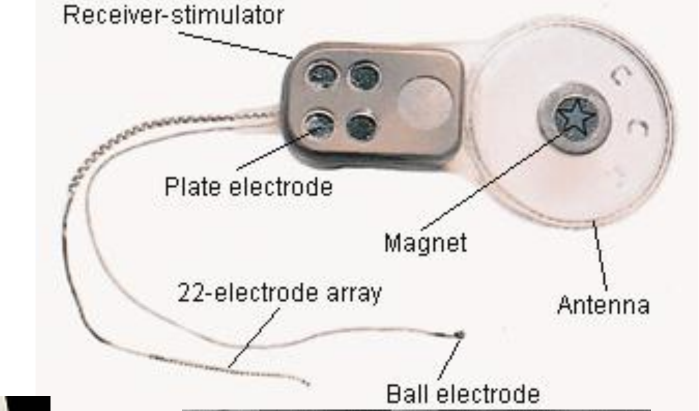

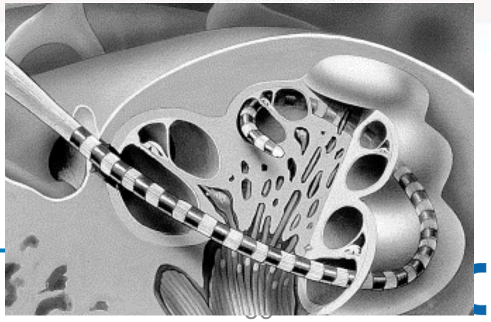

Cochlear implants materials and signals

Hearing frequencies → **20 Hz-20 kHz**
1-80 dB

Nerve → excitability 200 to 300 Hz

Sound encoding on a nerve array

Limited number of electrodes(22)

Activation séquencielle des électrodes
(Cross-talk entre électrodes)

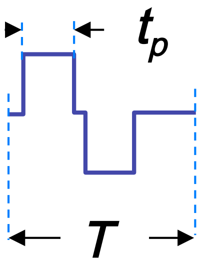

T : 1-8 kHz

t_p : 20-400 µs

I : 50-450 mA cm^{-2}

I = 90 ou 290 mA cm^{-2}

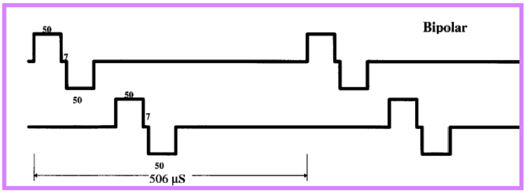

Xu et al, Hear. Res, , 105 (1997) 1

Platinum electrodes in teflon tubing

Surface modification → high surface area

Bipolar electrodes (paires)
Unipolar electrode with ground

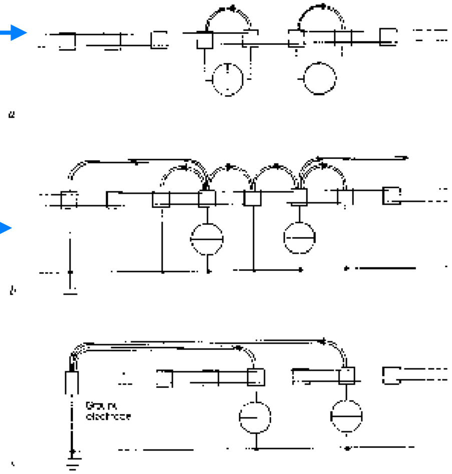

Sound power → $W = f\,I^{\alpha}$ → Electrode size
Nerve density
Electrode position

Cochlear implants : electrochemical behaviour

Electrodes de platine de grande surface développée

0.43 mm^2
Bipolar or unipolar

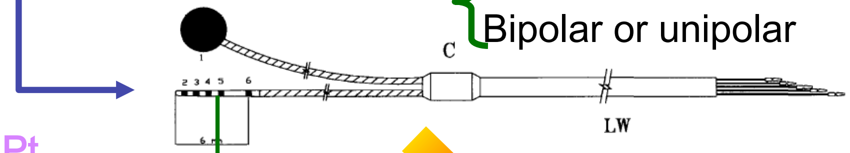

Pt

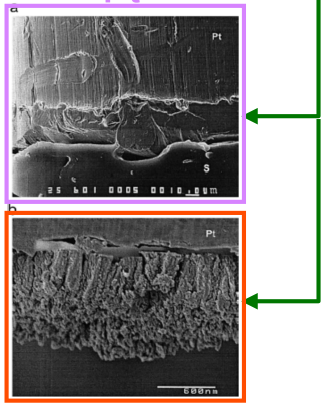

Pt - porous Pt

(Current level: 1mA, 50 µs/phase, 30 Hz)

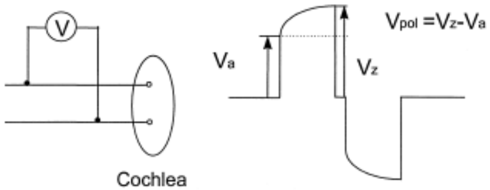

Typical chronopotetiometric response

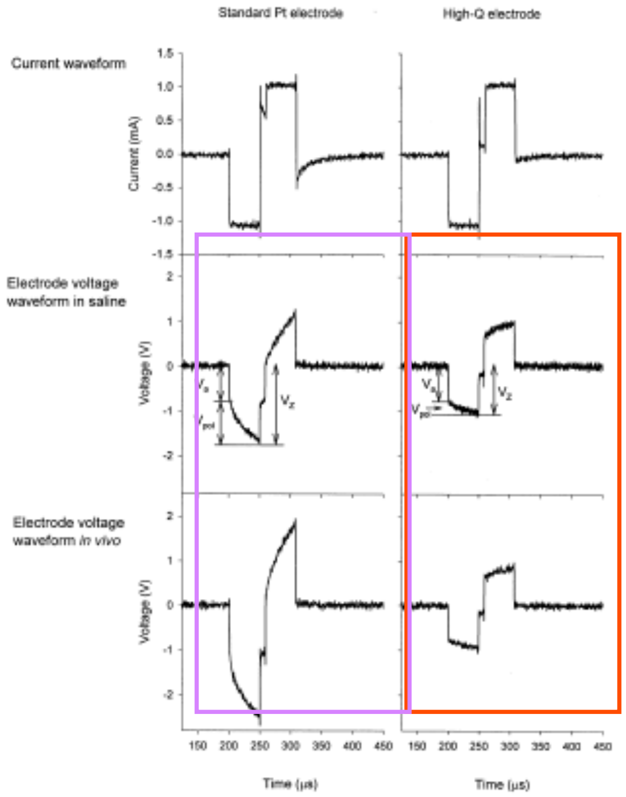

***Bolzan et al**, Electrochim Acta 33 (1988) 1743*

i. Formation of PtOH on Pt
ii. Reductionofe PtOH on Pt

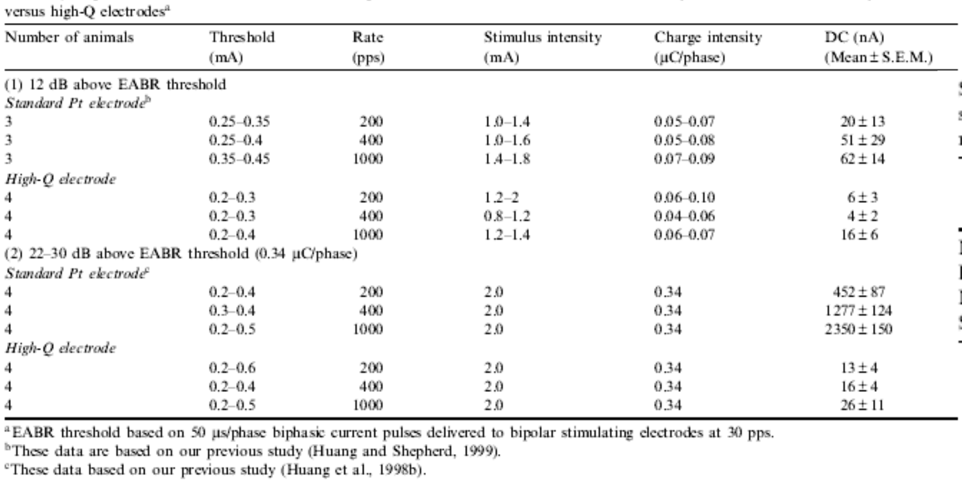

Summary of pre-stimulus EABR thresholds, stimulus parameters and mean residual DC levels during the acute stimulation using standard Pt versus high-Q electrodes[a]

Number of animals	Threshold (mA)	Rate (pps)	Stimulus intensity (mA)	Charge intensity (µC/phase)	DC (nA) (Mean ± S.E.M.)
(1) 12 dB above EABR threshold					
Standard Pt electrode[b]					
3	0.25–0.35	200	1.0–1.4	0.05–0.07	20 ± 13
3	0.25–0.4	400	1.0–1.6	0.05–0.08	51 ± 29
3	0.35–0.45	1000	1.4–1.8	0.07–0.09	62 ± 14
High-Q electrode					
4	0.2–0.3	200	1.2–2	0.06–0.10	6 ± 3
4	0.2–0.3	400	0.8–1.2	0.04–0.06	4 ± 2
4	0.2–0.4	1000	1.2–1.4	0.06–0.07	16 ± 6
(2) 22–30 dB above EABR threshold (0.34 µC/phase)					
Standard Pt electrode[c]					
4	0.2–0.4	200	2.0	0.34	452 ± 87
4	0.3–0.4	400	2.0	0.34	1277 ± 124
4	0.2–0.5	1000	2.0	0.34	2350 ± 150
High-Q electrode					
4	0.2–0.6	200	2.0	0.34	13 ± 4
4	0.2–0.4	400	2.0	0.34	16 ± 4
4	0.2–0.5	1000	2.0	0.34	26 ± 11

[a] EABR threshold based on 50 µs/phase biphasic current pulses delivered to bipolar stimulating electrodes at 30 pps.
[b] These data are based on our previous study (Huang and Shepherd, 1999).
[c] These data based on our previous study (Huang et al., 1998b).

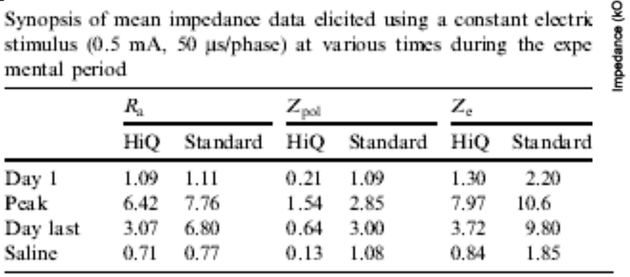

Synopsis of mean impedance data elicited using a constant electric stimulus (0.5 mA, 50 µs/phase) at various times during the expe mental period

	R_a		Z_{pol}		Z_e	
	HiQ	Standard	HiQ	Standard	HiQ	Standard
Day 1	1.09	1.11	0.21	1.09	1.30	2.20
Peak	6.42	7.76	1.54	2.85	7.97	10.6
Day last	3.07	6.80	0.64	3.00	3.72	9.80
Saline	0.71	0.77	0.13	1.08	0.84	1.85

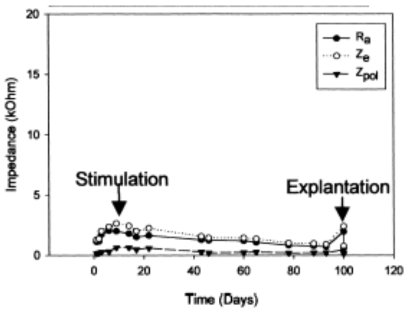

***Huang et al**, Hear. Res. 146 (2000) 57*
***Tyconcinsski et al**, Hear. Res. 159 (2001) 53*

Artificial retina

Margalit et al, *Survey of Ophtalmology 47 (2002) 335*

3 stimulation routes

- Retine
- Optical nerve
- Cortex

Subretinal implant (ASR)

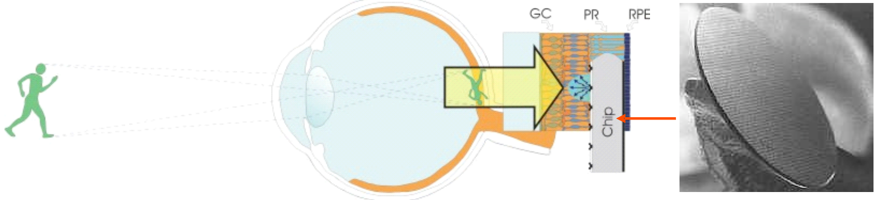

µelectrode and µphotodiodes array

Integrated system

Retina implant

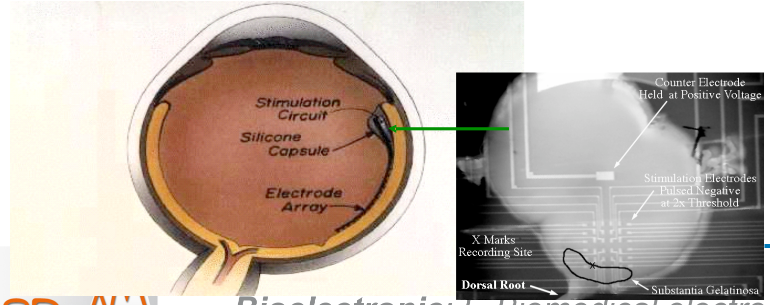

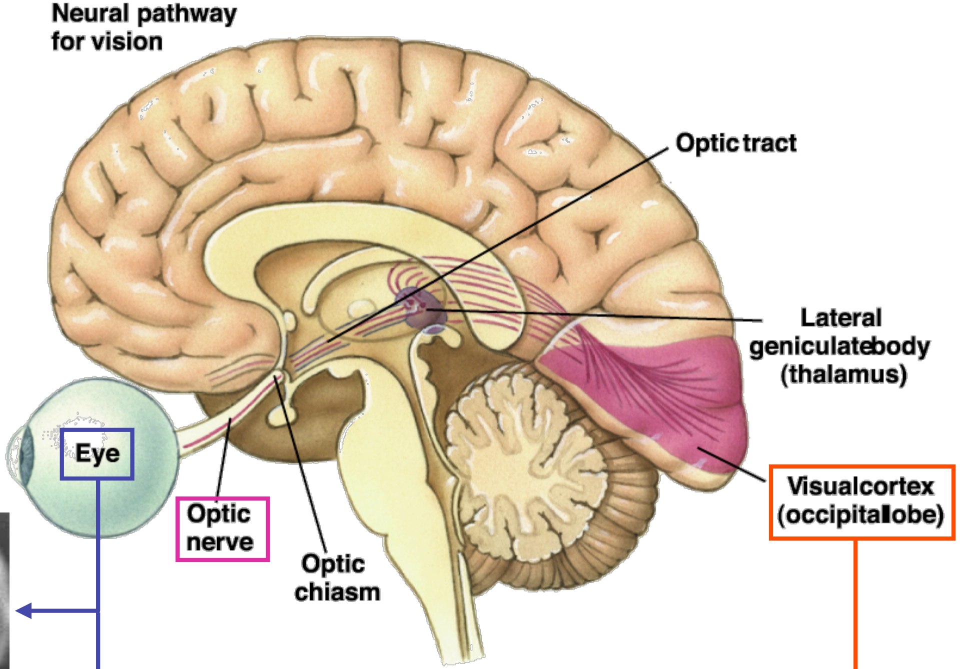

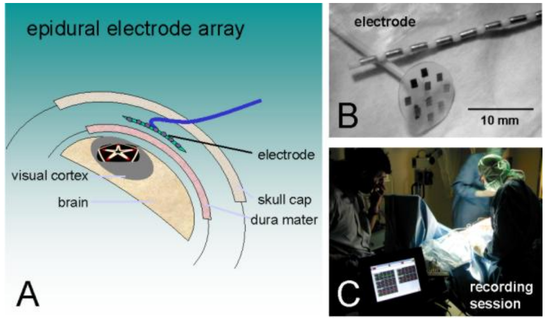

Basic requirements in retina implants

- **Unaided Mobility**
  - 256-600 pixels

- **Reading Large Print/Recognizing faces**
  - 1024 pixels

- **Reading regular print at regular reading speed**
  - 10,000 pixels

- **Stimulus Threshold**
  - Electrode Size
    - Best Case: 6 uA -> 15 micron diameter (irOx, 1 mC/cm^2)
    - Conservative: 100 uA - > 200 micron diameter (Pt, 0.1 mC/cm^2)
  - Device Power
    - Smaller electrode size will lead to higher impedance, but $P=I^2R$, so lowering threshold stimulus has large effect on decreasing power

Retinal neuron network and subretinal implants

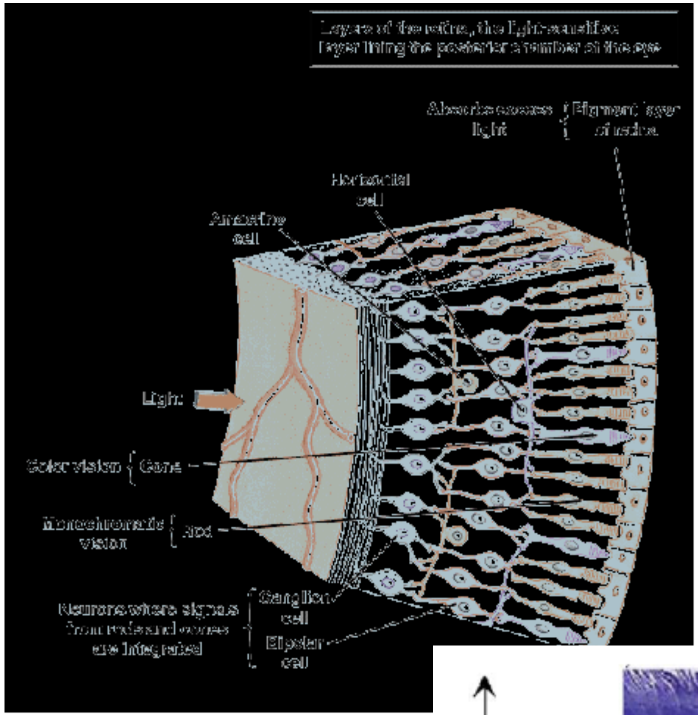

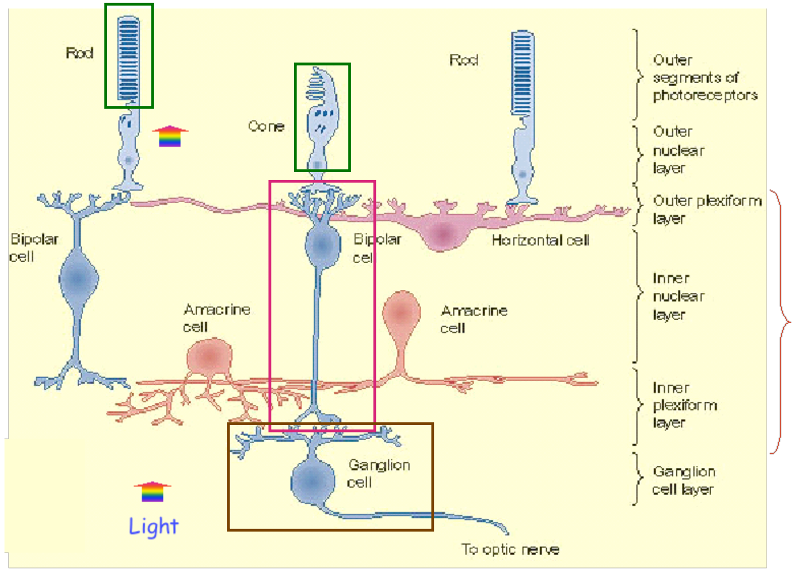

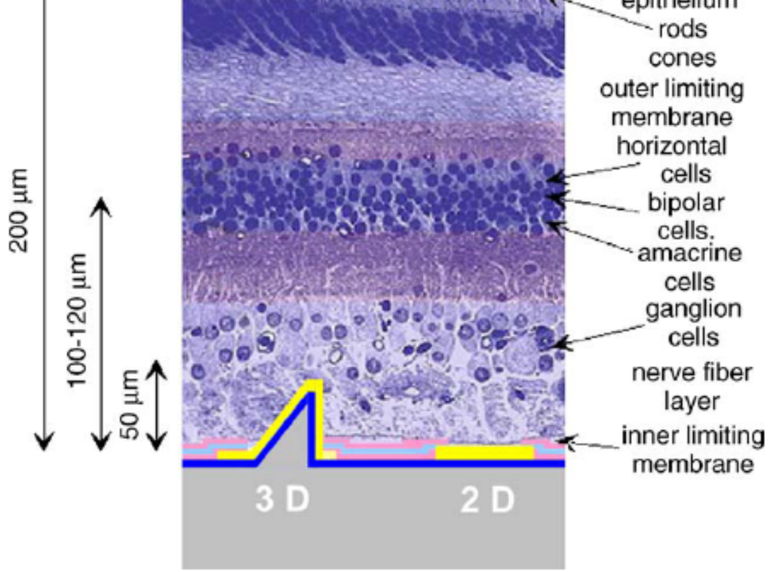

Epiretinal and subretinal implants

Epiretinal

- Less disruptive to the retina.
- More flexibility in component placement
- More complex stimulus algorithms required

Subretinal

- In natural position of photoreceptors
- Disruptive to retina
- Devices relying on incident light for power cannot generate effective stimulus

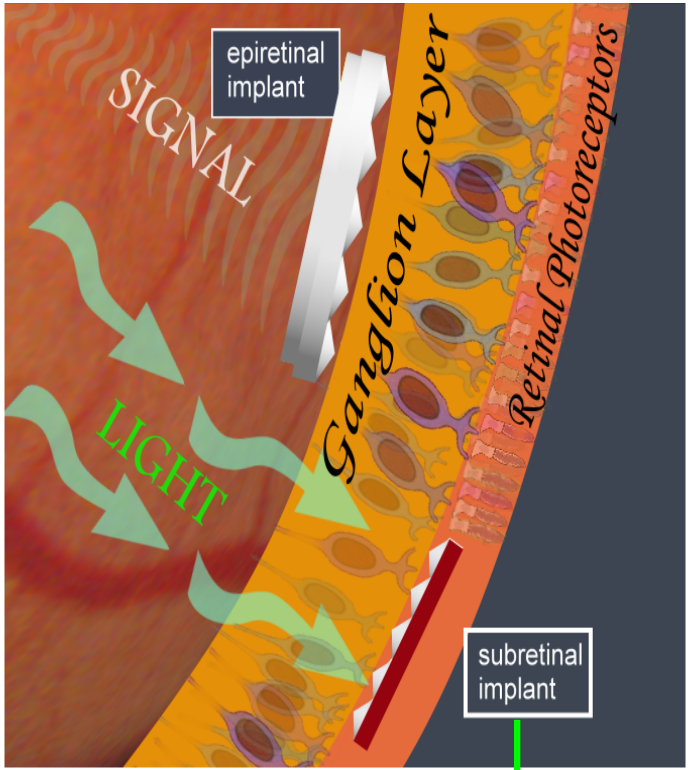

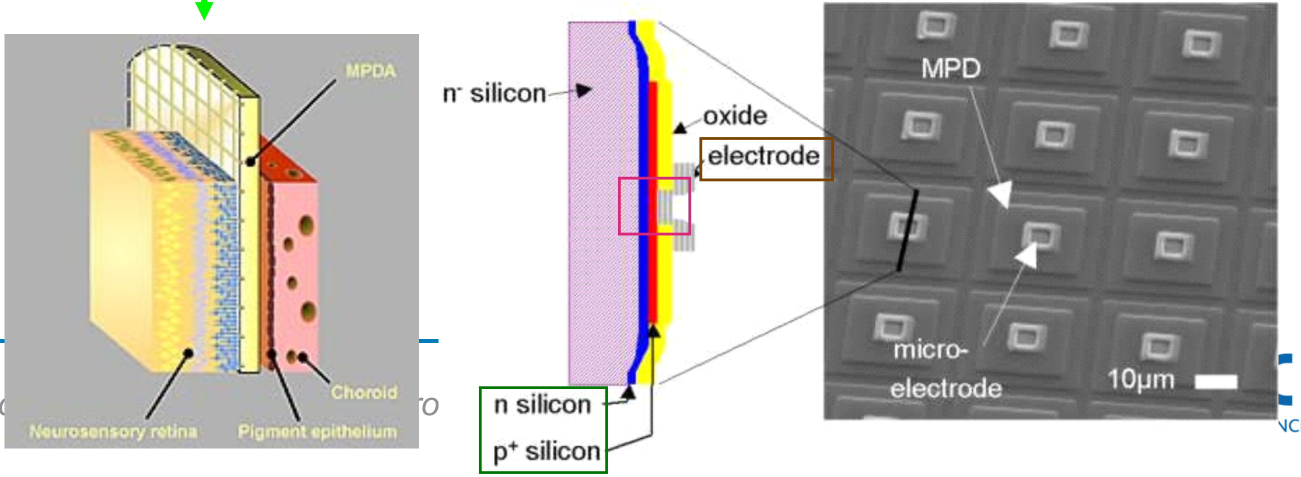

- Light conversion
- Electrochemical transduction
- Retina stimulation

State of the arts in artificial retina

- **Epiretinal and Subretinal** at Investigational Device Exemption Stage
- **Epiretinal** - encouraging results, but better technology required
- **Subretinal** – No direct evidence demonstrating functional electrical stimulation, but patients report subjective improvements in vision

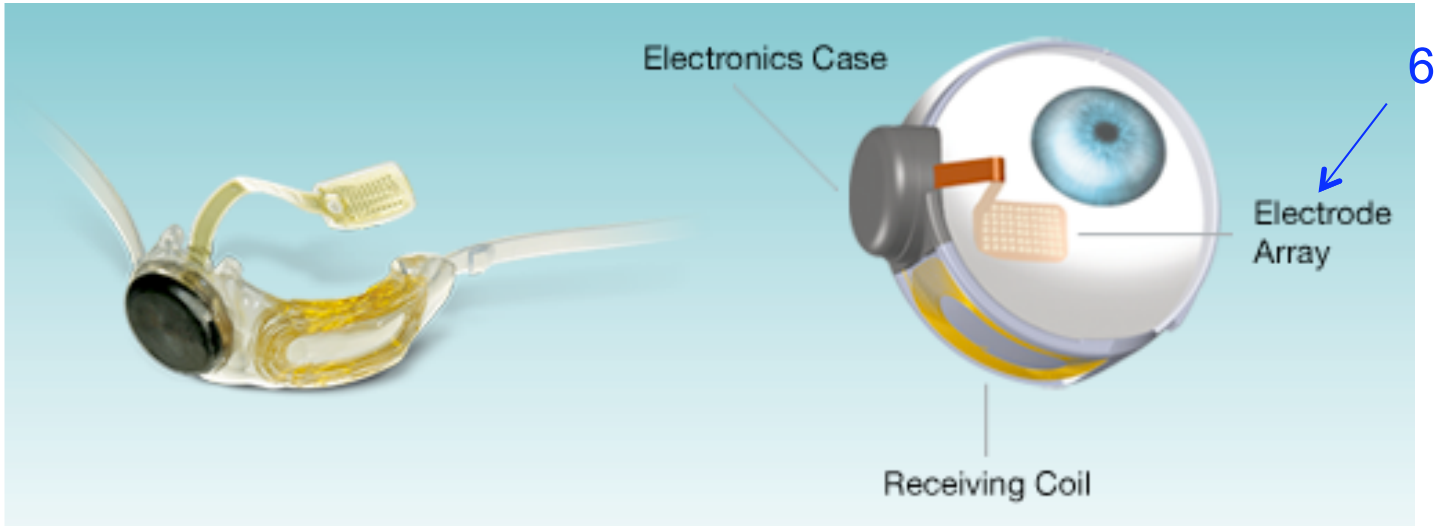

64 electrodes array

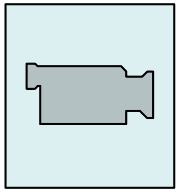

Second Sight Epiretinal implant Argus II^{TM}

Penetrating electrode retinal array

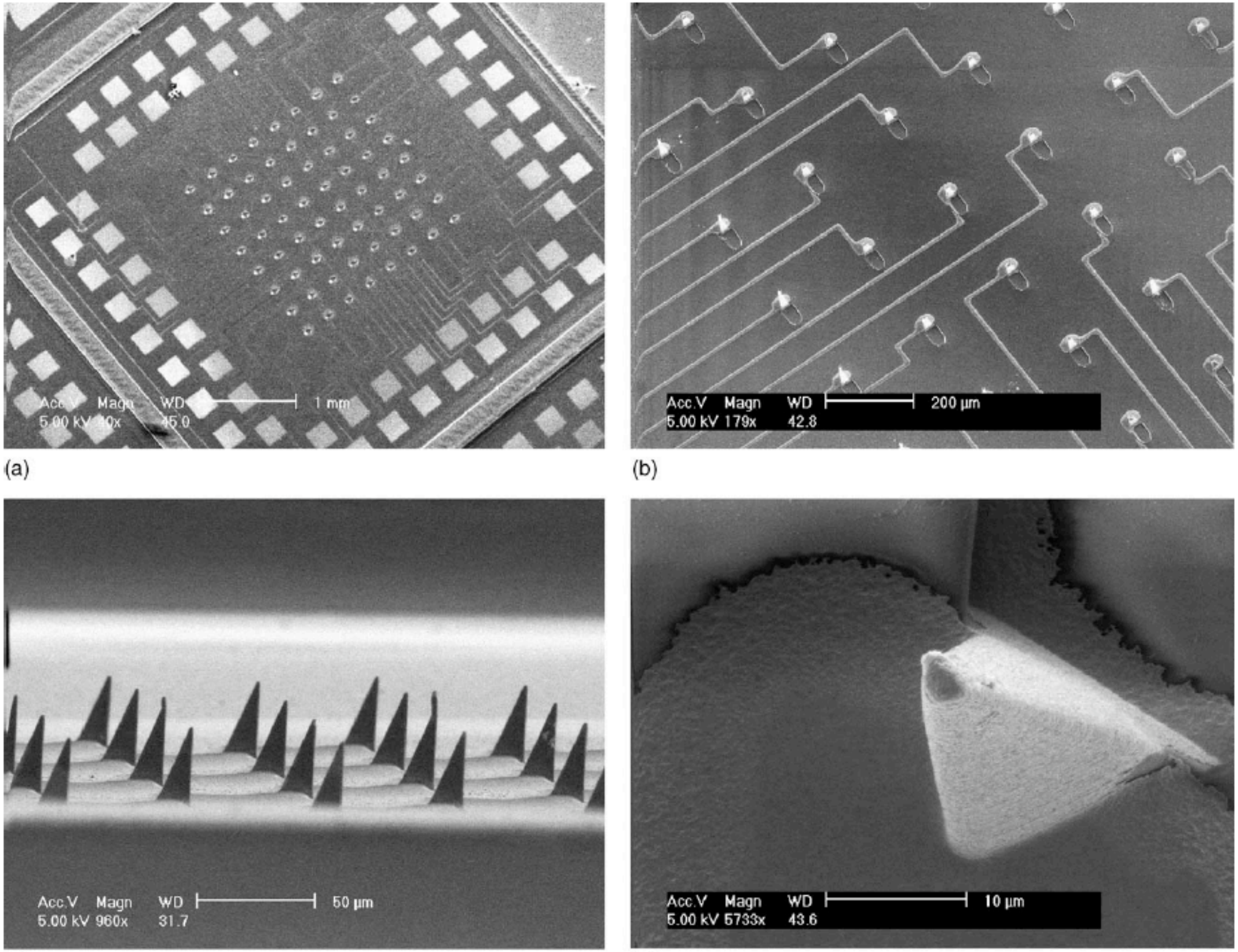

MEMS electrodes for epiretinal implants

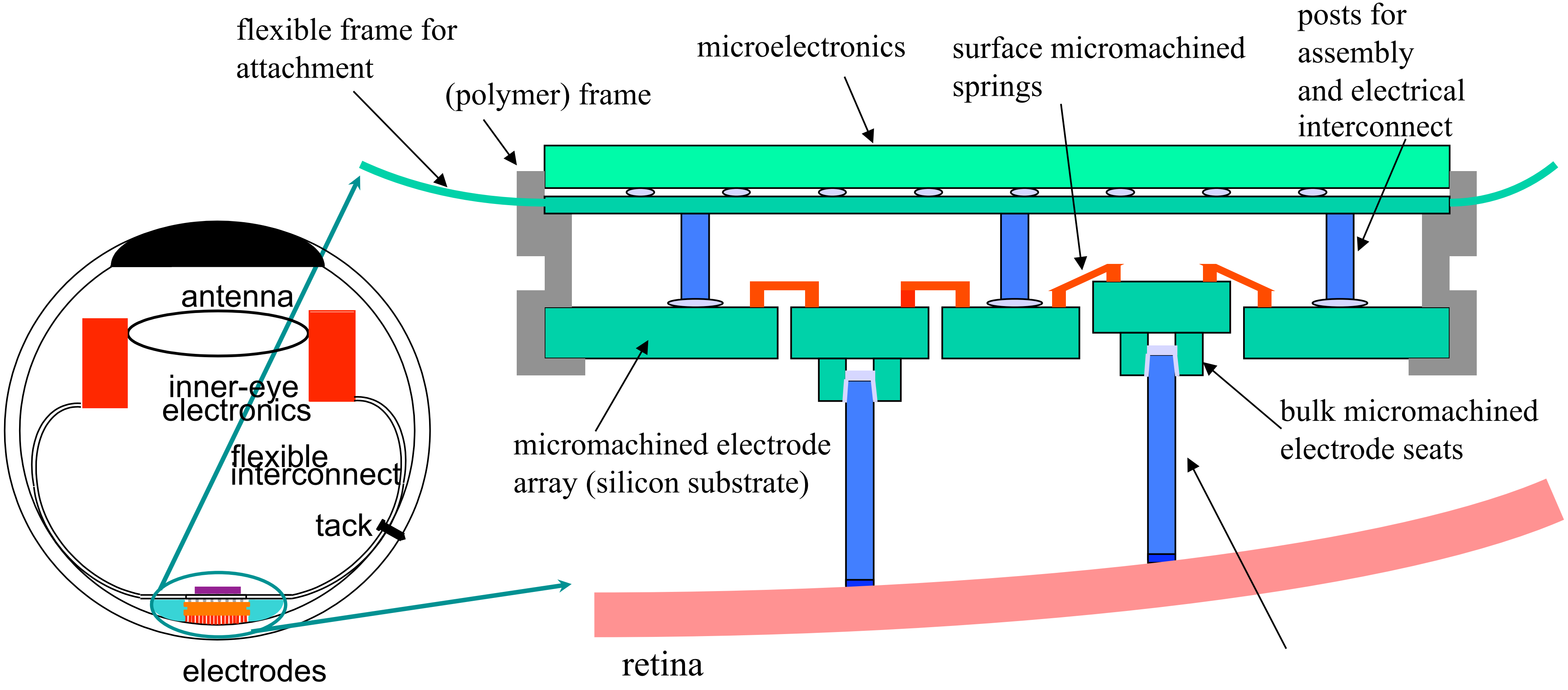

flexible frame for attachment

(polymer) frame

microelectronics

surface micromachined springs

posts for assembly and electrical interconnect

antenna

inner-eye electronics

flexible interconnect

tack

electrodes

micromachined electrode array (silicon substrate)

bulk micromachined electrode seats

retina

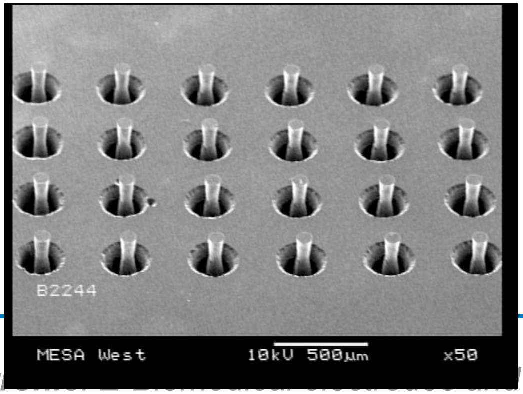

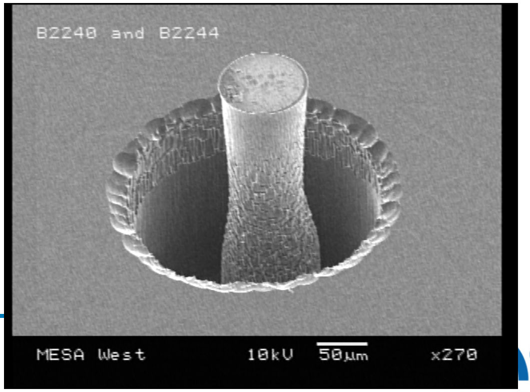

Flexible connectors

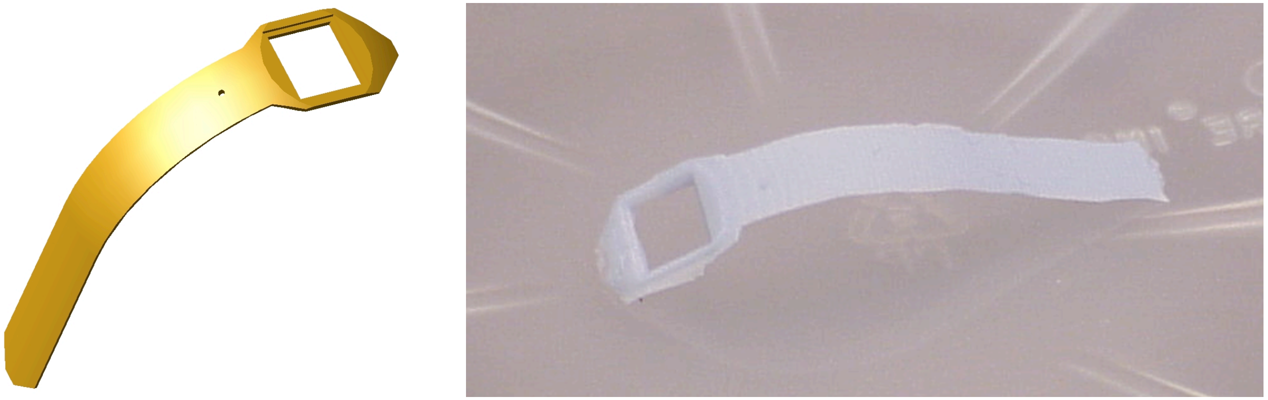

3D model
and fabricated
polymer mold

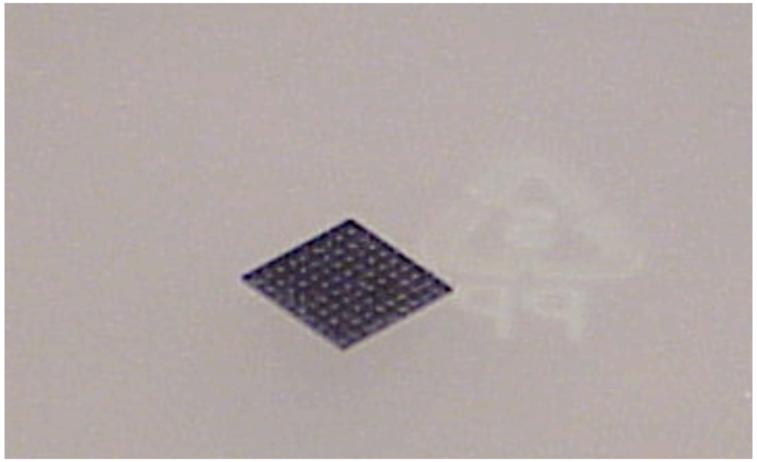

9x9 electrode array
(test part/ no posts)

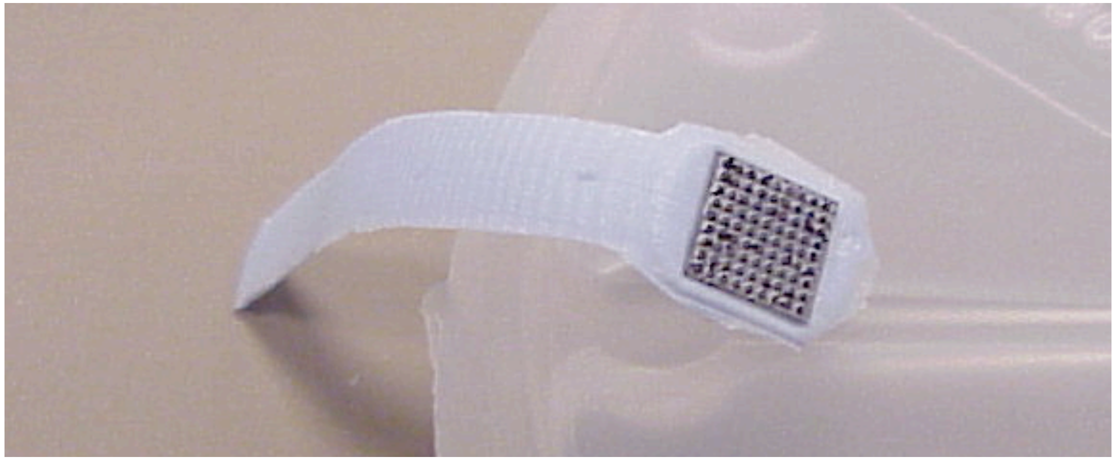

array placed in the polymer frame

Argon lab, USA

Diamond based artificial retina

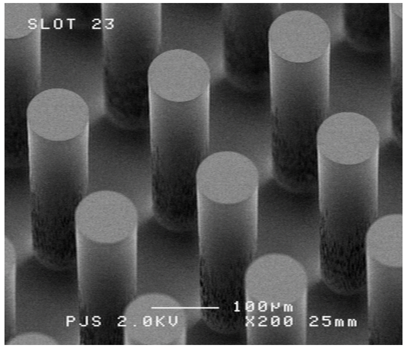

SEM picture of SNL MEMS Si electrode test structures

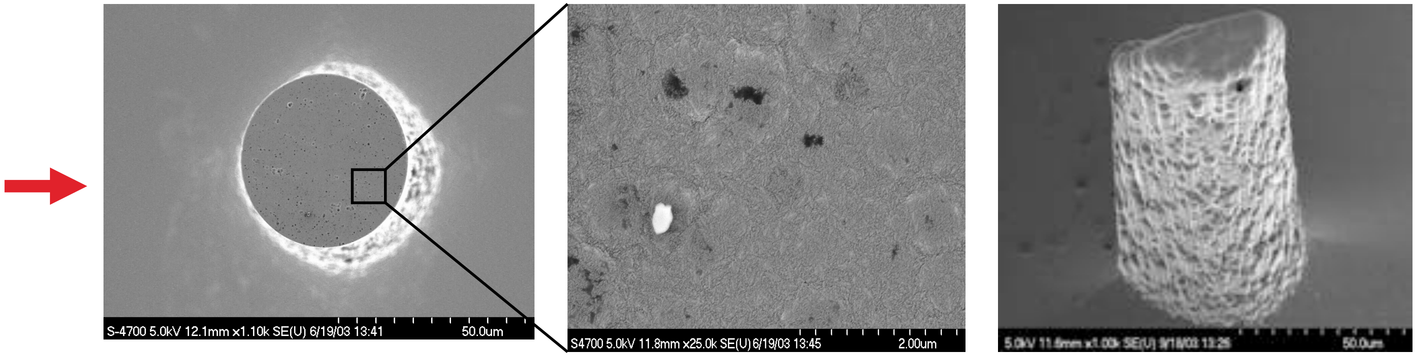

SEM pictures of SNL MEMS Si electrode test structure coated with UNCD film

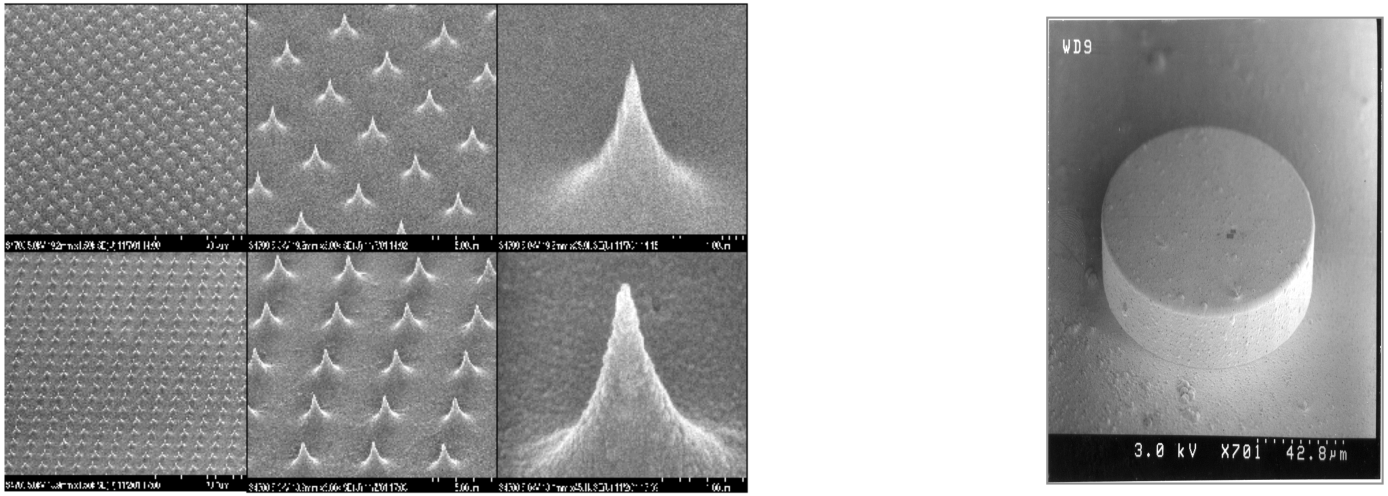

SEM pictures of ANL Si tips and posts coated with UNCD film

Diamond based flexible epiretinal implant

e.g., on polyimide :

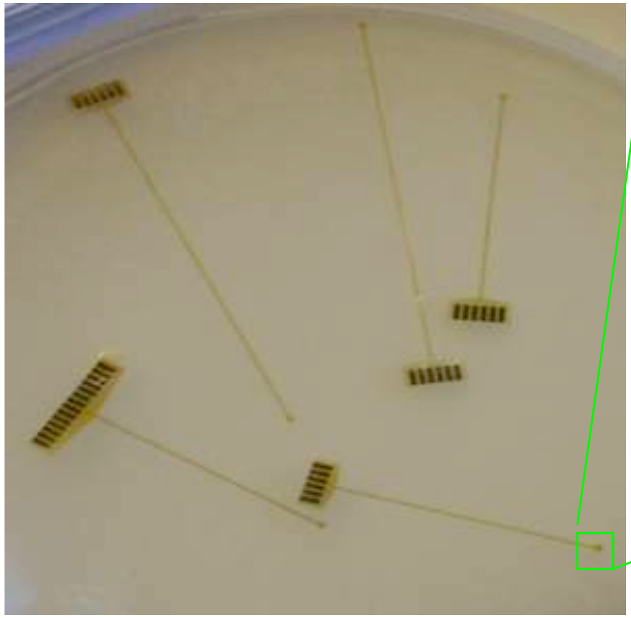

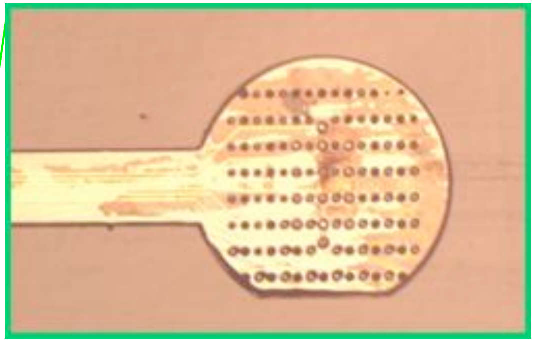

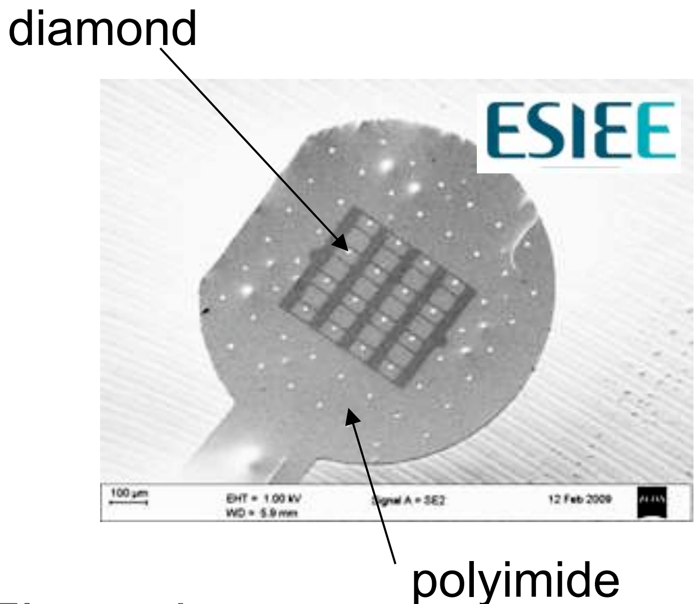

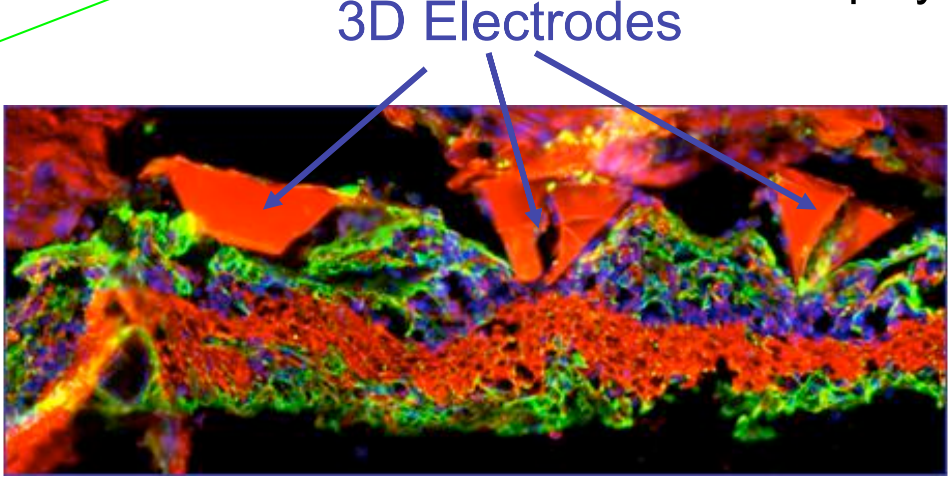

Bipolar cells + glial cells + nucleii

G0α + GFAP + DAPI

As subretinal retina implant
(14 weeks)

INSTITUT DE LA VISION
PARIS

SPrAM
Structures et Propriétés d'Architectures Moléculaires

INAC
INSTITUT NANOSCIENCES ET CRYOGÉNIE

Subretinal implant

OPTOBIONICS™
Technology for Vision™

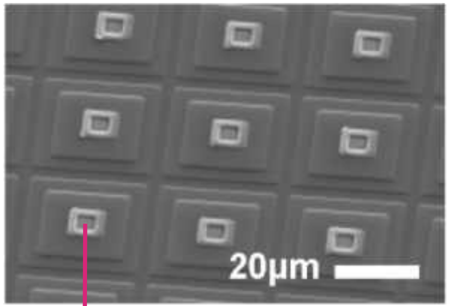

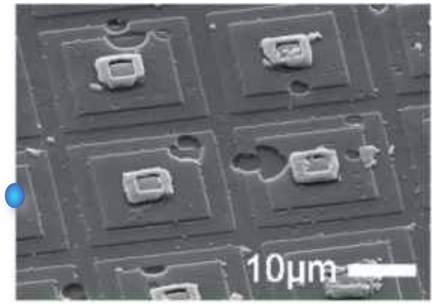

Explantation after 10 monthes

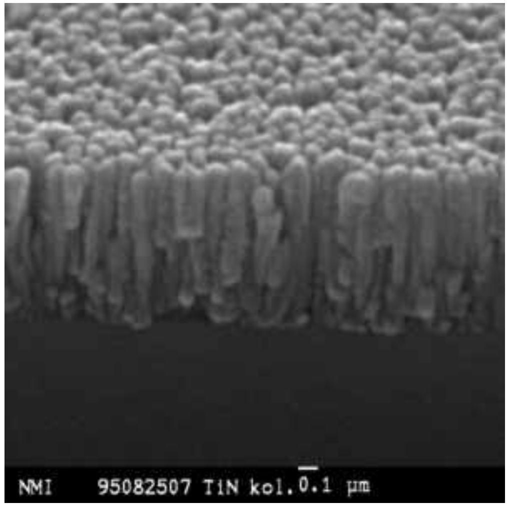

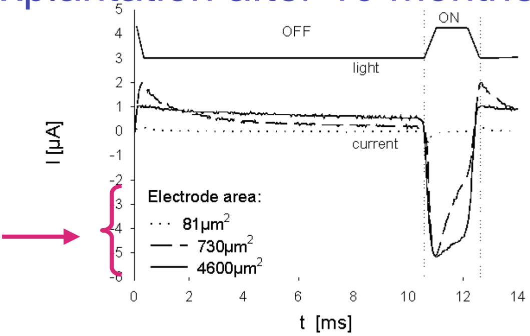

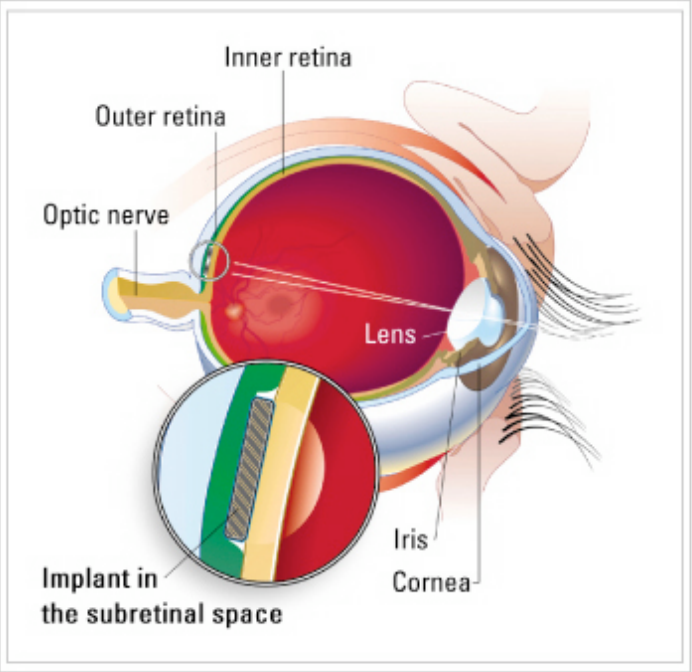

Drawing by Mike Zang

- Diamter 3mm, thickness50 µm
- Theoretical vision field12°
- 7600 Photodiodes of 40 µm^2
- Electrode of 50 µm^2 ⇨ high developed surface
- Requires photonic amplification (IR)

Electrode en TiN

Gekeler et al, Séminaires d'ophtalmologie d'IPSEN, 12 (2001) 77